

# Improving photon and proton radiotherapy of locally advanced non-small cell lung cancer

Kristine Fjellanger

Thesis for the degree of Philosophiae Doctor (PhD)  
University of Bergen, Norway  
2024

UNIVERSITY OF BERGEN



# Improving photon and proton radiotherapy of locally advanced non- small cell lung cancer

Kristine Fjellanger



Thesis for the degree of Philosophiae Doctor (PhD)  
at the University of Bergen

Date of defense: 19.03.2024

© Copyright Kristine Fjellanger

The material in this publication is covered by the provisions of the Copyright Act.

Year: 2024

Title: Improving photon and proton radiotherapy of locally advanced non-small cell lung cancer

Name: Kristine Fjellanger

Print: Skipnes Kommunikasjon / University of Bergen

## **Scientific environment**

The research in this thesis has been performed at Haukeland University Hospital (HUH), in the research group at the Section for Medical Physics at the Department of Oncology and Medical Physics, in collaboration with the research group at the Department of Radiotherapy, Erasmus University Medical Center (EMC), Rotterdam, The Netherlands. The candidate has been affiliated with the Institute of Physics and Technology at the University of Bergen (UiB). The work has been supervised by Liv B. Hysing (HUH, UiB), Ben J. M. Heijmen (EMC) and Helge E. S. Pettersen (HUH).

## Acknowledgements

This thesis marks the end of three and a half eventful and educational years. The PhD project was made possible by the main funder Helse Vest RHF and also benefited from funding from the Trond Mohn Foundation. It could not have been performed without the support and guidance from the amazing people around me and I am grateful for the opportunity to work with you all.

First, I would like to thank my supervisors, Liv Hysing, Ben Heijmen and Helge Pettersen. Liv, from the first ideas and grant application to the final touches on this thesis you have always been available for discussions, and you helped me see the questions I did not know to ask. Working with you has been a pleasure. Ben, you have readily shared your vast experience and knowledge and always contribute with a new perspective. Your very thorough feedback has given me many hours of work but most importantly substantially improved our manuscripts. It is a pity covid sabotaged my plans to join your group at EMC in 2020, but remote collaboration went smoothly and our many hours of online meetings have always been a constructive pleasure. Helge, thank you for sharing your expertise; having a scripting oracle in the office next door is a luxury.

I have been fortunate to collaborate with many proficient colleagues during these years. I am especially grateful to Inger Marie Sandvik for including patients and spending hours and hours delineating and re-delineating their tumors; to Turid Sulen for teaching me the significance of high-quality treatment planning; to Linda Rossi for spending many hours of covid-time online with me while patiently and thoroughly guiding me through the Erasmus-iCycle system; and to Sebastiaan Breedveld for sharing your expertise on all things related to automation. Also a special thanks to the Haukelandsbakken crew and the medical physics research group who make every day at the office better.

This research would not have been possible without the patients who contributed with their data. I am grateful to them and to the clinical personnel at the Department of Oncology and Medical Physics at HUH who contributed to the data collection -

radiation therapists, treatment planners, oncologists and physicists. I also thank the heads of the department and the sections for medical physics and radiation therapy for supporting the project.

I would not be where I am today without mom and dad, who always have believed in me and taught me to believe in myself. Mom, you were my biggest supporter and I really wish you were here to struggle through this entertaining piece of literature. Thank you to my family and friends for their continuous support and encouragement during this period, and a special thanks to mormor for being the best babysitter.

Most of all, thank you Niklas and Julian for bringing joy to every day. Niklas, you are my steady support and partner in everything, who remind me what is important. Julian, you are the best thing we have created. You motivate me to work hard so that I can come home to your big smile. With the two of you in it, I am looking forward to the next chapter no matter what it brings.

## Abstract in English

Patients with locally advanced non-small cell lung cancer (LA-NSCLC) have tumors that are large, invade other intrathoracic structures and/or have spread to regional lymph nodes. These patients are often inoperable, and the standard treatment is radiotherapy in combination with chemotherapy, followed by immunotherapy for selected patients.

Intensity-modulated photon radiotherapy (IMRT) in free breathing (FB) is the current standard radiotherapy technique for LA-NSCLC patients. Due to large treatment volumes in proximity to important organs at risk (OARs), the patients often experience side effects from treatment. Radiation-induced side effects such as radiation pneumonitis and cardiac disease can be severe and potentially fatal.

The aim of this project was to investigate the potential of different methods to reduce OAR doses and the risk of side effects in radiotherapy of LA-NSCLC. The three main topics of investigation were automated treatment planning (autoplanning), deep inspiration breath hold (DIBH) and proton therapy. Prospectively collected image data both from before and during radiotherapy treatment were used in five different simulation studies.

Autoplanning in IMRT was investigated in papers I-II. The delivery of radiotherapy is based on a treatment plan that defines all settings determining the radiation dose and location for each individual patient. Manual treatment planning is time consuming and results in heterogeneous plan quality between patients. In paper I, a system for automated IMRT treatment planning was developed based on the Erasmus-iCycle system, which generates treatment plans according to a pre-defined wish-list for the specific patient group. These plans are however not clinically deliverable, and Erasmus-iCycle was therefore coupled to the clinical treatment planning system at HUH to recreate the dose distributions. The developed system (“iCE”) generated plans with lower doses to the heart and esophagus compared to manually created, clinically delivered treatment plans.

---

In the second paper, iCE was exploited to improve treatment planning in the radiotherapy clinic at HUH. This was achieved by using iCE plans to train a clinically available commercial system for automated planning which is dependent on a library of input training plans. Paper II showed that training the system with plans from iCE improved the output plans compared to training with manually created plans. This knowledge is important because most centers using such systems for automated planning use manually created plans for training, thereby potentially generating suboptimal plans for many future patients.

In paper III, we investigated the effect of patients holding their breath while receiving radiotherapy. With similar target coverage and inter-fraction robustness, DIBH reduced the lung dose for around 90% and heart dose for around 70% of the patients compared to FB. Heart sparing depended on tumor position. The autoplanning system developed in paper I was applied to ensure bias-free generation of high-quality treatment plans for this study.

In the last two studies we investigated proton therapy for LA-NSCLC. Paper IV compared different optimization techniques for pencil beam scanning proton therapy with regard to target and OAR doses and robustness. 3D robust intensity-modulated proton therapy (IMPT) was the preferred technique because OAR doses were reduced with minimal loss of robustness compared to single-field optimized and 4D robust plans. This technique was therefore used in paper V.

In paper V, the methods were combined: We implemented a system for autoplanning of IMPT and used it to compare DIBH and FB also in proton therapy. DIBH reduced lung dose compared to FB, and regardless of breathing technique, OAR doses were far lower in IMPT than IMRT.

Overall, this thesis has provided knowledge that can improve radiotherapy of LA-NSCLC. With proper training or tuning, autoplanning has great potential for ensuring high and homogeneous plan quality between patients. DIBH can reduce the risk of side effects in both IMRT and IMPT. IMPT is costly and technically demanding but has potential to drastically reduce OAR doses compared to photon therapy. The results from this thesis have already had a direct impact in our clinic;



autoplanning for IMRT and routine use of DIBH for LA-NSCLC has already been or will be implemented in the clinic at HUH due to this work.

---

## Abstract in Norwegian

Pasienter med lokalavansert ikke-småcellet lungekreft (LA-NSCLC) har svulster som er store, vokser inn i andre strukturer i brystkassen, og/eller har spredt seg til regionale lymfeknuter. Disse pasientene er som oftest ikke kandidater for kirurgi, og standardbehandlingen er stråleterapi kombinert med kjemoterapi, med påfølgende immunterapi for utvalgte pasienter.

Intensitetsmodulert stråleterapi med fotoner (IMRT) i fripust er standard teknikk for stråleterapi for pasienter med LA-NSCLC. På grunn av store behandlingsvolum som ligger i nærheten av viktige risikoorganer får pasientene ofte bivirkninger av behandlingen. Bivirkninger av strålingen, som stråleindusert lungebetennelse og hjertesykdom, kan være alvorlige og potensielt dødelige.

Målet for dette prosjektet var å undersøke potensialet for å redusere risikoorgandoser og risikoen for bivirkninger i stråleterapi av LA-NSCLC ved bruk av ulike metoder: automatisk doseplanlegging, dyp innpust (DIBH) og protonterapi. Prospektivt innsamlet bildedata både fra før og underveis i strålebehandlingen ble brukt i fem ulike simuleringsstudier.

I artikkel I-II undersøkte vi automatisk doseplanlegging for IMRT. Stråleterapi leveres basert på en doseplan som definerer alle innstillinger som bestemmer hvor og hvor mye stråling som gis hver enkelt pasient. Manuell doseplanlegging er tidkrevende og gir varierende plankvalitet mellom pasienter. I artikkel I utviklet vi et system for automatisk doseplanlegging basert på Erasmus-iCycle, et system som genererer doseplaner ut fra en forhåndsdefinert «ønskeliste» for den aktuelle pasientgruppen. Disse planene er ikke klinisk leverbare, og Erasmus-iCycle ble derfor koblet sammen med det kliniske doseplansystemet som brukes på Haukeland Universitetssykehus (HUH) slik at dosefordelingene kunne gjenskapes der. Systemet vi utviklet («iCE») genererte planer med lavere dose til hjerte og spiserør sammenlignet med manuelt planlagte, kliniske leverte doseplaner.

I den andre studien dro vi nytte av iCE for å forbedre doseplanlegging i stråleterapiklinikken ved HUH. Dette gjorde vi ved å bruke iCE-planer for å «trene»

et kommersielt tilgjengelig system for automatisk doseplanlegging som er avhengig av et bibliotek med treningsplaner. Artikkel II viste at når dette systemet ble trent med iCE-planer genererte det bedre doseplaner enn når det ble trent med manuelle planer. Dette er viktig kunnskap fordi de fleste klinikker som bruker denne typen systemer for automatisk doseplanlegging bruker manuelle planer til trening, og dermed potensielt genererer suboptimale planer for mange framtidige pasienter.

I artikkel III undersøkte vi effekten av at pasientene holder pusten mens de får strålebehandling. Med tilsvarende målvolumsdekning og robusthet mellom fraksjoner reduserte DIBH lungedosen for rundt 90 % og hjertedosen for rundt 70 % av pasientene sammenlignet med fripust. Sparing av hjertet var avhengig av svulstens posisjon. Vi brukte systemet for automatisk doseplanlegging utviklet i artikkel I for å sikre doseplaner av høy kvalitet uten påvirkning av eventuell partiskhet hos en menneskelig doseplanlegger.

I de to siste studiene undersøkte vi protonterapi for LA-NSCLC. Artikkel IV sammenlignet ulike optimeringsteknikker for moderne protonterapi («pencil beam scanning») med hensyn til dose til målvolument og risikoorganer samt robusthet. 3D-robust intensitetsmodulert protonterapi (IMPT) kom best ut på grunn av reduksjon i risikoorgandoser sammen med minimalt tap av robusthet sammenlignet med enkeltfeltoptimerte og 4D-robuste planer. Denne teknikken ble derfor brukt i artikkel V.

I artikkel V kombinerte vi metodene: Vi implementerte et system for automatisk doseplanlegging av IMPT og brukte det for å sammenligne DIBH og fripust også i protonterapi. DIBH reduserte lungedosen sammenlignet med fripust, og uavhengig av pusteteknikk var risikoorgandosene langt lavere i IMPT enn IMRT.

Totalt sett har dette doktorgradsarbeidet gitt kunnskap som kan forbedre stråleterapi av LA-NSCLC. Med god trening eller innstilling har automatisk doseplanlegging stort potensial for å sikre høy og homogen plankvalitet mellom pasienter. DIBH kan redusere risikoen for bivirkninger i både IMRT og IMPT. IMPT er kostbart og teknisk krevende, men har potensial til å redusere risikoorgandoser drastisk sammenlignet med fotonterapi. Resultatene i denne avhandlingen har

---

allerede hatt direkte innvirkning i vår klinikk; automatisk doseplanlegging for IMRT og rutinemessig bruk av DIBH for LA-NSCLC har eller vil snart bli tatt i bruk i klinikken på HUH på grunn av dette arbeidet.

## List of Publications

Papers included in this thesis:

- Paper I            **Fjellanger K**, Hysing LB, Heijmen BJM, Pettersen HES, Sandvik IM, Sulen TH, Breedveld S, Rossi L. *Enhancing Radiotherapy for Locally Advanced Non-Small Cell Lung Cancer Patients with iCE, a Novel System for Automated Multi-Criterial Treatment Planning Including Beam Angle Optimization*. *Cancers* (Basel). 2021 Nov 13;13(22):5683.
- Paper II            **Fjellanger K**, Hordnes M, Sandvik IM, Sulen TH, Heijmen BJM, Breedveld S, Rossi L, Pettersen HES, Hysing LB. *Improving knowledge-based treatment planning for lung cancer radiotherapy with automatic multi-criteria optimized training plans*. *Acta Oncol*. 2023 Aug 17:1-7.
- Paper III           **Fjellanger K**, Rossi L, Heijmen BJM, Pettersen HES, Sandvik IM, Breedveld S, Sulen TH, Hysing LB. *Patient selection, inter-fraction plan robustness and reduction of toxicity risk with deep inspiration breath hold in intensity-modulated radiotherapy of locally advanced non-small cell lung cancer*. *Front Oncol*. 2022 Aug 30;12:966134.
- Paper IV            Boer CG, **Fjellanger K**, Sandvik IM, Ugland M, Engeseth GM, Hysing LB. *Substantial Sparing of Organs at Risk with Modern Proton Therapy in Lung Cancer, but Altered Breathing Patterns Can Jeopardize Target Coverage*. *Cancers* (Basel). 2022 Mar 8;14(6):1365.
- Paper V            **Fjellanger K**, Heijmen BJM, Breedveld S, Sandvik IM, Hysing LB. *Deep inspiration breath hold in intensity modulated proton therapy of locally advanced lung cancer - a dose and robustness analysis*. Submitted to *Radiotherapy and Oncology*.

Papers I-IV are open access under the Creative Commons Attribution (CC BY) 4.0 license. The use, distribution and reproduction is permitted provided the original work is properly cited.

---

## Conference contributions

Presentations at international medical physics conferences related to this thesis:

1. **Fjellanger K**, Hysing LB, Heijmen BJM, Pettersen HES, Sandvik IM, Sulen TH, Breedveld S, Rossi L. *iCycle-Eclipse: a novel approach to automated multi-criterial treatment planning*. European Society for Radiotherapy and Oncology (ESTRO), August 2021, Madrid, Spain/online (poster presentation).
2. **Fjellanger K**, Hysing LB, Heijmen BJM, Pettersen HES, Sandvik IM, Sulen TH, Breedveld S, Rossi L. *Advantages of DIBH in IMRT of locally advanced NSCLC systematically investigated with autoplanning*. ESTRO, May 2022, Copenhagen, Denmark (oral presentation).
3. **Fjellanger K**, Hysing LB, Heijmen BJM, Pettersen HES, Sandvik IM, Sulen TH, Breedveld S, Rossi L. *Integrated beam angle optimization in IMRT autoplanning for lung cancer*. ESTRO, May 2022, Copenhagen, Denmark (poster presentation).
4. **Fjellanger K**, Rossi L, Heijmen BJM, Pettersen HES, Sandvik IM, Breedveld S, Sulen TH, Hysing LB. *Inter-fraction plan robustness and reduction of toxicity risk with deep inspiration breath hold in intensity-modulated radiotherapy of locally advanced non-small cell lung cancer*. Nordic Association for Clinical Physics (NACP), March 2023, Reykjavik, Iceland (oral presentation).
5. **Fjellanger K**, Rossi L, Heijmen BJM, Pettersen HES, Sandvik IM, Breedveld S, Sulen TH, Hysing LB. *Patient selection for DIBH radiotherapy of locally advanced non-small cell lung cancer*. NACP, March 2023, Reykjavik, Iceland (poster presentation).
6. **Fjellanger K**, Rossi L, Heijmen BJM, Pettersen HES, Sandvik IM, Breedveld S, Sulen TH, Hysing LB. *Patient selection for DIBH radiotherapy of locally advanced non-small cell lung cancer*. ESTRO, May 2023, Vienna, Austria (oral presentation).

## Abbreviations

3D-CRT	3D Conformal RadioTherapy
AET	Acute Esophageal Toxicity
AIP	Average Intensity Projection
BAO	Beam Angle Optimization
CBCT	Cone Beam CT
CLIN	CLINical
CT	Computed Tomography
CTV	Clinical Target Volume
DIBH	Deep Inspiration Breath Hold
DVH	Dose-Volume Histogram
EMC	Erasmus Medical Center
FB	Free Breathing
GTV	Gross Tumor Volume
HUH	Haukeland University Hospital
iCE	iCycle-Eclipse
IGTV	Internal Gross Target Volume
IMPT	Intensity-Modulated Proton Therapy
IMRT	Intensity-Modulated Radiotherapy
LA-NSCLC	Locally Advanced Non-Small Cell Lung Cancer
MCO	Multi-Criteria Optimization
NSCLC	Non-Small Cell Lung Cancer
NTCP	Normal Tissue Complication Probability
OAR	Organ At Risk
PBS-PT	Pencil Beam Scanning Proton Therapy
PSPT	Passive Scattering Proton Therapy
PTV	Planning Target Volume
RP	Radiation Pneumonitis
RTT	Radiation Therapist
SFUD	Single-Field Uniform Dose
TPS	Treatment Planning System
VMAT	Volumetric Modulated Arc Therapy

---

# Contents

Scientific environment .....	iii
Acknowledgements.....	iv
Abstract in English .....	vi
Abstract in Norwegian .....	ix
List of Publications .....	xii
Conference contributions.....	xiii
Abbreviations .....	xiv
Contents .....	xv
<b>1. Introduction .....</b>	<b>1</b>
1.1 <i>Locally advanced non-small cell lung cancer</i> .....	1
1.1.1 Treatment of locally advanced NSCLC .....	2
1.2 <i>Radiotherapy with photons and protons</i> .....	3
1.2.1 Photon therapy .....	3
1.2.2 Proton therapy .....	3
1.2.3 Robustness .....	4
1.2.4 Radiotherapy side effects .....	5
1.3 <i>Radiotherapy treatment planning</i> .....	6
1.4 <i>Automated treatment planning</i> .....	8
1.5 <i>Respiratory gating</i> .....	9
<b>2. Aims of the thesis.....</b>	<b>11</b>
<b>3. Material and methods.....</b>	<b>13</b>
3.1 <i>Patients</i> .....	13
3.2 <i>Patient material</i> .....	13
3.3 <i>Clinical radiotherapy treatment</i> .....	14
3.4 <i>Software</i> .....	15



---

3.5	<i>IMRT treatment planning</i> .....	16
3.5.1	Manual IMRT treatment planning.....	16
3.5.2	Automated IMRT treatment planning.....	16
3.6	<i>Proton therapy treatment planning</i> .....	17
3.6.1	Manual proton therapy treatment planning.....	18
3.6.2	Automated IMPT treatment planning.....	18
3.7	<i>Data analysis</i> .....	19
3.7.1	Dose-volume parameters.....	19
3.7.2	NTCP .....	20
3.7.3	Statistics .....	21
3.8	<i>Ethical considerations</i> .....	21
<b>4.</b>	<b>Summary of results</b> .....	<b>23</b>
4.1	<i>Patients and images</i> .....	23
4.2	<i>Paper I</i> .....	25
4.3	<i>Paper II</i> .....	27
4.4	<i>Paper IV</i> .....	28
4.5	<i>Papers III and V</i> .....	29
<b>5.</b>	<b>Discussion</b> .....	<b>35</b>
5.1	<i>Main issues and findings</i> .....	35
5.1.1	Autoplanning.....	35
5.1.2	DIBH .....	36
5.1.3	Proton therapy .....	38
5.2	<i>Benefits of the investigated methods</i> .....	40
5.2.1	Autoplanning.....	40
5.2.2	DIBH .....	40
5.2.3	Proton therapy .....	41
5.3	<i>Resource requirements of the investigated methods</i> .....	41
5.3.1	Autoplanning.....	42
5.3.2	DIBH .....	42
5.3.3	Proton therapy .....	43
5.4	<i>Patient safety in implementation of new methods</i> .....	43
5.4.1	Autoplanning.....	43
5.4.2	DIBH .....	44

---

5.4.3	Proton therapy .....	45
5.5	<i>Methodological considerations</i> .....	46
5.6	<i>Limitations</i> .....	47
5.6.1	NTCP models .....	47
5.6.2	Autoplanning.....	47
5.6.3	Proton therapy optimization.....	48
5.6.4	Planner bias.....	48
5.7	<i>Strengths</i> .....	49
5.7.1	Number of patients.....	49
6.	<b>Conclusions</b> .....	51
7.	<b>Future perspectives</b> .....	53
	<b>References</b> .....	55
	<b>Publications</b> .....	63



# 1. Introduction

Cancer is a group of diseases characterized by uncontrolled cell growth which can spread to other parts of the body (metastasize). In Norway, more than 38 000 people were diagnosed with cancer in 2022, of which almost 10% lung cancer [1]. Lung cancer is the cancer that takes most lives, both in Norway and worldwide [2].

Radiotherapy is one of the main types of cancer treatment, along with surgery, chemotherapy and immunotherapy. 50% of cancer patients need radiotherapy as part of their treatment [3]. The goal in radiotherapy is to deliver the prescribed radiation dose to the tumor while damaging as little healthy tissue as possible.

## 1.1 Locally advanced non-small cell lung cancer

There are two main types of lung cancer: small cell and non-small cell. Non-small cell accounts for around 80%-85% of lung cancers and is usually less aggressive than small cell lung cancer.

In stage I non-small cell lung cancer, the tumor is  $<3$  cm in the greatest dimension and there is no lymph node metastasis. In stage II, the tumor can be up to 7 cm or there can be metastasis in nearby lymph nodes. Stage III is often referred to as locally advanced disease, and is characterized by one or more of the following:

- Primary tumor  $>7$  cm
- Primary tumor invading intrathoracic structures such as the diaphragm, mediastinum, heart or esophagus
- Separate tumor nodules in a different ipsilateral lobe than the primary tumor
- Spread to regional lymph nodes

There is large heterogeneity in anatomy between patients with stage III NSCLC (Figure 1). In stage IV there is distant metastasis [4].



Figure 1. Examples of patients studied in this thesis. Left: Stage IIIA NSCLC, with a 1.6 cm primary tumor in the left lower lobe and lymph node metastases in the hilar and superior mediastinal nodes. Right: Stage IIIC NSCLC, with a 10.5 cm primary tumor in the left upper lobe and lymph node metastases in the hilar, superior mediastinal, subcarinal, aortic and low cervical nodes. The gross tumor volume (GTV) is shown in red, heart in yellow, esophagus in brown, spinal canal in cyan and lungs in shaded blue.

### 1.1.1 Treatment of locally advanced NSCLC

While surgery can be an option for selected patients with stage IIIA NSCLC, most patients with stage III NSCLC have unresectable disease and receive radiotherapy as part of their treatment. Treatment for these patients has evolved over the last decades, slowly improving survival. Adding cisplatin based chemotherapy to radiotherapy gave an absolute benefit in survival of 4% at two years and 2% at five years [5], and changing chemoradiotherapy from sequential to concomitant improved 5-year overall survival from 10.6% to 15.1% due to reduction in locoregional progression [6]. Changing radiotherapy technique from 3D conformal radiotherapy (3D-CRT) to intensity-modulated radiotherapy (IMRT) did not impact survival or local control but reduced the rate of grade  $\geq 3$  radiation pneumonitis (RP) [7].

The current standard of care for inoperable locally advanced NSCLC (LA-NSCLC) is concurrent chemotherapy and radiotherapy [8], and external beam photon radiotherapy delivered as IMRT or volumetric modulated arc therapy (VMAT) is the most common radiotherapy technique. Following the success of the PACIFIC trial, immunotherapy is administered after chemoradiotherapy for a subgroup of patients (PD-L1  $\geq 1\%$  and no disease progression after chemoradiotherapy according to

---

Norwegian recommendations) [9]. However, even the most successful treatment so far has only achieved a 5-year overall survival of 42.9% and progression-free survival of 33.1% in stage III NSCLC [9]. Local tumor control is still suboptimal, but the possibility for radiotherapy dose escalation is limited by severe and potentially deadly treatment-related toxicity [10].

## **1.2 Radiotherapy with photons and protons**

Ionizing radiation consists of charged (directly ionizing) or uncharged (indirectly ionizing) particles with enough energy to create ionizations in a medium. When ionizing radiation interacts with cells in the body it can cause lethal damage to the deoxyribonucleic acid (DNA). In radiotherapy, ionizing radiation is used to kill cancer cells.

### **1.2.1 Photon therapy**

The most common radiotherapy is external beam radiotherapy with photons delivered by a linear accelerator (linac). In the linac, electrons are generated and accelerated before colliding with a high-Z material target to produce x-ray photons. In the head of the linac (gantry), the photon beam is shaped by a multileaf collimator and directed towards the patient.

When photons interact with tissue, energy is transferred to electrons or positrons which in turn deposit energy through interactions of their electric field with the electric fields of atoms they pass. Photons therefore deposit the most radiation dose (energy per mass) in the region of one to a few centimeters inside the body, and the dose gradually decreases with depth. To achieve a high dose in a deep-seated target volume and lower dose in surrounding tissues, the radiation can be delivered from several different angles or as arc therapy where the gantry rotates around the patient.

### **1.2.2 Proton therapy**

Protons interact differently with tissue than photons. They give a relatively low entrance dose, deposit most of the energy at a depth in the patient body determined by

their energy, then stop sharply and do not deliver any exit dose. This can be advantageous because the dose to healthy tissue, particularly behind the target volume, can be substantially reduced compared to photon therapy.

In proton radiotherapy, protons are accelerated in a cyclotron or synchrotron and emitted as a narrow so-called pencil beam. The range of the protons is selected either by adjusting the beam energy output from the accelerator, or by introducing degrading material in the beam. In passive scattering proton therapy (PSPT), the beam is spread by a scattering material to cover the target volume. Pencil beam scanning proton therapy (PBS-PT) is a modern delivery method where the pencil beam is magnetically scanned across the target volume. This allows for more conformal dose distributions than in photon therapy and PSPT, but also increases sensitivity to factors such as changes in tissue density (range) and breathing motion. PBS-PT can be optimized so that all the fields cover the target volume with uniform dose (single-field uniform dose, SFUD) or that each field contributes differently to different areas of the target volume, while all fields in sum give a homogeneous target dose (intensity-modulated proton therapy, IMPT).

The number of proton facilities has increased steadily the last years and there are now more than 100 operational centers around the world [11]. Two centers will open in Norway in 2024 (Oslo) and 2025 (HUH). While proton therapy is not a standard treatment for lung cancer, it is used both in clinical studies and in other settings such as within the model-based selection framework in the Netherlands; there, patients can qualify for proton therapy based on comparative treatment planning and estimated reductions in the risk of side effects [12].

### 1.2.3 Robustness

Different factors can cause the delivered radiation dose to differ from the planned dose, such as tumor growth or shrinkage, weight changes, changes in tissue density (e.g. atelectasis), positioning variations and intra-fraction motion (e.g. breathing motion). The treatment is considered robust if any variations in the target and OAR doses are within acceptable limits.

---

Anatomical and positioning changes can have more impact on the delivered dose in proton therapy than photon therapy [13]. Proton dose distributions are more conformal with steep dose gradients, and in IMPT the individual fields can have steep gradients within the target volume. There is also a range uncertainty originating from the conversion from Hounsfield units in CT images to stopping power of protons. Robust optimization algorithms available in commercial treatment planning systems (TPSs) can incorporate uncertainties related to positioning shifts and range uncertainties (3D) as well as breathing motion (4D) in the treatment plan optimization (section 1.3).

#### 1.2.4 Radiotherapy side effects

Radiotherapy destroys cancer cells but will inevitably also damage healthy tissue near the tumor, and this can induce short- and long-term side effects. The probability of both tumor control and side effects increases with radiation dose [14].

In radiotherapy of LA-NSCLC, side effects due to radiation of the lungs, heart and esophagus are relatively common [15]. The risk of side effects can limit the dose that can be delivered to the tumor and may therefore hinder tumor control. Radiation pneumonitis (RP) is a severe side effect that can cause interruption of treatment, preclude immunotherapy or even be deadly. The incidence increases with increasing lung dose, and there is no “safe” threshold below which RP does not occur. According to the QUANTEC report, keeping the mean lung dose  $\leq 20$  Gy and the lung  $V_{20\text{Gy}} \leq 30\%$  limits the risk of RP to  $\leq 20\%$  [16]. Radiation can also cause chronic lung fibrosis, a late side effect with symptoms such as progressive shortness of breath and coughing [17].

Focus on the effects of radiation on the heart has increased in recent years, as IMRT has increased the possibility of heart sparing and more lung cancer patients survive the first years after radiotherapy. In particular, attention increased after the RTOG0617 dose escalation trial which surprisingly showed worse survival for patients in the high-dose arm, where higher heart dose emerged as a contributing factor which increased risk of death [10]. Radiation-induced cardiac toxicities include stenosis of valves or arteries, myocardial atrophy, constrictive pericarditis, ischemia



and heart failure. Heart dose is associated with overall survival for LA-NSCLC patients [18]. While consistent dose limits have not been defined, mean heart dose,  $V_{5\text{Gy}}$  and  $V_{30\text{Gy}}$  have been associated with the risk of cardiac toxicity [19].

Acute esophagitis is a common side effect after radiotherapy of LA-NSCLC, with symptoms such as throat pain and swallowing problems. Correlations to both the mean and maximum esophagus dose have been reported [20,21]. Esophageal perforation and fistula are rare but potentially deadly side effects.

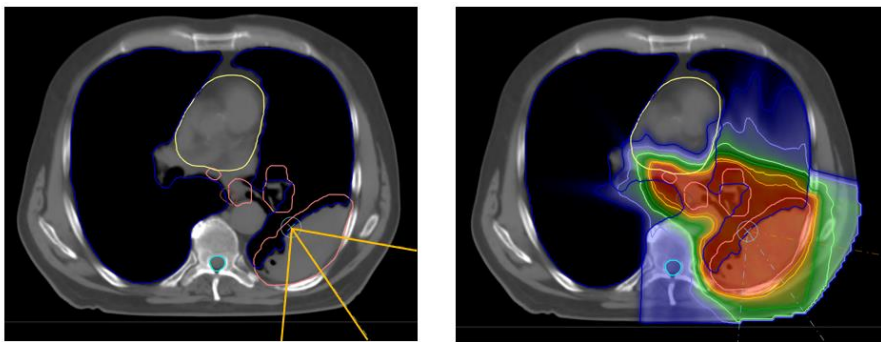
Radiation myelopathy (spinal cord injury) is a rare but severe late side-effect with symptoms such as pain, sensory deficits or paralysis. A commonly used tolerance dose of 50 Gy gives an incidence of myelopathy of 0.2% [22]. Radiation can also induce neuropathy in the brachial plexus, with symptoms such as pain, lymphedema and progressive sensory-motor deficits of the arm. The risk is low when the brachial plexus maximum dose is kept below 66 Gy [23]. Other side effects after radiotherapy of LA-NSCLC include fatigue and lymphopenia.

The individual risk of a specific radiation-induced side effect can be estimated using a normal tissue complication probability (NTCP) model. NTCP models are mathematical models that estimate the risk of side effects based on planned radiation dose in OARs, and other patient, disease and treatment variables.

### **1.3 Radiotherapy treatment planning**

A radiotherapy treatment plan defines all aspects of the treatment for the individual patient, such as the radiation type and energy, the physical arrangement and shape of the radiation beams, and the amount of radiation given from each angle. Treatment planning is usually performed by a radiation therapist (RTT) or medical physicist. The goal is to create a plan that delivers the prescribed dose to the target volume and as little as possible to surrounding healthy tissue. In particular, organs at risk (OARs) linked to radiation-induced complications must be spared when possible, and most of these organs have dose constraints (limit for acceptable risk of complications).

The treatment planning process, performed in a computerized TPS, is illustrated in Figure 2. A CT scan of the patient with the target volume (tumor with margins for subclinical disease, motion etc.) and OARs defined is used as basis. For each patient, the planner must decide the beam configuration (how many radiation beams and which angles to irradiate from) and define a list of constraints and objectives for the dose in different structures. A constraint is a fixed limit that cannot be violated, while an objective is a goal that is adapted to the anatomy of the individual patient and given a certain priority. The resulting mathematical optimization problem is solved to create a radiation dose distribution. The solution to the optimization problem is mathematically optimal, but not clinically optimal for the patient unless the beam configuration, constraints and objectives are optimal. The planner evaluates the dose distribution and tries to identify potential improvements.



Function	Constraint	Dose	ROI	Description	Robust	Weight
■ Physical composite objective						
Uniform dose		Plan (RBE)	CTV	Uniform dose 66.00 Gy (RBE)	★	500.00
Max dose		Plan (RBE)	BODY	Max dose 66.50 Gy (RBE)		1500.00
Dose fall-off		Plan (RBE)	BODY	Dose fall-off [H]66.00 Gy (RBE) [L]10.00 Gy (RBE), Low dose distance 1.50 cm		5.00
Max EUD		Plan (RBE)	Heart	Max EUD 4.34 Gy (RBE), Parameter A 1		5.00
Max EUD		Plan (RBE)	Lungs	Max EUD 9.74 Gy (RBE), Parameter A 1		5.00
Max EUD		Plan (RBE)	Esophagus	Max EUD 25.14 Gy (RBE), Parameter A 1		5.00
Max dose		Plan (RBE)	SpinalCanal	Max dose 22.96 Gy (RBE)		5.00

1) CT scan with target volumes (red) and OARs defined

2) Definition of beam configuration

3) Definition of planning objectives and constraints

4) Computerized optimization of dose distribution

5) Evaluation of dose distribution

Repeat until satisfied

Figure 2. The treatment planning process. Upper left: CT scan with target volume (pink) and OARs defined. Yellow lines show the selected beam angles. Upper right: Optimized treatment plan with radiation dose shown in colors from red (high) to blue (low). Center: Individual planning objectives for the clinical target volume (CTV), OARs and patient body. Bottom: Steps in the treatment planning process.

They adjust the beams and/or planning objectives and restart the optimization. This loop is continued until the planner does not see room for improvement. The treatment plan is then evaluated by an oncologist, who approves the plan for treatment or requests changes.

Manual treatment planning is a trial-and-error process, where the planner tries to make improvements to the dose distribution until they are satisfied or out of time. The number of possible combinations of beam angles, constraints, objectives and priorities is countless, and the planner has no way of knowing when an optimal dose distribution is achieved. The resulting dose distribution is therefore in general not optimal, and the quality is impacted by the skill and performance of the treatment planner [24–26].

## **1.4 Automated treatment planning**

Automated treatment planning, also called autoplanning, is gaining attention and popularity due to evidence of improved plan quality (reduced OAR doses), reduced inter-patient variation in plan quality and large time savings for the treatment planners, combined with better availability and performance of commercial solutions for photon therapy autoplanning [26]. With autoplanning, some or all tasks usually performed by the treatment planner are replaced by sophisticated computer algorithms.

There are several different strategies for autoplanning. Knowledge-based planning or machine learning planning systems predict the achievable dose for new patients based on previous treatment plans. Commercially available knowledge-based planning can give modest reductions in OAR doses for different diagnoses including LA-NSCLC [27–30]. However, the output depends on the input plans, which are usually manually planned and not optimal, and the systems are not applicable for new techniques or diagnoses when a set of high-quality previous plans is not available [31–36].

---

Other autoplanning systems are based on certain rules or characteristics that are indicative of an “ideal” dose distribution for each patient. The Erasmus-iCycle system for multi-criterial optimization (MCO), developed by our collaborators at the Erasmus Medical Center, creates a Pareto-optimal dose distribution based on a prioritized list (“wish-list”) of required and desired qualities [37]. Pareto-optimality describes a situation where no improvements can be made for any objective functions without deteriorating another. This system does not produce clinically deliverable treatment plans and must therefore be coupled to a clinical system [38,39]. Erasmus-iCycle can also perform beam angle optimization (BAO), where the optimal beam angles for each patient are determined based on the same wish-list. Another strategy in this category is scripted treatment planning, which can be implemented in various ways, e.g. to try and mimic the actions and assessments performed by human planners in a consistent way [40,41].

While autoplanning has become quite common in photon therapy and a number of papers have demonstrated benefits of autoplanning over manual planning, there is less experience with autoplanning in proton therapy. Some studies have reported successful implementation of different autoplanning methods for specific diagnoses and settings, but the improvements in OAR doses seen with autoplanning in photon therapy has so far not been demonstrated in proton therapy [42–46].

## **1.5 Respiratory gating**

Radiotherapy in the thorax and abdomen is influenced by breathing; attempting to hit a moving target can be a challenge. Large margins can be required to ensure the target volume receives the planned dose in different breathing phases, increasing dose to OARs. Respiratory gating is used to monitor or alter the patients’ breathing pattern during radiotherapy delivery and adapt the treatment to the breathing. With gating in free breathing, the patient breathes normally but radiation is only delivered in a specific part of the breathing cycle, when the tumor is in a pre-defined position. With gating in breath hold, radiation is delivered while the patient holds their breath either during inspiration or expiration.

Inspiration or deep inspiration breath hold (DIBH) is the most commonly used respiratory gating technique [47]. In DIBH, the patient holds their breath at a specific level of inspiration during radiotherapy delivery. Different approaches can be used for monitoring and reproducing the breathing level: tracking an external marker (e.g. a box placed on the patient's chest), tracking the patient surface directly (surface tracking), or spirometry (a mechanical device with a mouthpiece measuring air flow). A screen where the current and desired breathing level are visualized can help the patient achieve the correct level. Compared to gating in free breathing or expiration breath hold, DIBH has the potential additional advantage of increasing the separation between the target volume and OARs. It is however more demanding for the patient, and patients with cognitive impairments or severe comorbidities may be unable to carry out treatment in DIBH.

There have been some studies showing promise for DIBH in LA-NSCLC in terms of patient compliance [48], reproducibility [48,49] and OAR dose sparing [50]. Still, the use of DIBH in radiotherapy of LA-NSCLC is limited: in a survey of 200 radiotherapy centers, 17% used DIBH for lung cancer and most of them used it for less than 25% of lung cancer patients [47]. This motivates further studies to validate potential benefits of DIBH, also with respect to different sub-groups of patients.

## **2. Aims of the thesis**

The overall aim of this thesis was to identify methods that can improve radiotherapy of LA-NSCLC by reducing the radiation dose to OARs and thereby the risk of complications from radiotherapy.

Specific objectives of each paper were:

### **Papers I and II**

- Develop a system for autoplanning taking advantage of the MCO and BAO in Erasmus-iCycle while creating clinically deliverable plans (paper I).
- Use the autoplanning system to improve plan quality compared to manually created, clinically delivered plans, and investigate the impact of beam angles and beam number on plan quality (paper I).
- Use the generated autoplans to train and improve a system for knowledge-based treatment planning in clinical use at HUH (paper II).

### **Paper III**

- Compare FB and DIBH in IMRT of LA-NSCLC with focus on dose-volume parameters, NTCPs and inter-fraction robustness, and investigate which patients are most likely to benefit from DIBH.

### **Paper IV**

- Identify the best optimization technique for PBS-PT in terms of target coverage and OAR sparing with attention to delivery uncertainties and anatomical changes.

### **Paper V**

- Compare FB and DIBH in IMPT of LA-NSCLC with focus on dose-volume parameters, NTCPs and inter-fraction robustness, and compare FB and DIBH IMPT to FB and DIBH IMRT.

---

## 3. Material and methods

### 3.1 Patients

In all studies in this thesis, we have used prospectively collected data from patients treated at Haukeland University Hospital (HUH) between October 2019 and November 2022. Patients receiving radiotherapy with curative intent according to the protocol for LA-NSCLC were invited to participate. While most patients had stage III disease, stage II could also be included if the tumor was inoperable and not suited for stereotactic radiotherapy, and stage IV in case of oligometastatic disease where metastases could be treated separately, leaving a target volume in the lungs receiving radiotherapy with curative intent. One patient with stage IB that had an inoperable tumor due to the position in the main bronchus and received radiotherapy according to the protocol for LA-NSCLC was included.

### 3.2 Patient material

In the planning CT session prior to treatment, a 10-phase 4DCT, 3 DIBH CTs and a static CT with intravenous contrast were acquired for each patient. Imaging was performed on a Big Bore CT scanner (Philips Healthcare, Best, The Netherlands), using a Posirest-2 support device (Civco Radiotherapy, Coralville, USA) for fixation in the supine position with arms resting above the head. The breathing curve for the 4DCT was acquired using the Philips Bellows device. DIBH was performed with the Respiratory Gating for Scanners (RGSC) system (Varian Medical Systems, Palo Alto, USA), using a marker box placed on the sternum, 2-3 mm gating window and visual feedback. The patients practiced breath holds before image acquisition at the planning CT session.

Target volumes were defined by an oncologist and OARs by a treatment planner. Gross tumor volumes (GTVs) for the primary tumor and lymph nodes were delineated according to ESTRO guidelines [51]. For FB, the OARs and GTVs were delineated on the average intensity projection (AIP) of the 4DCT, and the internal GTV (IGTV) incorporated the GTV positions in all 4DCT phases. For DIBH, the



OARs and GTVs were delineated on one of the DIBH CTs, and the IGTV incorporated the GTV positions in the two other DIBH CTs. For both FB and DIBH, the clinical target volume (CTV) was defined by expanding the IGTV by 5 mm without extending into uninvolved organs such as bone, heart, esophagus and major vessels. A 5 mm isotropic margin from the CTV was used to define the planning target volume (PTV). As OARs, the lungs, heart, esophagus, spinal canal and brachial plexus (if relevant) were delineated according to RTOG guidelines [52].

Additionally, a repeat 4DCT and DIBH CT were acquired during the first week (w1, usually fraction 2-3) and third week (w3, usually fraction 13-14) of treatment. The time point for the w1 scan was selected to get an impression of inter-fraction variations before major anatomical changes are expected. The time point for the w3 scan was selected to assess the impact of anatomical changes and need for treatment adaptation while there is still time to adapt the treatment. Target volumes and OARs were re-delineated by an oncologist and a treatment planner, respectively, on the repeat CTs following the procedure described above. However, in w1 and w3 only one DIBH CT was acquired; the three DIBH CTs at planning were used to establish patient-specific IGTV margins, and the repeated CTs were used to evaluate if these were appropriate for the actual situation during treatment. Hence no IGTV was delineated on w1 and w3 DIBH CTs.

Patient and disease characteristics were recorded by an oncologist at inclusion, and treatment characteristics were recorded by the candidate at completion of radiotherapy. These were used e.g. in NTCP calculations and to describe the patient population. The study did not include clinical follow-up after treatment.

### **3.3 Clinical radiotherapy treatment**

Clinical (CLIN) treatments were delivered with IMRT in FB as a standard. For some patients the oncologist chose treatment in DIBH instead, mainly due to high lung doses with FB. Most patients were treated with 6 IMRT beams. Based on patient-specific assessments, a few patients were treated with VMAT or 5 IMRT beams.

---

In accordance with national guidelines, the prescribed dose was 60 or 66 Gy for concomitant treatment and 66 or 70 Gy for sequential treatment (depending on lung function, lung dose and proximity of the brachial plexus to the PTV), delivered in 2 Gy daily fractions 5 days per week. The plans were normalized to the median PTV dose ( $PTV D_{\text{median}} = 100\%$ ).

Daily cone beam CTs (CBCTs) followed by table corrections with six degrees of freedom were used for online positioning. Automatic online matching with focus on bony structures was standard, but according to the adaptive protocol (“traffic light protocol”), CTV match could be used in case of deviations with attention to lymph node and spinal canal positions. The adaptive protocol provided guidance for when offline or online evaluations by a physicist and oncologist were required. Treatment plan adaptation(s) were performed for 13% of patients.

### 3.4 Software

The Eclipse system (Varian Medical Systems Inc., Palo Alto, USA) is used for clinical treatment planning for photon therapy at HUH. The RapidPlan system for automated knowledge-based treatment planning is integrated in Eclipse. All IMRT plans used in this thesis were created in Eclipse. For proton therapy planning, we used a research version of RayStation (RaySearch Laboratories, Stockholm, Sweden). The Erasmus-iCycle system for automated treatment planning is not commercially available but could be accessed for this project through our collaboration with Erasmus Medical Center. Erasmus-iCycle does not produce clinically deliverable plans and was therefore coupled to Eclipse (paper 1).

DVH Toolkit, an openly available python program developed by co-supervisor H. Pettersen, was used for tasks such as collection of dose-volume parameters and calculation of average dose-volume histograms (DVHs) [53]. SPSS Statistics v. 26 (IBM Corp., Armonk, USA) was used for statistical analyses.

## 3.5 IMRT treatment planning

### 3.5.1 Manual IMRT treatment planning

The manually created IMRT plans used as a reference in papers I-II were created by expert treatment planners as part of clinical routine, approved by the responsible oncologist and used for clinical treatment.

In the clinical treatment planning, there were maximum dose objectives for the spinal canal, brachial plexus and patient body. Additionally, the goal was to achieve sufficient target coverage and as low dose as possible to normal tissue, with the following order of priority: (1) PTV, (2) lungs, (3) heart, (4) esophagus, and (5) undefined normal tissue. Planning dose objectives are listed in Table 1. Cases where all objectives could not be fulfilled were evaluated individually by the oncologist. Possible actions could be to accept either reduced target dose in certain areas or higher OAR dose than the objective, change prescribed dose from 66 Gy to 60 Gy, change from FB to DIBH treatment, or change to palliative fractionation.

Table 1. Planning objectives for the PTV, OARs and normal tissue.  $D_p$  = prescribed dose.

<b>Volume</b>	<b>Dose objective</b>
PTV	$V_{95\%} > 98\%$
Lungs	$V_{5Gy} < 65\%$ $V_{20Gy} < 35\%$ $D_{mean} < 20$ Gy
Heart	$V_{30Gy} < 40\%$
Esophagus	$D_{mean} < 34$ Gy
Spinal canal	$D_{max} < 50$ Gy
Brachial plexus	$D_{max} < 66$ Gy
Patient body	$D_{max} < D_p \cdot 1.07$

### 3.5.2 Automated IMRT treatment planning

Two methods for automated IMRT planning were used in this thesis: iCE (papers I-III) and RapidPlan (paper II).

iCE (short for iCycle-Eclipse) is an in-house method developed in this thesis for mimicking Erasmus-iCycle treatment plans in Eclipse, thereby creating

---

deliverable plans with similar DVHs to the Pareto optimal Erasmus-iCycle plans. The idea behind iCE was to take advantage of RapidPlan functionality already existing in Eclipse. In RapidPlan, a patient-specific DVH is predicted and translated to OAR line objectives. These are used in plan optimization to approach the predicted DVH. Similarly in iCE, a patient-specific DVH is generated by Erasmus-iCycle and translated to OAR line objectives used in plan optimization. Line objectives are not accessible to the user in the Eclipse optimization interface. They can however be defined in an objective template outside Eclipse, which can be imported and used for plan optimization. A method for this was developed by the candidate in paper I, consisting of an empty Eclipse objective template and a Python script that transfers dose-volume data from a DVH into the objective template. The candidate also performed the wish-list creation and tuning in Erasmus-iCycle.

In paper II, two RapidPlan models were created and compared. One had a library containing manually created clinical plans, and the other iCE plans. The RapidPlan model creation was performed by master's student M. Hordnes under the supervision of the candidate.

### **3.6 Proton therapy treatment planning**

Treatment plans for proton therapy were created manually in paper IV and automatically in paper V. Both in manual and automated proton therapy planning, a relative biological effectiveness of 1.1 was assumed for protons. A density override representative for tumor tissue was used for the IGTV on the AIPs to avoid areas with a non-biological intermediate density (averaged between lung/air and tumor/soft tissue) [13].

For SFUD and IMPT plans, 3D robust optimization was applied for the CTV, and for the spinal canal if close to the CTV. A setup uncertainty of 5 mm in each direction and 3.5% range uncertainty resulted in 21 scenarios. With the minimax approach implemented in RayStation, the reference plan is evaluated in each uncertainty scenario, and in each iteration, the scenario with the currently worst objective value is optimized [54]. For 4D robust planning in paper IV, the same setup

and range uncertainty was applied to all 4DCT phases, resulting in 230 scenarios [55]. Deformable registration was used to delineate the CTV on each phase, so the CTV dose in all phases could be optimized during planning.

### 3.6.1 Manual proton therapy treatment planning

For paper IV, SFUD, IMPT and 4D robust IMPT plans were manually created by an experienced treatment planner (C. Boer). A generic IBA beam model was used. Each plan consisted of 2-3 coplanar fields with range shifters of 4 or 7.5 cm (same configuration in the 3 plans for each patient). Split fields with field-specific targets were not possible due to a limitation in the 4D robust optimization algorithm. The SFUD plan was created first followed by IMPT and 4DIMPT.

The process followed a set planning procedure: in the first round of optimization, there were only objectives for CTV coverage, dose fall-off around the CTV and maximum dose in the patient. The beam angles were evaluated, and if necessary, they were changed and a new optimization was performed. The dose distribution was evaluated and objectives for OARs were added. A new optimization was performed, the dose distribution was evaluated again, and the objectives were changed if they were achieved or if the function value (the relative weight put on that objective in the optimization) was low. This process of changing objectives and reoptimizing was continued until no more room for improvement was seen. Many rounds of optimization could be required and to speed up the process, a pencil beam algorithm was used for initial optimization, and Monte Carlo was used for a final optimization and computation of final dose.

### 3.6.2 Automated IMPT treatment planning

The candidate developed a Python script for automated IMPT treatment planning in RayStation, which was used to automatically generate all FB and DIBH IMPT plans used in paper V. The approach was inspired by the manual planning procedure described in section 3.6.1 and the main steps performed by the script were:

1. Add fixed objectives for CTV (uniform dose, robust) and patient body (max dose and dose fall-off around the CTV). Run optimization.

- 
2. Add personalized objectives for OARs based on achieved OAR doses in step 1. Run new optimization.
  3. If achieved dose for lungs, heart and/or esophagus is lower than objective, lower objective further, reset and run new optimization (starting from 2).
  4. Compute final dose.

Beam angles were manually selected prior to automated planning for each patient. Most patients had 3 co-planar fields with 30°-40° separation, while 4-5 co-planar fields with field specific targets were used in some cases with separated target volumes. The same beam configuration was used for the FB and DIBH plan for each patient, and to reduce bias the FB plan was created first for half the patients and the DIBH plan for the other half. A 4 cm range shifter was used for shallow targets. Machine settings for a Varian ProBeam system were used for planning and a Monte Carlo optimization algorithm was used in all steps. The differences in settings compared to paper IV are due to new possibilities after software updates in the two years between the treatment planning for these studies.

## 3.7 Data analysis

### 3.7.1 Dose-volume parameters

For comparison of treatment plans made with different techniques or strategies, a set of dose-volume parameters for targets and normal tissue were selected in collaboration with an oncologist based on available literature and recommendations:

- Target volume (PTV in photon therapy and CTV in robust optimized proton therapy)  $V_{95\%}$  (mainly) or  $D_{98\%}$
- Lungs  $D_{\text{mean}}$ ,  $V_{5\text{Gy}}$  and  $V_{20\text{Gy}}$
- Heart  $D_{\text{mean}}$ ,  $V_{5\text{Gy}}$  and  $V_{30\text{Gy}}$
- Esophagus  $D_{\text{mean}}$ ,  $V_{20\text{Gy}}$  and  $V_{60\text{Gy}}$
- The maximum dose in the patient body and spinal canal

While most or all OAR parameters above are reported in the papers, most emphasis is put on the  $D_{\text{mean}}$  to the lungs, heart and esophagus; these are for example used in several of the illustrations (see e.g. Figure 4). They were chosen to condensedly

represent the data as they are the most reported parameters and linked to the risk of complications (section 3.7.2).

### 3.7.2 NTCP

For NTCP calculations in papers II, III and V, we used the set of models that are in use for proton therapy patient selection in the Netherlands. The three selected models have been thoroughly evaluated and validated in that framework, and depend on the lung, heart and esophagus dose, respectively, along with other patient and treatment factors.

The NTCP for RP grade  $\geq 2$  was calculated using a QUANTEC model refined by Appelt et al. [12,56]:

$$NTCP = \frac{1}{1+e^{-S}} \text{ with } S = -4.12 + 0.138 \cdot MLD - 0.3711 \cdot (\text{Former smoker}) - 0.478 \cdot (\text{Current smoker}) + 0.8198 \cdot (\text{Co-morbidity}) + 0.6259 \cdot (\text{Tumor location}) + 0.5068 \cdot (\text{Old age}) + 0.47 \cdot (\text{Sequential chemo}),$$

where MLD is the mean lung dose in Gy and the other parameters are assigned value 1 or 0 according to Table 2.

Table 2. Variables in the NTCP model for radiation pneumonitis.

<b>Variable</b>	<b>Value = 1</b>	<b>Value = 0</b>
Former smoker	Yes	Never smoked/active smoker
Current smoker	Yes	Never smoked/stopped smoking
Co-morbidity <sup>1</sup>	Yes	No
Tumor location	Middle/lower lobe	Upper lobe
Old age	$\geq 63$ years	$< 63$ years
Sequential chemo	Yes	No

<sup>1</sup> Chronic obstructive pulmonary disease or other pre-existing lung disease.

The NTCP for 2-year mortality based on heart dose was calculated using a model developed by Defraene et al. and revised after external validation in several patient cohorts [12,57]:

$$NTCP = \frac{1}{1+e^{-S}} \text{ with } S = -1.3409 + 0.0590 \cdot \sqrt{GTV} + 0.2635 \cdot \sqrt{MHD},$$

where GTV is the combined GTV volume of the primary tumor and nodes in cm<sup>3</sup> and MHD is the mean heart dose in Gy.

The NTCP for acute esophageal toxicity (AET) grade  $\geq 2$  was calculated using a model developed by Wijsman et al. and revised after external validation in several patient cohorts [12,58]:

$$NTCP = \frac{1}{1+e^{-S}} \text{ with } S = -3.634 + 1.496 \cdot \ln(MED) - 0.0297 \cdot OTT,$$

where MED is the mean esophagus dose in Gy and OTT is the overall radiotherapy treatment time in days.

### 3.7.3 Statistics

The parameters evaluated and compared between techniques in the studies of this thesis were in general not all normally distributed. Non-parametric statistics were therefore applied. For comparison of two related samples, the two-tailed Wilcoxon signed-rank test was used (papers I-III, paper V). For comparison of three related samples in paper IV, the Friedman's test (non-parametric two-way analysis of variance by ranks) was used. Bonferroni correction was applied to adjust the  $p$ -value for multiple testing in post hoc analysis. In paper III, linear regression was used to test correlations between continuous variables.

## 3.8 Ethical considerations

The study was approved by the regional committee for medical and health research ethics in Western Norway (protocol code 2019/749) and all participants gave written informed consent. The patient data were pseudonymized by the candidate before they were used for research purposes (i.e., an anonymization key was stored on a research server with limited access).

Study participation entailed collection of image data (both routine images and extra study images) but not treatment intervention; the standard treatment was still IMRT in FB. However, since DIBH images were available through the study, it was



decided that these could be used for planning and treatment could be given in DIBH at the oncologist's discretion. This was mainly done for patients where lung dose constraints could not be met in FB without compromising target coverage.

Similarly, the repeat CTs taken for the study were not intended to be regularly evaluated and used for adaptive treatment, but in cases where RTTs or physicists were concerned about potential changes they were allowed to use the available images and delineations for recalculation and replanning.

## 4. Summary of results

### 4.1 Patients and images

Of 49 patients originally included, the curative treatment strategy was upheld after target delineation and treatment planning for 45 patients, and 26, 45, 38, 15 and 41 of these were used in papers I-V, respectively (Figure 3). Table 3 gives an overview of patient and treatment characteristics. Average age was 66 years (range 49-82) and average GTV volume was 106 cm<sup>3</sup> (range 13-1021).

44 patients had FB and DIBH images at planning, while one had only DIBH because of machine issues. Repeat FB and DIBH CTs from w1 and w3 were available for 43 and 40 patients. Some patients did not complete all scans due to poor condition or covid-19.

Table 3. Patient and treatment characteristics for the 45 patients in the study. Not all percentages add up to 100% due to rounding.

Characteristic		Number of Patients	
Stage	IB	1	2%
	IIA	1	2%
	IIB	2	4%
	IIIA	17	38%
	IIIB	18	40%
	IIIC	3	7%
	IVA	3	7%
Target volume	Primary tumor and lymph nodes	34	76%
	Primary tumor only	9	20%
	Lymph nodes only	2	4%
Primary tumor location (lobe)	Right upper	16	36%
	Right upper + middle	1	2%
	Right lower	8	18%
	Left upper	8	18%
	Left lower	10	22%
	No primary tumor	2	4%
Prescribed dose	60 Gy	15	33%
	66 Gy	29	64%
	70 Gy	1	2%
Chemotherapy	Concurrent	43	96%
	Sequential	2	4%
Breathing technique	Free breathing	32	71%
	Deep inspiration breath hold	13	29%



---

## 4.2 Paper I

### **Enhancing Radiotherapy for Locally Advanced Non-Small Cell Lung Cancer Patients with iCE, a Novel System for Automated Multi-Criterial Treatment Planning Including Beam Angle Optimization**

In this paper we compared automated treatment planning with the developed iCE system to manual treatment planning for 26 patients, and exploited iCE to investigate the effect of beam configuration and number on OAR sparing.

Overall, the iCE plans were clearly superior to the manually created clinical (CLIN) plans. The PTV coverage and lung doses were similar, while iCE reduced the median heart  $D_{\text{mean}}$  from 9.0 Gy to 8.1 Gy ( $p = 0.02$ ) and the median esophagus  $D_{\text{mean}}$  from 20.3 Gy to 18.5 Gy ( $p = 0.02$ ) compared with CLIN. Heart  $V_{30\text{Gy}}$  and esophagus  $V_{20\text{Gy}}$  were also reduced. Substantial OAR sparing with iCE was seen for individual patients, with reductions of more than 5 Gy in the  $D_{\text{mean}}$  observed for both heart and esophagus compared to CLIN (Figure 4).

The BAO in iCE contributed to the observed OAR dose reductions. In general, the beam configurations used in the CLIN plans had most weight on the anterior-posterior direction, with little variation in the angles chosen for each patient. In contrast, the optimized beam angles in the iCE plans were well dispersed across the candidate beam space, revealing a large difference in optimal angles between patients (Figure 5). In addition to 6-beam IMRT plans (as used clinically), iCE-plans with 4 and 8 beams were generated. Median OAR doses decreased with an increasing number of beams, but the effect varied considerably between patients.

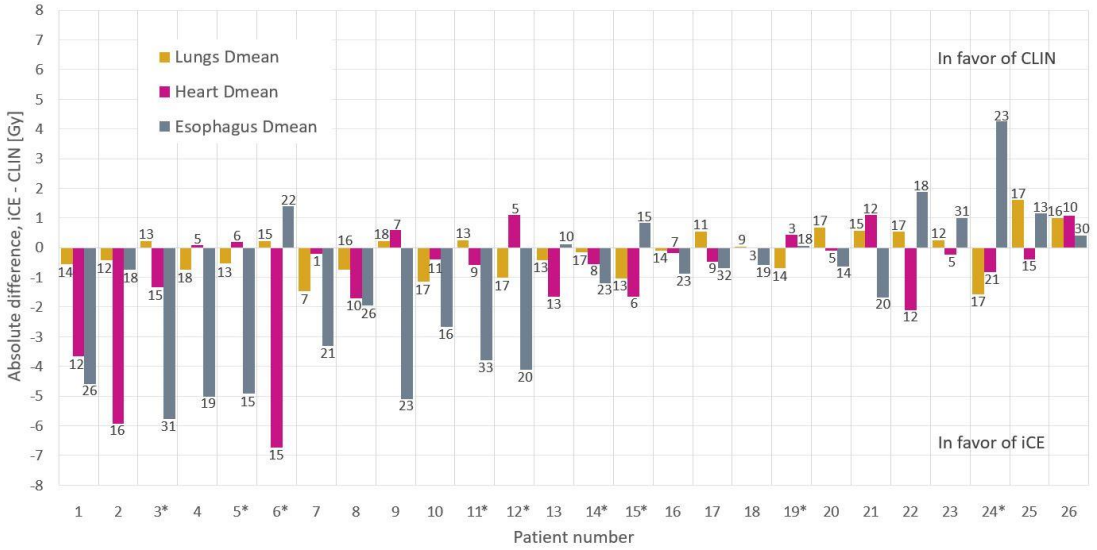


Figure 4. Differences in OAR mean doses between CLIN and iCE plans per patient. The numbers on the bars indicate the  $D_{mean}$  values [Gy] in the CLIN plans. The patients are sorted according to the sum of differences for all OARs. Patients marked with \* were used in wish-list tuning.

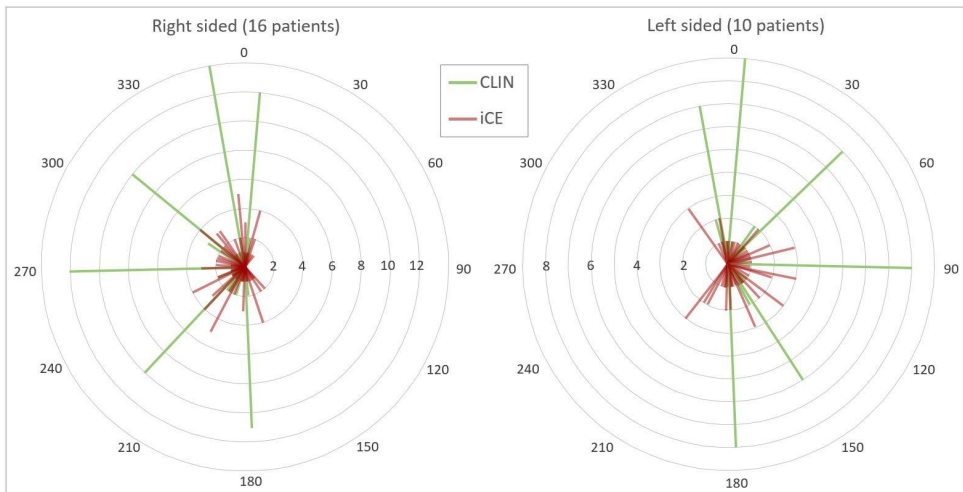


Figure 5. Selected beam angles in the CLIN plans (green) and optimized beam angles in the iCE plans (red) for patients with right-sided and left-sided tumors. Angles are rounded to the nearest 5 degrees. The number of patients is shown on the radial axis, and the angular axis shows beam angle in degrees.

### 4.3 Paper II

#### Improving knowledge-based treatment planning for lung cancer radiotherapy with automatic multi-criteria optimized training plans

In this paper we used 30 iCE treatment plans from paper I to train a RapidPlan model, and compared plans generated by this model (RP\_MCO) to plans generated by a RapidPlan model trained with CLIN plans (RP\_CLIN) and to the CLIN plans for a validation group of 15 patients.

Heart and esophagus doses were lower in RP\_MCO plans than RP\_CLIN plans. This was not surprising as the dose to the same OARs were lower in the iCE plans than the CLIN plans (paper I). The dose reductions translated into modest but consistent NTCP reductions for 2-year mortality and AET (Figure 6). The PTV coverage and lung dose were similar, except for lungs  $V_{5Gy}$  which was slightly lower with RP\_MCO. In blind comparison, the oncologist preferred the RP\_MCO plan for 53% and the CLIN plan for 47% of patients while the RP\_CLIN plan was not preferred for any patients. The RP\_MCO model was based on these results selected for implementation in the clinic.

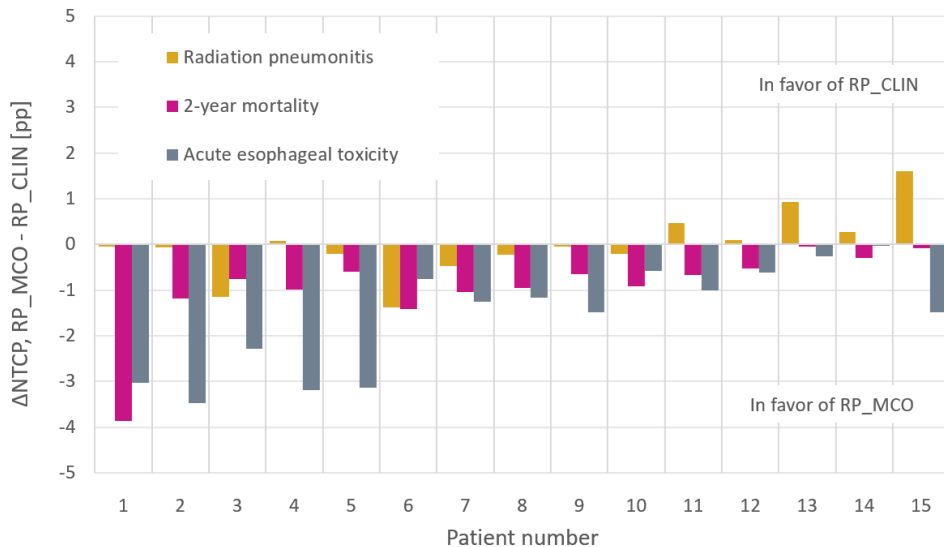


Figure 6. Differences in NTCPs between RP\_CLIN and RP\_MCO plans per patient. The patients are sorted according to the sum of differences for the three NTCPs.

## 4.4 Paper IV

### **Substantial Sparing of Organs at Risk with Modern Proton Therapy in Lung Cancer, but Altered Breathing Patterns Can Jeopardize Target Coverage**

In this paper we performed a detailed comparison of SFUD, IMPT and 4D robust IMPT (4DIMPT) proton plans and IMRT plans for 15 patients. Target coverage and OAR doses were compared in the nominal plans, with respect to setup and range uncertainties and breathing motion at planning, and in recalculations on w1 CTs.

OAR doses were lower for all proton techniques than for IMRT. Among the proton techniques, significant differences were found between SFUD and IMPT in  $D_{\text{mean}}$  for the lungs and esophagus and  $V_{20\text{Gy}}$  for the lungs, all in favor of IMPT. The mean rank was worst with IMRT and best with IMPT for all the evaluated OAR parameters.

All proton techniques had satisfying target robustness at planning (setup and range and interplay evaluations, recalculation on extreme 4DCT phases). In recalculations on the w1 CT, 2 patients with SFUD and 4DIMPT and 3 patients with IMPT had CTV  $D_{98\%} < 95\%$ . These 3 patients had a change in breathing pattern between the planning and w1 CTs causing a baseline shift for the tumor.

IMPT achieved lowest OAR doses of the investigated techniques and there were only minor differences in robustness. We therefore concluded that robust optimized IMPT was the best proton technique for these patients and could improve treatment of LA-NSCLC, but strategies to recognize patients with altered breathing motion between planning and treatment should be implemented.

---

## 4.5 Papers III and V

**Patient selection, inter-fraction plan robustness and reduction of toxicity risk with deep inspiration breath hold in intensity-modulated radiotherapy of locally advanced non-small cell lung cancer**

**Deep inspiration breath hold in intensity modulated proton therapy of locally advanced lung cancer - a dose and robustness analysis**

In these papers we compared FB and DIBH in IMRT (paper III) and IMPT (paper V) of LA-NSCLC. 41 patients were included in Paper V and 38 of these were included in paper III. All treatment plans were automatically generated with the iCE system (IMRT) or the RayStation script (IMPT).

The average lung volume was 50% larger and PTV and heart volumes 6% and 7% smaller with DIBH than FB. In IMRT, all investigated dose parameters for the lungs and heart were lower with DIBH than FB, with reductions in the median  $D_{\text{mean}}$  for lungs from 15.2 Gy to 13.8 Gy ( $p < 0.001$ ) and heart from 9.3 Gy to 8.2 Gy ( $p = 0.002$ ). This translated into reductions in median NTCP for RP from 20.3% to 18.3%, and for 2-year mortality from 51.4% to 50.3%.

In IMPT, DIBH reduced the lung dose compared to FB while other OAR doses were similar. Median lung  $D_{\text{mean}}$  was reduced from 9.3 Gy to 8.0 Gy ( $p < 0.001$ ) and NTCP for RP from 10.9% to 9.4% ( $p < 0.001$ ) with DIBH compared to FB. Regardless of breathing technique, IMPT substantially reduced the dose to all OARs compared to IMRT, and these differences were much larger than between FB and DIBH within each modality (Figure 7, Figure 8). Also in terms of NTCPs, IMPT with both FB and DIBH was better than IMRT for all investigated complications and for almost all patients (Figure 9).



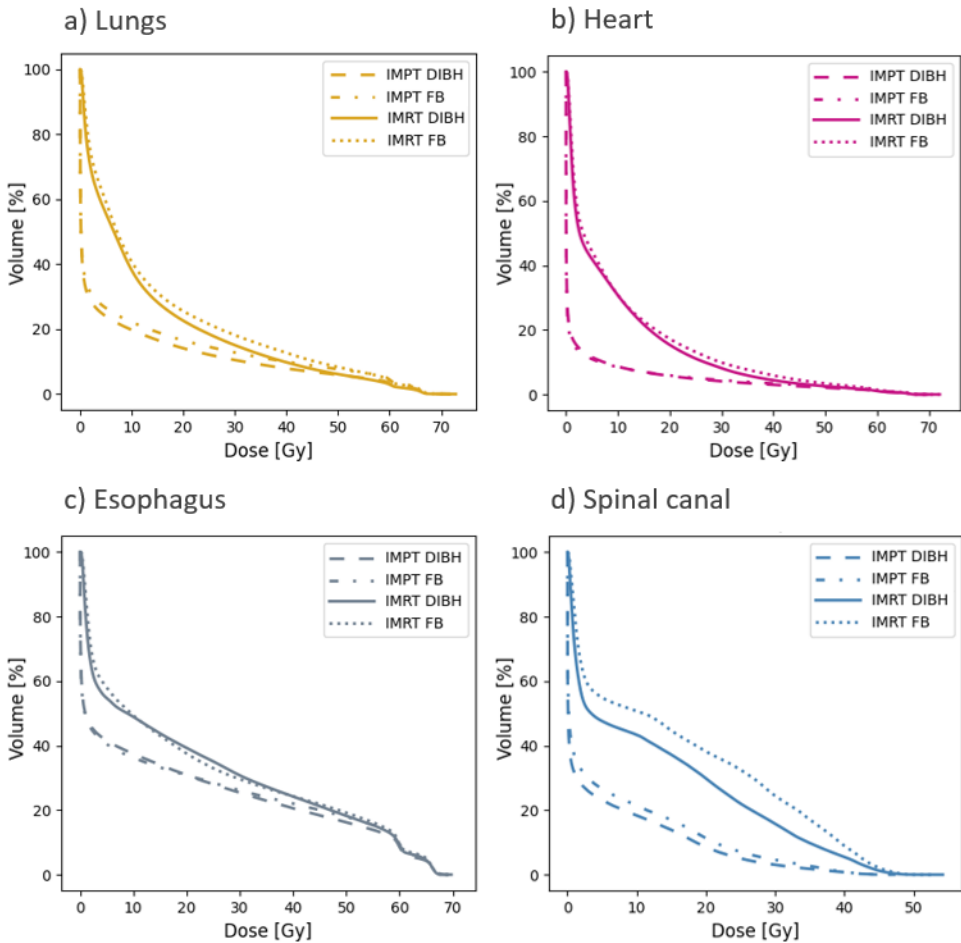


Figure 7. Population average DVHs for organs at risk for the nominal planning scenario in the FB and DIBH plans, both for IMPT and IMRT.

Robustness of the target coverage was similar for FB and DIBH, but different for IMRT and IMPT. In the recalculated IMRT plans on the w1 and w3 CTs, CTV  $V_{95\%}$  was below 98% in 5% of DIBH and 8% of FB plans. In 3% of the plans, CTV  $V_{95\%}$  was below 95%, and in zero plans CTV  $V_{95\%}$  was below 90%. In IMPT, corresponding numbers were 21% (FB)-22% (DIBH) with CTV  $V_{95\%}$  below 98%, 9-10% below 95% and 3-4% below 90% (Figure 10).

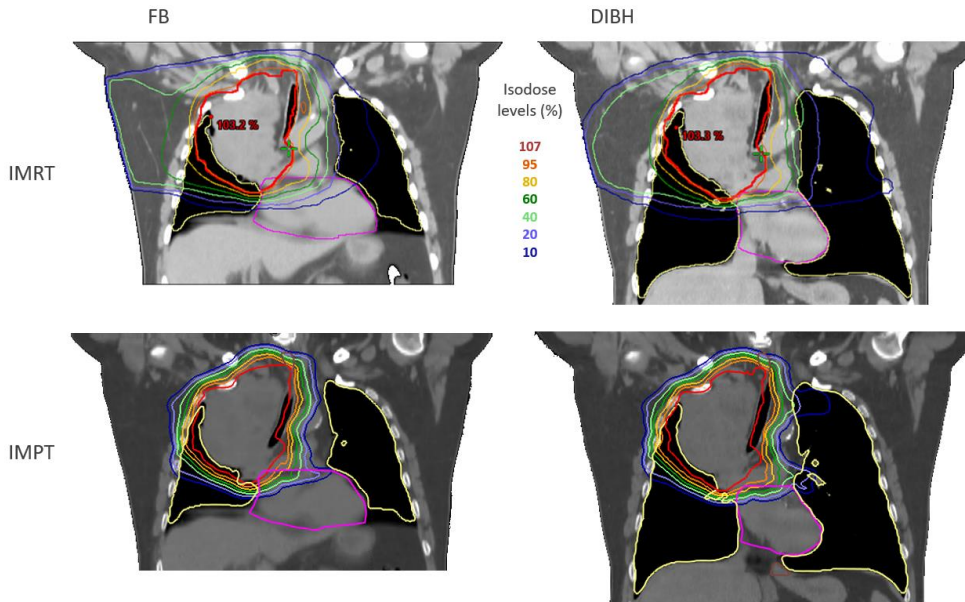
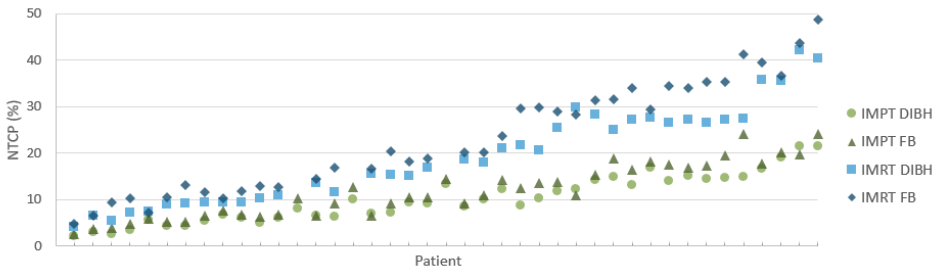


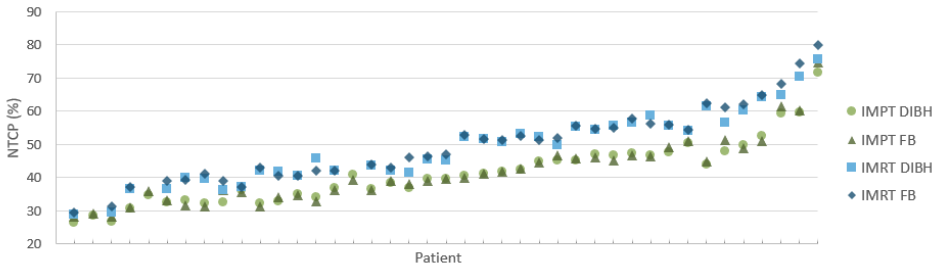
Figure 8. Dose distributions superimposed on planning CT scans of patient 1, showing enhanced sparing of OARs in DIBH (right) compared to FB (left) and in IMPT (bottom) compared to IMRT (top). Contours are shown for the PTV (red), lungs (yellow) and heart (magenta). Isodoses are shown in percentage of the prescribed dose (60 Gy).

In paper III we also explored correlations between the benefit of DIBH and patient and treatment characteristics. The NTCPs for RP and 2-year mortality was reduced with DIBH compared to FB for 92% and 74% of patients. The risk of RP was consistently reduced with DIBH regardless of tumor location, breathing motion and lung expansion with DIBH, while the ability to reduce the risk of 2-year mortality was evident among patients with upper and left lower lobe tumors but not right lower lobe tumors (Figure 11).

a) Radiation pneumonitis



b) 2-year mortality



c) Acute esophageal toxicity

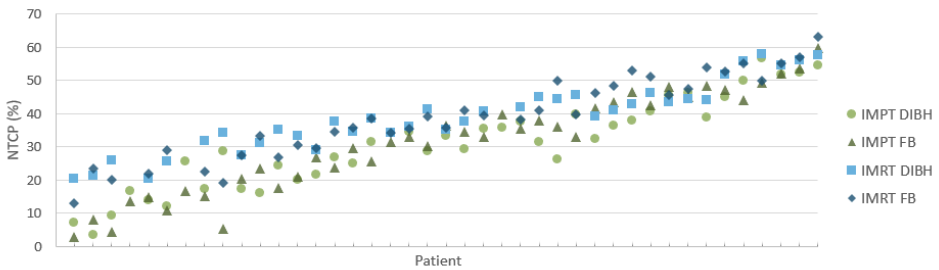
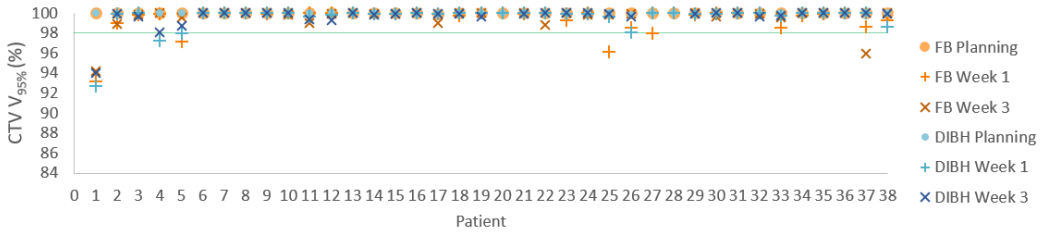


Figure 9. NTCPs for a) radiation pneumonitis, b) 2-year mortality and c) acute esophageal toxicity for FB and DIBH IMRT and IMPT plans for each patient. The patients are sorted according to the average NTCP for all techniques in each plot.

## IMRT



## IMPT

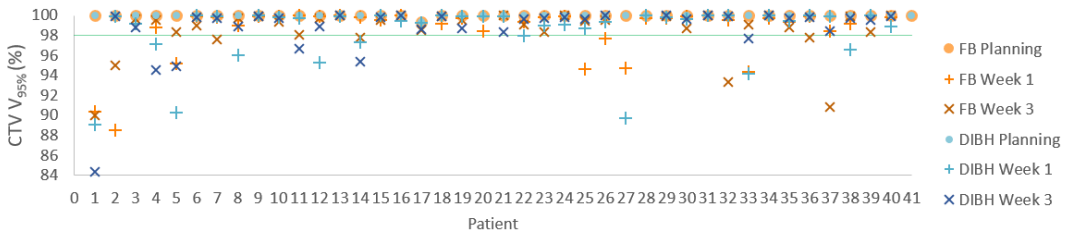


Figure 10. CTV  $V_{95\%}$  in nominal and recalculated FB and DIBH plans for IMRT (top) and IMPT (bottom). The green line indicates the planning objective of CTV  $V_{95\%} > 98\%$  used in IMPT (planning objectives in IMRT are for the PTV).

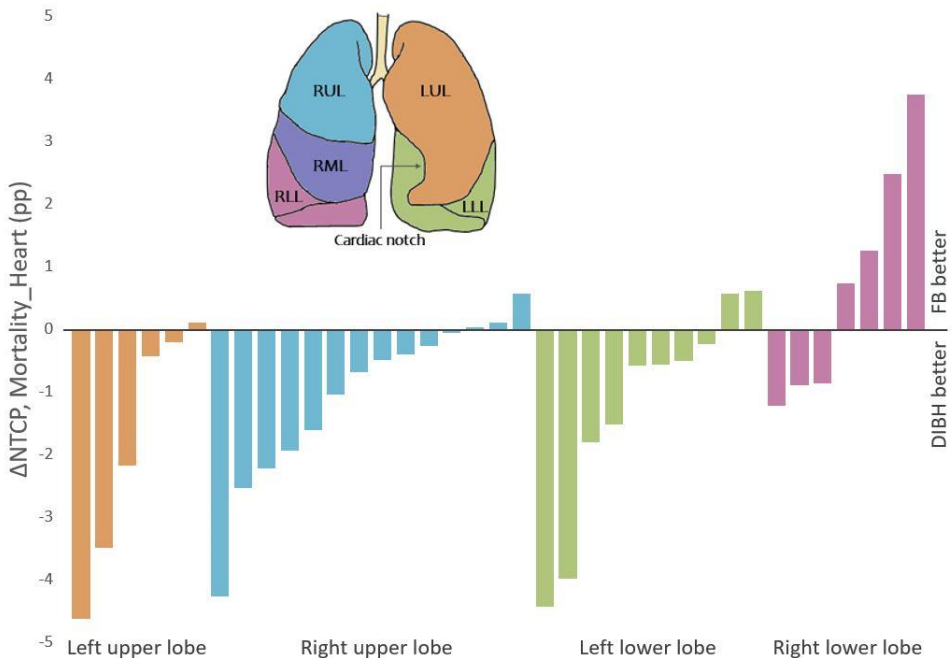


Figure 11.  $\Delta$ NTCP for 2-year mortality between DIBH and FB in the IMRT plans per patient, sorted according to primary tumor position. There were no patients with primary tumor in the right middle lobe. Negative  $\Delta$ NTCP values are in favor of DIBH and positive values are in favor of FB. pp =percentage points.



---

## 5. Discussion

This thesis has shown the potential of autoplanning, DIBH and proton therapy to reduce radiotherapy side effects for LA-NSCLC patients. This is important in a patient group with substantial risk of severe side effects that could reduce quality of life in the short or long term and limit the potential for curative radiation doses or immunotherapy.

### 5.1 Main issues and findings

#### 5.1.1 Autoplanning

Autoplanning has been both a topic of investigation and an essential tool in this thesis. While there are a number of studies on different autoplanning systems and applications in photon therapy, a major limitation is the availability of the systems in the clinic. Most clinics depend on solutions from their TPS vendor, and in-house developed systems or systems from other vendors are often not possible to use for patient treatment.

In paper I, we demonstrated that the developed iCE system for autoplanning reduced heart and esophagus dose compared to manual planning. While iCE generates deliverable Eclipse treatment plans, the system is suited in a research setting rather than clinical routine because it requires transfer of patient images and contours to EMC systems for the Erasmus-iCycle part and back to HUH for the Eclipse part. This would be impractical in a clinical setting and would also require approval of Erasmus-iCycle as a medical device at HUH. Instead, in paper II, we aimed to take advantage of this MCO-based system without routine access at our hospital. For this, we used the autoplanning system we have available at HUH, RapidPlan.

The main limitation of knowledge-based systems such as RapidPlan is the dependency of the output on the input training data. Several studies have shown how improving the RapidPlan library can improve the output plans [31,33–36]. In line with this, we showed in paper II that a RapidPlan model trained with MCO iCE plans

improved the output plans compared to a model trained with manual plans. While the study did not show any major differences in dose distributions between RP\_iCE and manual plans, other advantages such as homogeneous plan quality between patients and time saved in the planning process will follow the clinical implementation of the RP\_iCE model.

For proton therapy, autoplanning is less widespread, with few clinical systems available and little data showing a benefit compared to manual planning. For paper V, we needed more than 80 IMPT plans, and wanted to generate these automatically to ensure efficiency, quality and reduction of bias. Some studies have reported successful implementation of different autoplanning methods for specific diagnoses and settings. Machine learning planning produced robustly optimized IMPT plans for H&N cancer with comparable quality to clinical plans [46]. RapidPlanPT generated plans comparable to manual plans for prostate, head and neck and gastroesophageal cancer [42–45]. Both these methods require a set of training plans for configuration, which we did not have available for LA-NSCLC.

With a lack of applicable commercial systems for high-quality, robust IMPT planning, we decided to develop a script for automated, robust planning in RayStation. Scripted autoplanning in RayStation has previously been described for both photon [40] and proton [59] therapy, using different approaches to determine patient-specific optimization objectives. For our script we chose an approach inspired by the manual planning in paper IV where the target coverage was optimized first, and appropriate OAR dose objectives were automatically selected for each patient based on the results of the first optimization. A preliminary validation showed improvement in dose distributions compared to manual plans and this was considered sufficient for the purpose of paper V (comparing two techniques with plans created by the same script). We plan to further develop and validate the system for potential clinical use.

### 5.1.2 DIBH

DIBH is standard of care in radiotherapy of left-sided breast cancer as it reduces the heart dose by increasing the separation between the breast and heart. It is also used to

---

varying extents for other thoracic and abdominal tumors such as lymphoma and pancreatic cancer and stereotactic radiotherapy of lung and liver lesions [47,60,61]. Use of DIBH for LA-NSCLC has so far been limited [47]. Possible reasons are assumptions that these patients are too frail or lack lung capacity to perform DIBH, and lack of concrete evidence of benefits. However, studies have shown that most LA-NSCLC patients are able to perform DIBH throughout treatment. One study reported that 10% of patients were considered not suited for treatment in DIBH during a coaching session and 3% during the CT session, while 94% of the patients who started treatment in DIBH were able to perform DIBH throughout treatment [48].

A clinical study of various respiratory gating techniques in 3D-CRT for lung cancer patients with different stages and prescriptions treated in 2004-2008 found less pulmonary and esophageal toxicity with respiratory gating compared to FB [62]. Recent clinical data with modern radiotherapy techniques is lacking. One VMAT treatment planning study of 17 LA-NSCLC patients found dose reductions for the lungs, heart, esophagus, trachea and bronchi with DIBH compared to FB [50]. In proton therapy, there is even less data on potential benefits of DIBH. One treatment planning study with only 6 patients and no robustness measures suggested a potential for heart and lung sparing with DIBH compared to FB [63].

At HUH, DIBH has been used sporadically for LA-NSCLC patients with lower lobe tumors and large breathing motion based on experience from stereotactic treatment of early-stage lung cancer. This practice was not well founded in evidence, and the need for better data inspired this project.

The main difference we found between FB and DIBH for both IMRT and IMPT was a consistent reduction in lung dose and RP with DIBH. In addition, the heart dose was reduced for most patients for IMRT. The dose reductions were smaller than in the previous VMAT study [50], possibly because of the small number of patients with mostly upper lobe tumors in that study. Especially for the heart, separation from the target volume with DIBH is more likely for upper than lower lobe tumors. They also used manual planning which could have introduced planner bias.



For IMPT, we found very low heart doses both for FB and DIBH (median  $D_{\text{mean}}$  2-3 Gy), so there was not much dose to spare.

We did not see a correlation between tumor breathing motion and benefit of DIBH, contradictory to the criteria for patient selection previously used in our clinic. The only correlation we found was between the reduction in heart dose and tumor position; for tumors in the right lower lobe, the heart could be pushed closer to the treatment volume during DIBH, increasing the heart dose for some patients. Dividing the patients in groups based on tumor position resulted in few patients in each group, and these exploratory results should be verified in a separate and preferably larger cohort. Persson et al. did not find a pattern in benefit regarding OAR doses between FB and DIBH depending on tumor position; however, their study included only three patients with lower lobe tumors, all in the left lung [50].

Based on the results in paper III, the interdisciplinary lung cancer radiotherapy group at HUH has decided that DIBH should be standard for LA-NSCLC patients, except for patients with tumors in the right lower lobe where treatment plans for both FB and DIBH will be created, and an individual choice will be made for each patient.

### 5.1.3 Proton therapy

While early clinical experience with proton therapy for LA-NSCLC was with PSPT, more recent studies have showed promising results for PBS-PT [64–66]. Different approaches for optimization of PBS-PT result in different compromises between OAR dose and target coverage robustness. In theory, IMPT should produce the most conformal treatment plans while SFUD and 4D robust optimization are expected to increase robustness [13]. In paper IV we investigated differences between these techniques in FB treatment and found only small differences in target coverage robustness in evaluations both on the planning and w1 CTs. This indicates that the setup and range robustness criteria applied in the optimization of all techniques in most cases was sufficient to ensure robust target coverage. Change in breathing motion pattern from planning to w1 causing major baseline shifts were not handled by any of the optimization techniques and would require treatment adaptation in any

---

case. As expected, IMPT achieved best OAR sparing and was therefore preferred and used in paper V.

Our findings are in line with previous encouraging reports on robustness of 3D robust optimized IMPT. Inoue et al. found limited impact of setup and range uncertainties, breathing motion and interplay effects on 3D robust optimized IMPT plans for LA-NSCLC evaluated at planning [67]. Ribeiro et al. performed a comprehensive robustness analysis including weekly imaging during treatment, and also concluded that 3D robust optimized IMPT provided sufficiently robust plans for most patients and was preferred over 4D robust optimization. Their study included 10 LA-NSCLC patients with small to moderate tumor motion, and paper IV confirms their findings in a population with larger motion variability.

In papers IV and V, we showed a clear advantage of robust optimized IMPT over IMRT in terms of OAR sparing and risk of complications. On average, IMPT reduced the volume of lungs, heart and esophagus receiving up to 40-50 Gy. The spinal canal dose was also considerably reduced, which could give more room for optimization of other OARs and make possible reirradiation safer and easier. A randomized clinical trial comparing PSPT and IMRT for LA-NSCLC did not find any difference in RP between the groups [68]. However, in that study, the patients receiving proton therapy actually had more lung exposed to dose levels  $\geq 20$  Gy. While RP grade  $\geq 3$  occurred in IMRT patients regardless of time of treatment, it only occurred in the proton group for patients treated before the study midpoint. To discover any differences in side effects between photon and proton therapy of LA-NSCLC, future clinical trials should compare modern photon therapy to modern proton therapy, after the learning phase of introducing new techniques.

Previous studies have found that more frequent treatment adaptations are necessary in proton therapy than IMRT of LA-NSCLC. In a randomized clinical trial, Yang et al. reported 12% replanning for IMRT and 29% for PSPT [69]. In a simulation study by Hoffmann et al., 0% and 61% of the patients would require adaptation with IMRT and IMPT, respectively, when a robustness criterion of CTV  $V_{95\%} > 95\%$  was applied to recalculated plans at two time points during treatment

[70]. However, robust proton planning was not used in any of these studies. Previous data on the need for adaptations in robustly planned IMPT for LA-NSCLC is lacking.

In paper V, we showed that inter-fraction uncertainties such as tumor growth, baseline shift and change in atelectasis deteriorated target coverage more in IMPT than IMRT. In comparison to the study by Hoffmann et al. [70], 3% with IMRT and 13% (DIBH) – 18% (FB) with IMPT of the patients in our study would require adaptation with IMPT given a criteria of CTV  $V_{95\%} < 95\%$  in at least one repeated CT. This indicates that robust optimization greatly reduces the need for adaptations in IMPT compared to PTV-based optimization. Furthermore, some of the errors could be random and not require adaptation; 11/18 patients with CTV  $V_{95\%} < 98\%$  had an issue only for one of the two evaluated repeat CTs and one of the breathing techniques, and more data would be necessary to evaluate the actual need for adaptive replanning.

## **5.2 Benefits of the investigated methods**

The standard radiotherapy treatment for LA-NSCLC at HUH was until recently manually planned IMRT delivered during FB. All three methods investigated in this thesis spared OARs compared to standard treatment, to varying extents.

### **5.2.1 Autoplanning**

While autoplanning on average could spare some OAR dose, it has other and perhaps more important benefits. The occasional bad plans that typically occur with manual planning are avoided, which can be a large benefit for individual patients. It homogenizes plan quality between patients, so factors such as experience of the treatment planner and time available for planning have less impact on the treatment. It also spares a lot of resources for the clinic (section 5.2.1).

### **5.2.2 DIBH**

During DIBH, the lung volume increases, moving lung tissue away from the target volume, and tumor motion is restricted so the target volume can be reduced. The clinical benefit remains unclear. The main lung sparing with DIBH, particularly in

---

IMRT, is achieved at levels cranially and/or caudally to the target volume, and it is not clear which parts of the lungs are most important for RP or other side effects. Although it seems probable that a reduction in mean lung dose would give a similar benefit whether it is achieved with DIBH or other means, this has not been proven. A randomized clinical trial would give the best answer but also require a lot of resources, and the appropriateness in this setting could be questioned (section 5.5).

### 5.2.3 Proton therapy

Proton therapy, and IMRT in particular, was by far the method with most potential to limit OAR doses. This is not surprising as it is not only a technical detail but a different modality of radiation that interacts differently with tissue in the body. In paper V we demonstrated very low OAR doses in robustly optimized IMPT plans compared to previously published data on proton therapy [64,65,68,71]. This could mean that the potential of proton therapy to improve clinical outcomes is larger than what has been shown so far and underlines the need for more research on IMPT for LA-NSCLC.

An additional advantage of the investigated methods is that they can all be combined. The combination of autoplanning, DIBH and IMPT implemented in paper V achieved very low OAR doses compared to the alternative techniques and previous reports and would be the preferred choice to limit normal tissue complications in radiotherapy of LA-NSCLC.

## 5.3 Resource requirements of the investigated methods

In medical treatment there is always a balance between cost and benefit. In a public health care system such as the Norwegian, there are limited resources that must be distributed, and priorities must be made. While this thesis showed a benefit for all the investigated methods compared to standard treatment, the magnitude varied, as does the cost of implementation.

### 5.3.1 Autoplanning

Regardless of autoplanning system, tuning and validation for the desired patient group does require time and expertise, and updates could be required due to future changes in delineation, fractionation or planning procedures. However, the system can be used to generate plans for numerous future patients, and autoplanning should therefore normally save more resources than it requires. For example, Della Gala et al. reported a reduction in hands-on planning time of 3-4 hours per patient for VMAT planning of LA-NSCLC with automated MCO compared to manual planning [72]. Visak et al. reported a reduction of around 90 minutes per patient in dedicated planning time for stereotactic radiotherapy of LA-NSCLC with RapidPlan compared to manual planning [28].

As highlighted in paper II, it is important that efforts are made to configure the system in the best way. Its quality will impact the treatment plan quality for many future patients, and a well-functioning system that delivers good plans will save more time and give confidence to the treatment planners as they will not need to make frequent alterations to the autoplans.

### 5.3.2 DIBH

How easy it will be to implement DIBH in routine treatment of LA-NSCLC will vary. Treatment in DIBH requires equipment to monitor the patients' breathing level. Because DIBH is standard in radiotherapy of left-sided breast cancer this equipment is available in many clinics. The required time for the CT and treatment sessions is usually slightly longer for DIBH treatment; this could especially be the case in clinics with little experience with DIBH for LA-NSCLC. In contrast, the oncologists performing target volume delineation for our study noted that delineation on DIBH CTs was faster and easier than on 4DCTs; they felt more confident when the images were less blurred, and they only needed to evaluate 3 DIBH scans instead of 10 4DCT phases. In our clinic, where equipment is present, the staff are experienced with DIBH for LA-NSCLC and we have relatively few patients with this diagnosis, the extra resources required in terms of a slightly longer treatment time should hardly be noticeable.

---

Paper III showed that except for patients with tumors in the right lower lobe, DIBH is consistently a better choice than FB. This knowledge helps us spare resources because there is no need to acquire both 4DCTs and DIBH CTs and perform comparative treatment planning for most patients. Training patients in DIBH technique in a separate session prior to the planning CT session would require extra resources in terms of space and personnel but could identify patients who are not able to perform DIBH satisfactorily early on, and thereby reduce time on CT and the need to change from DIBH to FB during the treatment course.

### 5.3.3 Proton therapy

Proton therapy is in its own league both in terms of potential benefit and cost. In the Netherlands, the estimated cost per radiotherapy fraction (including building, equipment and personnel) for proton therapy is around 4 times higher than for photon therapy (€1062 vs. €256) [73]. In that study, proton therapy was not found to be cost-effective neither for all NSCLC patients nor for selected patients based on  $\Delta$ NTCP thresholds. However, the authors noted that this could change with improved clinical experience. The treatment time per fraction in this analysis was set to 35 minutes for proton therapy and 15 minutes for photon therapy; however, if the same time per fraction was assumed, proton therapy for selected patients would be cost-effective.

## 5.4 Patient safety in implementation of new methods

### 5.4.1 Autoplanning

Good autoplanning tools can increase patient safety because they ensure high and homogeneous treatment plan quality for all patients. In manual planning, the plan quality can be affected by factors such as time pressure and planner experience. It is however important that the autoplanning system is thoroughly validated and that careful controls of treatment plans by the planners, oncologists and physicists are retained. Treatment planners should still be trained in manual treatment planning; this will also make them better equipped to evaluate the autoplans.

### 5.4.2 DIBH

For clinical implementation of DIBH, the anatomical situation in each breath hold should closely match the situation in the CT used for treatment planning. Prior to delivery of each fraction of radiation, the RTTs acquire and evaluate a pre-treatment CBCT where positioning errors or major anatomical changes can be discovered. During the treatment, the position of the external marker placed on the patient's chest (or position of the patient surface if surface-guided systems are used) is used as surrogate for the tumor position – if the external marker is in the right position, it is assumed that the tumor is in the right position and radiation can be delivered. It is therefore important to know how well the position of external marker or signal correlates with the position of the internal target volume [61].

Scherman Rydhög et al. used fluoroscopic movies of liquid markers to evaluate intra- and inter-breath-hold tumor position uncertainty during the treatment course for 9 LA-NSCLC patients. They reported small uncertainties with average intra-breath-hold marker excursion  $\leq 2.1$  mm and mean inter-breath-hold shifts  $\leq 0.3$  mm in all directions [49]. In the INHALE trial, tumor positions on three consecutive DIBH CTs at planning were compared, and good inter-breath-hold reproducibility was reported with median position differences of  $\leq 1.3$  mm in all directions for both primary tumor and lymph nodes [48].

We also acquired three DIBH CTs during consecutive breath holds for treatment planning and used them to determine patient-specific margins to account for inter-breath-hold (intra-fraction) tumor position variation, i.e., how much the tumor position varied when the external marker was in the right position. However, more breath holds are needed to deliver each treatment fraction (usually 6-12 for our IMRT plans). A recent study found that the primary tumor position varied more between DIBHs in CBCTs pre and post treatment fractions than between four DIBH scans at the planning CT session, and that a few patients had large deviations and should be replanned or treated in FB [74]. Post-CBCT should be considered to identify these patients [61,74]. It is important to keep in mind that intra-fraction position uncertainty also affects treatment in FB. Changes in breathing pattern

---

(deeper or shallower breathing) can cause a baseline shift of the tumor, and particularly for lymph nodes which are difficult to see on CBCT, there is a risk of missing parts of the target volume also in FB [49,75]. Interplay between the motion of the radiation beam and breathing motion is also an issue in FB. However, although more of a concern in IMPT than IMRT, interplay is not expected to be an issue in normofractionated treatment regimens [76], confirmed in paper IV where a fraction dose of more than 90% was maintained in all interplay simulations.

### 5.4.3 Proton therapy

Proton therapy, including IMPT, for LA-NSCLC has been investigated in some clinical studies without evidence of worse local tumor control than in photon therapy. In a randomized clinical trial comparing PSPT with IMRT, rates of local failure (including marginal failure) and overall survival did not differ [68,69]. In a clinical study comparing IMPT with IMRT, rates of locoregional recurrence and overall survival were similar despite the IMPT population being more frail [66]. Another clinical study found similar locoregional control and overall survival for scanning beam proton therapy (mostly PBS-PT) and IMRT [65]. This indicates that proton therapy can be safely delivered.

However, as mentioned earlier, anatomical changes are expected to impact proton dose distributions more and adaptations will likely be more frequent with protons than photons. To improve robustness in IMPT, stricter robustness criteria could be applied in the treatment planning. However, altering the robustness settings for all patients would mean a general increase in OAR doses, and changes such as major tumor growth or shrinkage or change in atelectasis would require replanning anyway. The same is the case for SFUD and 4D robust optimization, which as shown in paper IV gave minor gains in robustness at the cost of increased OAR doses. Instead, a good adaptive protocol with methods to discover patients in need of adaptation is required. An appropriate strategy could be frequent routine control CTs during treatment and adaptation of treatment plans when needed. For proton therapy in DIBH, some machines have limitations on CBCT acquisition. In such cases, other alternatives for daily monitoring must be considered.



## 5.5 Methodological considerations

The investigations in this thesis are based on computer simulations – so-called treatment planning studies. The simulations show expected differences in radiation dose which in turn can be used in calculations of NTCP, but they do not reveal differences in actual clinical outcome. The gold standard for comparing treatments in evidence-based medicine is randomized clinical trials. They require far more resources than simulation studies as follow-up data must be collected, often over several years, and more patients must be included; in simulation studies, pairwise comparison where the patient is its own control reduces the number of patients needed. It has also been questioned whether randomizing patients is ethical when researchers know, or strongly suspect, that one group will be randomized to an inferior treatment that could cause unnecessary harm to the participants. As argued by Smith and Pell, validation in a randomized trial is not necessary or appropriate for all types of interventions [77].

The relationship between reduced radiation dose and reduced risk of common side effects is well established. For organs such as the lungs, heart and esophagus, there is no “safe” threshold dose, but it is clear that the risk increases with dose. For purely technical developments such as automated treatment planning, treatment planning studies to evaluate differences in dose distributions are the obvious choice. As mentioned in section 5.2.2, comparing DIBH and FB in IMRT and IMPT is somewhat more complex. Treatment planning studies are an appropriate tool to evaluate dose differences and NTCP models can indicate clinical differences, but NTCP models developed in the specific scenario would increase confidence in the results (section 5.6.1). Bearing in mind potential differences in robustness between techniques, treatment planning studies should preferably evaluate the delivered dose in addition to the planned dose.

Hansen et al. pointed out the important role of radiotherapy treatment planning studies both to facilitate the introduction of new techniques into clinical practice, and as a preparation for clinical studies. We have applied their “RATING” guidelines to ensure high quality in the design, execution and reporting of our studies [78].

---

## 5.6 Limitations

### 5.6.1 NTCP models

In this thesis, NTCP models have been used for scenarios and a patient population they are not validated for (IMPT or DIBH). The RP model is based on 3D-CRT data, but has been validated for proton therapy [79]. The AET model is based on IMRT/VMAT data, and the mortality model is based on data from 3D-CRT, VMAT and hybrid VMAT treatments, without validation for proton therapy. The applied models are currently used for patient selection for proton therapy in the Netherlands.

It is not optimal to use NTCP models for scenarios outside their scope, especially when there is a large difference in the dose distributions such as the case is for IMPT vs. photons. This was confirmed by our experience with the Mortality\_EDIC model investigated in study III. This model was based on one patient cohort with different dose characteristics than ours; especially the heart dose was clearly higher. The NTCP for 2-year mortality based on EDIC seemed to be driven mainly by the mean lung dose in our cohort, and compared to the Mortality\_Heart model (which has been externally validated), the estimated median 2-year mortality was 10-13 percentage points lower. Despite the uncertainties, NTCP values can give an impression of the magnitude of the clinical relevance of differences in dose distributions, and we have used them as a complement to dose-volume parameters.

### 5.6.2 Autoplanning

The script for automated IMPT planning developed for paper V is a rather simple approach to autoplanning. More iterations could give a result closer to a Pareto-optimal plan for each patient. In the current implementation, there is one round of lowering OAR objectives that were achieved in the previous round of optimization, because this indicates further room for improvement without compromising other objectives. This could instead have been a loop where the objectives were lowered in consecutive rounds until the achieved dose was higher than, or within a pre-defined threshold from, the objective. A more sophisticated but also much more complicated approach would be to push OAR doses as low as possible without losing target coverage or robustness.

The strength of the applied method is simplicity and speed. Because only 2-3 rounds of optimization were performed per plan, a Monte Carlo dose calculation algorithm could be used for the whole process, giving better initial indications of possible doses than preliminary, fast pencil beam calculations. Importantly, the method was feasible to implement in the limited time available for the last study of the thesis and gave robust plans with favorable dose distributions compared to previous publications.

### 5.6.3 Proton therapy optimization

Different settings and machine parameters can have a large impact on the proton therapy treatment plans. The manually created plans in paper IV and the automatically generated plans in paper V cannot be directly compared. In paper IV, a generic IBA beam model provided in RayStation v. 8B was used, with energy range 100-226 MeV/A and sigma of spot sizes in air at isocenter 3.7-7.2 mm. Range shifters of 4 or 7.5 cm were required for all patients. In paper V, a beam model with energy range 70-227 MeV/A (closer to the Varian ProBeam 360 system that will be installed at HUH) was used. Because of the lower energies available, a 4 cm range shifter was needed for around half the patients only, allowing more conformal dose distributions. This is an example of differences that makes comparing and evaluating different proton therapy studies, also clinical studies, challenging.

### 5.6.4 Planner bias

Planner bias refers to prejudice (conscious or unconscious) of the treatment planner in favor of one of the investigated techniques. Automated planning is a powerful tool to reduce bias, which was a main motivation for its use in papers III and V. To achieve the best results the autoplanning system should be configured or trained using representative cases and planned according to procedure. E.g., training a RapidPlan model with only FB plans and using it for both FB and DIBH could lead to systematically higher doses than achievable in the DIBH plans. In the RapidPlan models created in paper II, there were both FB and DIBH plans in the library (the same technique as for clinical treatment was used). When the clinical routine changes

---

and more patients are treated with DIBH, updating the model to reflect the new routine should be considered.

In paper IV where the plans were manually created, the three different plans were created in the same order for all patients. This introduces a high risk of planner bias because the objectives used and dose values obtained in the SFUD plan were always known when creating the other plans. For example, if the planner found that OAR doses could be pushed lower in the IMPT plan than the SFUD plan for the first patients, they could unconsciously try harder to lower doses in the IMPT plans for later patients as well. Without autoplanning available, planner bias could have been reduced by varying which technique was planned first for each patient.

## 5.7 Strengths

The prospective data collection for this thesis has several benefits. A representative patient population can be expected when all LA-NSCLC patients receiving radiotherapy during three years were invited to participate. All data including repeated delineations by the treatment planners and oncologist were collected within the same time period, avoiding uncertainty that could be introduced if this was done retrospectively when practice or guidelines could have changed. The repeat CTs taken during treatment were important as they allowed evaluation of the validity of the result during treatment and to get an impression of the inter-fraction robustness of the investigated techniques.

### 5.7.1 Number of patients

The number of patients in each paper varied because patients were included during the PhD period. More patients were therefore available for the studies performed last (papers II and V). Each study had enough patients to answer the research questions. Study II required most patients because both a library of training plans for knowledge-based model creation and an independent validation group were needed. Compared to other treatment planning studies, the number of included patients particularly in study III and V was fairly high. This was made possible by autoplanning; creating 82 IMPT plans for study V would for example not have been

feasible with manual treatment planning. The proton plans used in study IV were manually created as part of a master thesis before we had autoplanning available, and 15 patients with 3 plans each required substantial planning time.

---

## 6. Conclusions

This thesis has shown a potential to improve current standard radiotherapy of LA-NSCLC by reducing OAR doses and the risk of complications.

The developed iCE system for automated treatment planning enabled generation of deliverable MCO-based plans that reduced heart and esophagus doses compared to manual planning. Using iCE plans for RapidPlan training, automatic MCO could be exploited in a clinic without routine access to this system. Reduction of heart and esophagus doses in the output plans from RapidPlan trained with iCE plans compared to with manual plans highlights the importance of high-quality training data in machine learning based treatment planning. Implementation of autoplanning for both IMRT and IMPT was essential to ensure efficient, bias-free treatment planning for comparisons of DIBH and FB.

DIBH consistently reduced lung doses and risk of RP compared to FB in both IMRT and IMPT. In IMRT, the heart dose was also lower with DIBH for most patients, except for patients with tumor in the right lower lung where DIBH could push the heart closer to the target volume. Inter-fraction robustness was similar for DIBH and FB plans despite smaller target volumes with DIBH.

Comparing different optimization techniques for PBS-PT, IMPT gave the best compromise between target coverage robustness and OAR sparing and was preferred over SFUD and 4D robust IMPT. Comparison of IMPT with IMRT showed far lower OAR doses with IMPT, both for FB and DIBH. Dose differences between IMPT and IMRT were much larger than differences between FB and DIBH.

Autoplanning and DIBH are fairly easy to implement and is or will soon be routinely used in the clinic at HUH as a result of this work. Proton therapy is costly, technically challenging (at least in a start-up phase) and less available but has the potential to substantially reduce OAR doses compared to photon therapy. This potential should first be explored in clinical studies.

In conclusion, this thesis has provided tools, knowledge and experience that have improved clinical practice in radiotherapy of LA-NSCLC at HUH.



---

## 7. Future perspectives

There are several opportunities for further improvement in treatment of LA-NSCLC. In combination with other treatment advances, the techniques investigated in this thesis might have more potential than shown so far.

One particularly interesting area to investigate is the combination of proton therapy with immunotherapy. The PACIFIC trial on Durvalumab after chemotherapy and photon radiotherapy of LA-NSCLC reported unprecedented levels of survival and has changed standard of care [9]. Still, a 5-year overall survival of only 42.9% shows room for further improvement. Preliminary evidence suggests that the radiotherapy dose distribution is linked to lymphopenia, which could be a predictor for poorer progression free survival after chemoradiotherapy combined with immunotherapy in LA-NSCLC [80–82]. IMPT can spare immune cells by irradiating less circulating blood, in particular due to the drastic reduction of lung and heart volume receiving low radiation doses, and this could increase the effect of immunotherapy. DIBH also reduces the estimated dose to immune cells compared to FB and could therefore improve the effect of immunotherapy in combination with both IMRT and IMPT.

While immunotherapy has improved systemic control in LA-NSCLC, frequent intrathoracic progression is a concern that calls for improvement of the localized radiotherapy treatment [83]. The possibility of radiation dose escalation was investigated in the RTOG 0617 trial, which reported worse overall survival in the high dose arm (74 Gy) than the low dose arm (60 Gy) [10]. This has in part been explained by an increase in heart dose; heart  $V_{5\text{Gy}}$  and  $V_{30\text{Gy}}$  were both important predictors of patient survival. IMPT in particular, but also DIBH in IMRT, can reduce dose to heart and other OARs compared to standard FB IMRT and might enable safe dose escalation. However, high doses in small volumes of normal tissue inside or close to the target volume would still be a concern. Novel techniques such as linear energy transfer optimization of proton therapy could be explored to limit such adverse effects [84].



Both for lung cancer and many other diagnoses, the use of autoplanning has increased rapidly in the last years. Still, allocating the resources necessary for setting up and implementing autoplanning is a major barrier. Most centers depend on solutions from their commercial TPS provider, and these vary both in terms of resource requirements and quality of the resulting plans. There is a large potential for more sharing of models, scripts etc., preferably accompanied by further standardization of imaging, delineation and treatment planning protocols. For example, future clinical study protocols could include an autoplanning model that would ensure homogeneous plan quality and prioritizations across participating centers. Autoplanning is also a great tool to standardize and streamline both manual objective selection and model based selection of patients for photon vs. proton therapy.

On a local scale, a proton therapy center is opening in Bergen in 2025, with one clinical gantry and one reserved for research. The goal of the health authorities is for 80% of the patients to be included in clinical trials [85], and good capacity is expected in the first years. This will hopefully open opportunities for Norwegian LA-NSCLC patients to participate in clinical trials on proton therapy. These are sorely needed, as there is currently little data on outcomes especially after IMPT.

---

## References

- [1] Larsen I, Ursin G, Nystad W. Kreft i Norge. I: Folkehelse rapporten - Helsetilstanden i Norge. [Internet]. Oslo: Folkehelseinstituttet; 2023 [cited 2023 Oct 31]. Available from: <https://www.fhi.no/he/folkehelse rapporten/ikke-smittsomme/kreft/>.
- [2] World Health Organization. Lung cancer (fact sheet). [Internet]. 2023 [cited 2023 Oct 31]. Available from: <https://www.who.int/news-room/fact-sheets/detail/lung-cancer>.
- [3] Delaney GP, Barton MB. Evidence-based Estimates of the Demand for Radiotherapy. *Clinical Oncology*. 2015;27:70–76.
- [4] Brierly JD, Gospodarowicz MK, Wittekind C. TNM Classification of Malignant Tumors. 8th ed. Union for International Cancer Control; 2016.
- [5] Non-small Cell Lung Cancer Collaborative Group. Chemotherapy in non-small cell lung cancer: a meta-analysis using updated data on individual patients from 52 randomised clinical trials. *BMJ*. 1995;311:899–909.
- [6] Aupérin A, Le Péchoux C, Rolland E, et al. Meta-Analysis of Concomitant Versus Sequential Radiochemotherapy in Locally Advanced Non-Small-Cell Lung Cancer. *JCO*. 2010;28:2181–2190.
- [7] Chun SG, Hu C, Choy H, et al. Impact of Intensity-Modulated Radiation Therapy Technique for Locally Advanced Non-Small-Cell Lung Cancer: A Secondary Analysis of the NRG Oncology RTOG 0617 Randomized Clinical Trial. *JCO*. 2017;35:56–62.
- [8] Petrella F, Rizzo S, Attili I, et al. Stage III Non-Small-Cell Lung Cancer: An Overview of Treatment Options. *Current Oncology*. 2023;30:3160–3175.
- [9] Spigel DR, Faivre-Finn C, Gray JE, et al. Five-Year Survival Outcomes From the PACIFIC Trial: Durvalumab After Chemoradiotherapy in Stage III Non-Small-Cell Lung Cancer. *JCO*. 2022;40:1301–1311.
- [10] Bradley JD, Paulus R, Komaki R, et al. Standard-dose versus high-dose conformal radiotherapy with concurrent and consolidation carboplatin plus paclitaxel with or without cetuximab for patients with stage IIIA or IIIB non-small-cell lung cancer (RTOG 0617): a randomised, two-by-two factorial phase 3 study. *The Lancet Oncology*. 2015;16:187–199.
- [11] Particle Therapy Co-Operative Group. Particle therapy facilities in clinical operation [Internet]. 2023 [cited 2023 Nov 15]. Available from: <https://www.ptcog.site/index.php/facilities-in-operation-public>.

- 
- [12] Nederlandse Vereniging voor Radiotherapie en Oncologie. Landelijk Indicatie Protocol Protonen Therapie - Longcarcinoom [Internet]. 2019. Available from: [nvro.nl/images/documenten/rapporten/LIPP\\_longen\\_final\\_01122019.pdf](https://nvro.nl/images/documenten/rapporten/LIPP_longen_final_01122019.pdf).
- [13] Chang JY, Zhang X, Knopf A, et al. Consensus Guidelines for Implementing Pencil-Beam Scanning Proton Therapy for Thoracic Malignancies on Behalf of the PTCOG Thoracic and Lymphoma Subcommittee. *International Journal of Radiation Oncology\*Biology\*Physics*. 2017;99:41–50.
- [14] Deasy JO, Jeong J, Thor M, et al. Optimizing Lung Cancer Radiotherapy Treatments Using Personalized Dose-Response Curves. In: Jeremić B, editor. *Advances in Radiation Oncology in Lung Cancer* [Internet]. Cham: Springer International Publishing; 2022 [cited 2023 Dec 13]. p. 189–212. Available from: [https://link.springer.com/10.1007/174\\_2022\\_307](https://link.springer.com/10.1007/174_2022_307).
- [15] Verma V, Simone C, Werner-Wasik M. Acute and Late Toxicities of Concurrent Chemoradiotherapy for Locally-Advanced Non-Small Cell Lung Cancer. *Cancers*. 2017;9:120.
- [16] Marks LB, Bentzen SM, Deasy JO, et al. Radiation Dose–Volume Effects in the Lung. *International Journal of Radiation Oncology\*Biology\*Physics*. 2010;76:S70–S76.
- [17] Arroyo-Hernández M, Maldonado F, Lozano-Ruiz F, et al. Radiation-induced lung injury: current evidence. *BMC Pulm Med*. 2021;21:9.
- [18] Speirs CK, DeWees TA, Rehman S, et al. Heart Dose Is an Independent Dosimetric Predictor of Overall Survival in Locally Advanced Non–Small Cell Lung Cancer. *Journal of Thoracic Oncology*. 2017;12:293–301.
- [19] Banfill K, Giuliani M, Aznar M, et al. Cardiac Toxicity of Thoracic Radiotherapy: Existing Evidence and Future Directions. *Journal of Thoracic Oncology*. 2021;16:216–227.
- [20] Werner-Wasik M, Yorke E, Deasy J, et al. Radiation Dose-Volume Effects in the Esophagus. *International Journal of Radiation Oncology\*Biology\*Physics*. 2010;76:S86–S93.
- [21] Singh AK, Lockett MA, Bradley JD. Predictors of radiation-induced esophageal toxicity in patients with non-small-cell lung cancer treated with three-dimensional conformal radiotherapy. *International Journal of Radiation Oncology\*Biology\*Physics*. 2003;55:337–341.
- [22] Kirkpatrick JP, van der Kogel AJ, Schultheiss TE. Radiation Dose–Volume Effects in the Spinal Cord. *International Journal of Radiation Oncology\*Biology\*Physics*. 2010;76:S42–S49.

- 
- [23] Yan M, Kong W, Kerr A, et al. The radiation dose tolerance of the brachial plexus: A systematic review and meta-analysis. *Clinical and Translational Radiation Oncology*. 2019;18:23–31.
- [24] Nelms BE, Robinson G, Markham J, et al. Variation in external beam treatment plan quality: An inter-institutional study of planners and planning systems. *Practical Radiation Oncology*. 2012;2:296–305.
- [25] Berry SL, Boczkowski A, Ma R, et al. Interobserver variability in radiation therapy plan output: Results of a single-institution study. *Practical Radiation Oncology*. 2016;6:442–449.
- [26] Hussein M, Heijmen BJM, Verellen D, et al. Automation in intensity modulated radiotherapy treatment planning—a review of recent innovations. *BJR*. 2018;91:20180270.
- [27] Fogliata A, Belosi F, Clivio A, et al. On the pre-clinical validation of a commercial model-based optimisation engine: Application to volumetric modulated arc therapy for patients with lung or prostate cancer. *Radiotherapy and Oncology*. 2014;113:385–391.
- [28] Visak J, McGarry RC, Randall ME, et al. Development and clinical validation of a robust knowledge-based planning model for stereotactic body radiotherapy treatment of centrally located lung tumors. *J Appl Clin Med Phys*. 2021;22:146–155.
- [29] Fogliata A, Reggiori G, Stravato A, et al. RapidPlan head and neck model: the objectives and possible clinical benefit. *Radiat Oncol*. 2017;12:73.
- [30] Schubert C, Waletzko O, Weiss C, et al. Intercenter validation of a knowledge based model for automated planning of volumetric modulated arc therapy for prostate cancer. The experience of the German RapidPlan Consortium. Zhang Q, editor. *PLoS ONE*. 2017;12:e0178034.
- [31] Hundvin JA, Fjellanger K, Pettersen HES, et al. Clinical iterative model development improves knowledge-based plan quality for high-risk prostate cancer with four integrated dose levels. *Acta Oncologica*. 2021;60:237–244.
- [32] Fjellanger K, Hordnes M, Sandvik IM, et al. Improving knowledge-based treatment planning for lung cancer radiotherapy with automatic multi-criteria optimized training plans. *Acta Oncologica*. 2023;1–7.
- [33] Fogliata A, Cozzi L, Reggiori G, et al. RapidPlan knowledge based planning: iterative learning process and model ability to steer planning strategies. *Radiat Oncol*. 2019;14:187.
- [34] Hoffmann L, Knap MM, Alber M, et al. Optimal beam angle selection and knowledge-based planning significantly reduces radiotherapy dose to organs at risk for lung cancer patients. *Acta Oncologica*. 2021;60:293–299.

- [35] Scaggion A, Fusella M, Cavinato S, et al. Updating a clinical Knowledge-Based Planning prediction model for prostate radiotherapy. *Physica Medica*. 2023;107:102542.
- [36] Miguel-Chumacero E, Currie G, Johnston A, et al. Effectiveness of Multi-Criteria Optimization-based Trade-Off exploration in combination with RapidPlan for head & neck radiotherapy planning. *Radiat Oncol*. 2018;13:229.
- [37] Breedveld S, Storchi PRM, Voet PWJ, et al. iCycle: Integrated, multicriterial beam angle, and profile optimization for generation of coplanar and noncoplanar IMRT plans. *Med Phys*. 2012;39:951–963.
- [38] Fjellanger K, Hysing LB, Heijmen BJM, et al. Enhancing Radiotherapy for Locally Advanced Non-Small Cell Lung Cancer Patients with iCE, a Novel System for Automated Multi-Criterial Treatment Planning Including Beam Angle Optimization. *Cancers*. 2021;13:5683.
- [39] Bijman R, Sharfo AW, Rossi L, et al. Pre-clinical validation of a novel system for fully-automated treatment planning. *Radiotherapy and Oncology*. 2021;158:253–261.
- [40] Funderud M, Hoem IS, Guleng MAD, et al. Script-based automatic radiotherapy planning for cervical cancer. *Acta Oncologica*. 2023;62:1798–1807.
- [41] Xhaferllari I, Wong E, Bzdusek K, et al. Automated IMRT planning with regional optimization using planning scripts. *J Applied Clin Med Phys*. 2013;14:176–191.
- [42] Delaney A, Dong L, Mascia A, et al. Automated Knowledge-Based Intensity-Modulated Proton Planning: An International Multicenter Benchmarking Study. *Cancers*. 2018;10:420.
- [43] Xu Y, Brovold N, Cyriac J, et al. Assessment of Knowledge-Based Planning for Prostate Intensity Modulated Proton Therapy. *International Journal of Particle Therapy*. 2021;8:62–72.
- [44] Xu Y, Cyriac J, De Ornelas M, et al. Knowledge-Based Planning for Robustly Optimized Intensity-Modulated Proton Therapy of Head and Neck Cancer Patients. *Front Oncol*. 2021;11:737901.
- [45] Celik E, Baues C, Claus K, et al. Knowledge-based intensity-modulated proton planning for gastroesophageal carcinoma. *Acta Oncologica*. 2021;60:285–292.
- [46] van Bruggen IG, Huiskes M, de Vette SPM, et al. Automated Robust Planning for IMPT in Oropharyngeal Cancer Patients Using Machine Learning. *International Journal of Radiation Oncology\*Biography\*Physics*. 2023;115:1283–1290.

- 
- [47] Anastasi G, Bertholet J, Poulsen P, et al. Patterns of practice for adaptive and real-time radiation therapy (POP-ART RT) part I: Intra-fraction breathing motion management. *Radiotherapy and Oncology*. 2020;153:79–87.
- [48] Josipovic M, Aznar MC, Thomsen JB, et al. Deep inspiration breath hold in locally advanced lung cancer radiotherapy: validation of intrafractional geometric uncertainties in the INHALE trial. *BJR*. 2019;92:20190569.
- [49] Scherman Rydhög J, Riisgaard de Blanck S, Josipovic M, et al. Target position uncertainty during visually guided deep-inspiration breath-hold radiotherapy in locally advanced lung cancer. *Radiotherapy and Oncology*. 2017;123:78–84.
- [50] Persson GF, Scherman Rydhög J, Josipovic M, et al. Deep inspiration breath-hold volumetric modulated arc radiotherapy decreases dose to mediastinal structures in locally advanced lung cancer. *Acta Oncologica*. 2016;55:1053–1056.
- [51] Nestle U, De Ruysscher D, Ricardi U, et al. ESTRO ACROP guidelines for target volume definition in the treatment of locally advanced non-small cell lung cancer. *Radiotherapy and Oncology*. 2018;127:1–5.
- [52] Kong F-M (Spring), Ritter T, Quint DJ, et al. Consideration of Dose Limits for Organs at Risk of Thoracic Radiotherapy: Atlas for Lung, Proximal Bronchial Tree, Esophagus, Spinal Cord, Ribs, and Brachial Plexus. *International Journal of Radiation Oncology\*Biophysics\*Physics*. 2011;81:1442–1457.
- [53] Pettersen HES. DVHToolkit [Internet]. GitHub; [cited 2023 Dec 13]. Available from: <https://github.com/BergenParticleTherapy/DVHToolkit>.
- [54] Fredriksson A, Forsgren A, Hårdemark B. Minimax optimization for handling range and setup uncertainties in proton therapy: Minimax optimization for handling uncertainties in proton therapy. *Med Phys*. 2011;38:1672–1684.
- [55] Engwall E, Fredriksson A, Glimelius L. 4D robust optimization including uncertainties in time structures can reduce the interplay effect in proton pencil beam scanning radiation therapy. *Med Phys*. 2018;45:4020–4029.
- [56] Appelt AL, Vogelius IR, Farr KP, et al. Towards individualized dose constraints: Adjusting the QUANTEC radiation pneumonitis model for clinical risk factors. *Acta Oncologica*. 2014;53:605–612.
- [57] Defraene G, Dankers FJWM, Price G, et al. Multifactorial risk factors for mortality after chemotherapy and radiotherapy for non-small cell lung cancer. *Radiotherapy and Oncology*. 2020;152:117–125.
- [58] Wijsman R, Dankers F, Troost EGC, et al. Multivariable normal-tissue complication modeling of acute esophageal toxicity in advanced stage non-small cell lung cancer patients treated with intensity-modulated (chemo-)radiotherapy. *Radiotherapy and Oncology*. 2015;117:49–54.

- 
- [59] Hedrick SG, Petro S, Ward A, et al. Validation of automated complex head and neck treatment planning with pencil beam scanning proton therapy. *J Applied Clin Med Phys*. 2022;23:e13510.
- [60] Boda-Heggemann J, Knopf A-C, Simeonova-Chergou A, et al. Deep Inspiration Breath Hold—Based Radiation Therapy: A Clinical Review. *International Journal of Radiation Oncology\*Biography\*Physics*. 2016;94:478–492.
- [61] Aznar MC, carrasco de fez P, Corradini S, et al. ESTRO-ACROP guideline: Recommendations on implementation of breath-hold techniques in radiotherapy. *Radiotherapy and Oncology*. 2023;185:109734.
- [62] Giraud P, Morvan E, Claude L, et al. Respiratory Gating Techniques for Optimization of Lung Cancer Radiotherapy. *Journal of Thoracic Oncology*. 2011;6:2058–2068.
- [63] Mah D, Yorke E, Zemanaj E, et al. A Planning Comparison of IMRT vs. Pencil Beam Scanning for Deep Inspiration Breath Hold Lung Cancers. *Med Dosim*. 2022;47:26–31.
- [64] Gjyshi O, Xu T, Elhammali A, et al. Toxicity and Survival After Intensity-Modulated Proton Therapy Versus Passive Scattering Proton Therapy for NSCLC. *Journal of Thoracic Oncology*. 2021;16:269–277.
- [65] Zou Z, Bowen SR, Thomas HMT, et al. Scanning Beam Proton Therapy versus Photon IMRT for Stage III Lung Cancer: Comparison of Dosimetry, Toxicity, and Outcomes. *Advances in Radiation Oncology*. 2020;5:434–443.
- [66] Yu NY, DeWees TA, Liu C, et al. Early Outcomes of Patients With Locally Advanced Non-small Cell Lung Cancer Treated With Intensity-Modulated Proton Therapy Versus Intensity-Modulated Radiation Therapy: The Mayo Clinic Experience. *Advances in Radiation Oncology*. 2020;5:450–458.
- [67] Inoue T, Widder J, van Dijk LV, et al. Limited Impact of Setup and Range Uncertainties, Breathing Motion, and Interplay Effects in Robustly Optimized Intensity Modulated Proton Therapy for Stage III Non-small Cell Lung Cancer. *International Journal of Radiation Oncology\*Biography\*Physics*. 2016;96:661–669.
- [68] Liao Z, Lee JJ, Komaki R, et al. Bayesian Adaptive Randomization Trial of Passive Scattering Proton Therapy and Intensity-Modulated Photon Radiotherapy for Locally Advanced Non–Small-Cell Lung Cancer. *JCO*. 2018;36:1813–1822.
- [69] Yang P, Xu T, Gomez DR, et al. Patterns of Local-Regional Failure After Intensity Modulated Radiation Therapy or Passive Scattering Proton Therapy

- 
- With Concurrent Chemotherapy for Non-Small Cell Lung Cancer. *International Journal of Radiation Oncology\*Biography\*Physics*. 2019;103:123–131.
- [70] Hoffmann L, Alber M, Jensen MF, et al. Adaptation is mandatory for intensity modulated proton therapy of advanced lung cancer to ensure target coverage. *Radiotherapy and Oncology*. 2017;122:400–405.
- [71] Iwata H, Akita K, Yamaba Y, et al. Concurrent Chemo-Proton Therapy Using Adaptive Planning for Unresectable Stage 3 Non-Small Cell Lung Cancer: A Phase 2 Study. *International Journal of Radiation Oncology\*Biography\*Physics*. 2021;109:1359–1367.
- [72] Della Gala G, Dirkx MLP, Hoekstra N, et al. Fully automated VMAT treatment planning for advanced-stage NSCLC patients. *Strahlenther Onkol*. 2017;193:402–409.
- [73] Aldenhoven L, Ramaekers B, Degens J, et al. Cost-effectiveness of proton radiotherapy versus photon radiotherapy for non-small cell lung cancer patients: Exploring the model-based approach. *Radiotherapy and Oncology*. 2023;183:109417.
- [74] Hoffmann L, Ehmsen MI, Hansen J, et al. Repeated deep-inspiration breath-hold CT scans at planning underestimate the actual motion between breath-holds at treatment for lung cancer and lymphoma patients. *Radiotherapy and Oncology*. 2023;188:109887.
- [75] Boer CG, Fjellanger K, Sandvik IM, et al. Substantial Sparing of Organs at Risk with Modern Proton Therapy in Lung Cancer, but Altered Breathing Patterns Can Jeopardize Target Coverage. *Cancers*. 2022;14:1365.
- [76] Li Y, Kardar L, Li X, et al. On the interplay effects with proton scanning beams in stage III lung cancer. *Medical Physics*. 2014;41:021721.
- [77] Smith GCS. Parachute use to prevent death and major trauma related to gravitational challenge: systematic review of randomised controlled trials. *BMJ*. 2003;327:1459–1461.
- [78] Hansen CR, Crijns W, Hussein M, et al. Radiotherapy Treatment planning study Guidelines (RATING): A framework for setting up and reporting on scientific treatment planning studies. *Radiotherapy and Oncology*. 2020;153:67–78.
- [79] Niezink A, Jain V, Chouvalova O, et al. PO-0782 External validation of NTCP models for pneumonitis in lung cancer patients receiving proton therapy. *Radiotherapy and Oncology*. 2019;133:S404–S405.
- [80] Upadhyay R, Venkatesulu BP, Giridhar P, et al. Risk and impact of radiation related lymphopenia in lung cancer: A systematic review and meta-analysis. *Radiotherapy and Oncology*. 2021;157:225–233.



- [81] Friedes C, Chakrabarti T, Olson S, et al. Association of severe lymphopenia and disease progression in unresectable locally advanced non-small cell lung cancer treated with definitive chemoradiation and immunotherapy. *Lung Cancer*. 2021;154:36–43.
- [82] Cho Y, Kim Y, Chamseddine I, et al. Lymphocyte dynamics during and after chemo-radiation correlate to dose and outcome in stage III NSCLC patients undergoing maintenance immunotherapy. *Radiotherapy and Oncology*. 2022;168:1–7.
- [83] Pujol J-L. Durvalumab Induces Sustained Survival Benefit After Concurrent Chemoradiotherapy in Stage III Non–Small-Cell Lung Cancer. *JCO*. 2022;40:1271–1274.
- [84] McIntyre M, Wilson P, Gorayski P, et al. A Systematic Review of LET-Guided Treatment Plan Optimisation in Proton Therapy: Identifying the Current State and Future Needs. *Cancers*. 2023;15:4268.
- [85] Helse- og omsorgsdepartementet. Nasjonal handlingsplan for kliniske studier [Internet]. 2021 [cited 2023 Dec 18]. Available from: [https://www.regjeringen.no/contentassets/c3dcd95b7d741319c62642865afada/i-1206b\\_kliniske\\_studier\\_uu.pdf](https://www.regjeringen.no/contentassets/c3dcd95b7d741319c62642865afada/i-1206b_kliniske_studier_uu.pdf).

---

## **Publications**









Article

# Enhancing Radiotherapy for Locally Advanced Non-Small Cell Lung Cancer Patients with iCE, a Novel System for Automated Multi-Criterial Treatment Planning Including Beam Angle Optimization

Kristine Fjellanger <sup>1,2,\*</sup> , Liv Bolstad Hysing <sup>1,2</sup>, Ben J. M. Heijmen <sup>3</sup>, Helge Egil Seime Pettersen <sup>1</sup> , Inger Marie Sandvik <sup>1</sup>, Turid Husevåg Sulen <sup>1</sup>, Sebastiaan Breedveld <sup>3</sup> and Linda Rossi <sup>3</sup>

<sup>1</sup> Department of Oncology and Medical Physics, Haukeland University Hospital, 5021 Bergen, Norway; liv.bolstad.hysing@helse-bergen.no (L.B.H.); helge.egil.seime.pettersen@helse-bergen.no (H.E.S.P.); inger.marie.sandvik@helse-bergen.no (I.M.S.); turid.husevag.sulen@helse-bergen.no (T.H.S.)

<sup>2</sup> Institute of Physics and Technology, University of Bergen, 5007 Bergen, Norway

<sup>3</sup> Department of Radiotherapy, Erasmus University Medical Center (Erasmus MC), 3015 GD Rotterdam, The Netherlands; b.heijmen@erasmusmc.nl (B.J.M.H.); s.breedveld@erasmusmc.nl (S.B.); l.rossi@erasmusmc.nl (L.R.)

\* Correspondence: kristine.fjellanger@helse-bergen.no



**Citation:** Fjellanger, K.; Hysing, L.B.; Heijmen, B.J.M.; Pettersen, H.E.S.; Sandvik, I.M.; Sulen, T.H.; Breedveld, S.; Rossi, L. Enhancing Radiotherapy for Locally Advanced Non-Small Cell Lung Cancer Patients with iCE, a Novel System for Automated Multi-Criterial Treatment Planning Including Beam Angle Optimization. *Cancers* **2021**, *13*, 5683. <https://doi.org/10.3390/cancers13225683>

Academic Editors: Laura Cella, Giuseppe Palma and Andrew Hope

Received: 13 October 2021

Accepted: 10 November 2021

Published: 13 November 2021

**Publisher's Note:** MDPI stays neutral with regard to jurisdictional claims in published maps and institutional affiliations.



**Copyright:** © 2021 by the authors. Licensee MDPI, Basel, Switzerland. This article is an open access article distributed under the terms and conditions of the Creative Commons Attribution (CC BY) license (<https://creativecommons.org/licenses/by/4.0/>).

**Simple Summary:** In treatment planning for intensity-modulated radiotherapy (IMRT), optimization objectives and beam angle settings are individualized for the anatomy of each patient. This is a complex interactive process that is usually performed by a treatment planner. In this study, a novel system for automated optimization of IMRT plans with integrated beam angle optimization (BAO) was developed, and used to systematically investigate the impact of selected beam angles on treatment plan quality for locally advanced non-small cell lung cancer (LA-NSCLC). Automatically generated plans were of a higher quality than the manually generated, clinically delivered plans, while dramatically reducing the planning workload. The study demonstrates the potential for automated planning with integrated BAO to enhance radiotherapy for LA-NSCLC patients.

**Abstract:** In this study, the novel iCE radiotherapy treatment planning system (TPS) for automated multi-criterial planning with integrated beam angle optimization (BAO) was developed, and applied to optimize organ at risk (OAR) sparing and systematically investigate the impact of beam angles on radiotherapy dose in locally advanced non-small cell lung cancer (LA-NSCLC). iCE consists of an in-house, sophisticated multi-criterial optimizer with integrated BAO, coupled to a broadly used commercial TPS. The in-house optimizer performs fluence map optimization to automatically generate an intensity-modulated radiotherapy (IMRT) plan with optimal beam angles for each patient. The obtained angles and dose-volume histograms are then used to automatically generate the final deliverable plan with the commercial TPS. For the majority of 26 LA-NSCLC patients, iCE achieved improved heart and esophagus sparing compared to the manually created clinical plans, with significant reductions in the median heart  $D_{\text{mean}}$  (8.1 vs. 9.0 Gy,  $p = 0.02$ ) and esophagus  $D_{\text{mean}}$  (18.5 vs. 20.3 Gy,  $p = 0.02$ ), and reductions of up to 6.7 Gy and 5.8 Gy for individual patients. iCE was superior to automated planning using manually selected beam angles. Differences in the OAR doses of iCE plans with 6 beams compared to 4 and 8 beams were statistically significant overall, but highly patient-specific. In conclusion, automated planning with integrated BAO can further enhance and individualize radiotherapy for LA-NSCLC.

**Keywords:** autoplanning; automated treatment planning; beam angle optimization (BAO); beam configuration; Erasmus-iCycle and Eclipse; iCE; locally advanced non-small cell lung cancer (LA-NSCLC); intensity-modulated radiotherapy (IMRT); radiotherapy

## 1. Introduction

The standard treatment for locally advanced non-small cell lung cancer (LA-NSCLC) is concurrent chemoradiotherapy [1]. Intensity-modulated radiotherapy (IMRT) is the state-of-the-art radiation technique, allowing optimal shaping of the delivered dose to the target. IMRT has improved outcomes compared to conformal radiotherapy, but side effects are still common and potentially severe [2]. Decreasing the radiation dose to organs at risk (OARs) is desirable both for toxicity reduction and the potential for dose escalation [1,3].

The aim of radiotherapy treatment planning is to establish treatment unit settings for each patient that will result in a high-quality dose distribution, i.e., a high dose inside the target volume and limited dose outside, especially in the OARs. IMRT treatment plans are generated using a cost function that defines the planning objectives for the target, OARs and other tissues, and their relative weights. A mathematical optimizer derives patient-specific beam intensity profiles that minimize the cost function value. In manual IMRT treatment planning, the general approach is to begin the plan generation for a new patient using a tumor-site-specific template for the cost function. In an iterative trial-and-error process, the objectives and weights are then adapted by the manual planner to account for the patient's anatomy. For fixed-beam IMRT treatment in the thorax, the beam angles should also be individually tuned, as IMRT with carefully selected beam angles can reduce OAR doses compared to volumetric modulated arc therapy (VMAT) or IMRT with non-optimized beam angles [4]. In clinical routine, time pressure limits the possibility to test many different objective and beam angle settings, and the planner's experience or skills may affect the quality of the plans. A number of studies have demonstrated that manually created plans may be suboptimal [5–9].

In recent years, several systems for automated treatment planning have been presented. Compared to manual planning, automated planning can considerably increase the plan quality while dramatically reducing the planning workload [7].

Erasmus-iCycle, developed at the Erasmus University Medical Center (Erasmus MC, Rotterdam, The Netherlands), is a system for automated multi-criterial treatment planning that can generate beam profiles for pre-selected beam directions, but it also features integrated beam profile and beam angle optimization (BAO) [10–16]. With appropriate treatment-site-specific configuration (creation of a “wish-list”), the generated Pareto-optimal plans are also clinically favorable. Erasmus-iCycle generates plans using fluence map optimization (FMO), but there is no consecutive segmentation, and therefore the plans are not directly deliverable. For the generation of clinically deliverable plans at Erasmus MC, Erasmus-iCycle is used as a pre-optimizer, with consecutive automatic reconstruction of FMO plans into segmented plans in the Monaco treatment planning system (TPS) (Elekta AB, Stockholm, Sweden). For this purpose, patient-specific Monaco optimization templates are created based on the achieved constraint and objective values in the Erasmus-iCycle FMO plan. Several publications have demonstrated the effectiveness of this approach in reducing OAR doses and planning time for different treatment sites [17–21], including VMAT of LA-NSCLC [8]. The Erasmus-iCycle wish-list-based lexicographic optimization approach for automated multi-criterial treatment planning has recently been adopted by a commercial party [22].

The Eclipse TPS (Varian Medical Systems, Inc., Palo Alto, CA, USA) features the RapidPlan system for automated knowledge-based treatment planning, whereby a library of previous treatment plans is used to predict feasible patient-specific OAR dose-volume histograms (DVHs) for new patients [23]. The predicted DVHs are converted into optimization parameters for automatic generation of deliverable treatment plans. A limitation of RapidPlan for automated IMRT planning for LA-NSCLC is that it does not feature patient-specific BAO. Therefore, the beam configuration must be determined manually by trial-and-error.

While treatment planning systems featuring advanced BAO are not commercially available, BAO methods have been investigated for their use in radiotherapy of lung cancer. Yuan et al. used a wide range of lung tumors to tune a BAO system for coplanar

configurations, and applied it for more complex, non-coplanar plans [24]. Amit et al. presented a learning-based method which was applied for various thoracic indications [25]. In both studies, beam angle and beam profile optimization were not integrated; first, patient-specific beam angles were established, followed by IMRT optimization for the selected (fixed) angles. The results showed that plans with optimized beam angles had similar quality to clinical plans with manually selected beam angles.

The aim in this study was to automatically create IMRT plans with integrated optimization of beam angles for a prospective database of LA-NSCLC patients, in order to improve plan quality compared to manually created plans and to investigate the impact of beam angles on plan quality. For this purpose, Erasmus-iCycle was coupled with Eclipse to establish the novel “iCE” system. In iCE, Erasmus-iCycle is used as a pre-optimizer to automatically generate an initial Pareto-optimal FMO treatment plan with optimized beam angles for each patient. The OAR DVHs of this plan are converted into patient-specific optimization parameters for automated generation of the final deliverable plan in Eclipse. Both iCE plans and autoplans using the manually selected beam angles were compared to the manually generated, clinically delivered plans. Finally, iCE was used to investigate the effect of changing the number of IMRT beams.

## 2. Materials and Methods

### 2.1. Patients and Clinical Treatment Planning

Twenty-five consecutive patients with stage IIB-IIIc non-small cell lung cancer were prospectively included in this study. One patient with stage IVA, who had a single brain metastasis surgically removed prior to radiotherapy, received radiotherapy according to the protocol for LA-NSCLC and was also included. All patients received IMRT and concurrent or sequential chemotherapy at Haukeland University Hospital (HUH) between October 2019 and August 2021. The study was approved by the regional committee for medical and health research ethics (protocol code 2019/749) and all participants provided their informed consent.

All patients had both a 10-phase 4DCT and a deep inspiration breath-hold (DIBH) CT at planning. Treatment plans were created on the average intensity projection (AIP) of the 4DCT and treatment was given in free breathing (FB) conditions as a standard. However, for patients with very large breathing motion or where lung dose constraints could not be met with the AIP, the treatment plans were created on the DIBH CT instead (four patients).

The responsible oncologist delineated the gross tumor volumes (GTVs) for the primary tumor and lymph nodes according to ESTRO guidelines [26]. For FB treatment, the internal GTVs (IGTVs) included the GTV positions on all 4DCT phases. For DIBH treatment, three repeated DIBH scans were taken at planning and the IGTVs encompassed the GTV positions on all three scans. The clinical target volume (CTV) was defined by expanding the IGTV by 5 mm without extending into uninvolved organs such as bone, heart, esophagus and major vessels. A 5 mm isotropic margin from the CTV was used to define the planning target volume (PTV). As OARs, the lungs, heart, esophagus, spinal canal and brachial plexus (if relevant) were delineated according to RTOG guidelines [27].

The clinical plans (CLIN) were manually created by expert planners in Eclipse v. 15.6 or 16.1 using the Photon Optimizer algorithm for optimization and the Acuros External Beam algorithm for dose calculation. All plans included 6 coplanar IMRT beams with beam angles based on a template that was individually adapted. In accordance with national guidelines, the prescribed dose was 60 or 66 Gy for concomitant treatment (depending on lung function, lung dose and proximity of the brachial plexus to the PTV) and 70 Gy for sequential treatment, all administered in 2 Gy fractions. The plans were normalized to the median dose in the PTV. The dose constraints applied for planning are provided in Table 1.



**Table 1.** Planning dose constraints for the PTV, OARs and normal tissue.  $D_p$  = prescribed dose. In cases where fulfilling all constraints was impossible, the responsible oncologist decided whether target coverage or OAR constraints should be compromised.

Volume	Dose Constraint
PTV	$V_{95\%} > 98\%$
Lungs	$V_{5Gy} < 65\%$
	$V_{20Gy} < 35\%$
	$D_{mean} < 20$ Gy
Heart	$V_{30Gy} < 40\%$
Esophagus	$D_{mean} < 34$ Gy
Spinal canal	$D_{max} < 50$ Gy
Brachial plexus	$D_{max} < 66$ Gy
Patient body	$D_{max} < D_p \cdot 1.07$

## 2.2. iCE Treatment Planning

### 2.2.1. Erasmus-iCycle Wish-List Creation and FMO Plan Generation

A detailed description of Erasmus-iCycle functionality and wish-list creation can be found elsewhere [10,28]. In this study, an Erasmus-iCycle wish-list for LA-NSCLC was established and tuned according to clinical priorities at HUH. An oncologist (IMS) and an expert planner (THS) were involved in the evaluation of treatment plans during this process. In the first phase of tuning, five of the patients treated in FB with 66 Gy were used. The PTV coverage and high dose conformity were kept similar to the clinical plans, while the dose to the OARs and undefined normal tissue was minimized. The wish-list was then applied for an additional four patients with a 60 Gy prescription and/or DIBH CT, and some final adjustments were made.

In the final wish-list, hard constraints were used for the maximum dose to the spinal canal, brachial plexus and PTV, and for an external ring to prevent high entrance doses. Target and OAR objectives were added with the following order of priority (in line with clinical priorities): PTV coverage, lung  $D_{mean}$ , heart  $D_{mean}$  and esophagus  $D_{mean}$ . In addition, constraints and objectives were applied for normal tissue at specified distances from the PTV to steer conformity. The full wish-list is provided in Table 2.

In the multi-criterial plan generation, the objective functions are consecutively minimized following the allotted priorities. After the minimization of an objective function, a constraint is added to the problem to avoid quality loss for this objective when minimizing the following lower priority objectives. Two rounds of consecutive minimizations of objective functions are applied. In the first round, the constraint that is added after an objective minimization is the Goal value (second to last column in Table 2), if it could be obtained, regardless of the possibility for further improvement. If the Goal value is not achieved, the obtained objective value, with some relaxation, is added as a constraint. In the second round, all objectives without a Sufficient value (last column in Table 2) are minimized to the fullest extent, following the order of priority. In this way, the Goal and Sufficient values make sure undesired and unnecessary greediness in minimizing objectives is avoided, leaving room for minimizing lower priority objectives [10].

The candidate beam angles for BAO were in the range of 140–40° for right-sided tumors and 320–220° for left-sided tumors with 5° spacing.

**Table 2.** Applied Erasmus-iCycle wish-list.  $D_p$  = prescribed dose, 60/66/70 Gy; different logarithmic tumor control probability (LTCP) settings were used depending on  $D_p$ . Note that the goal value for constraints was set slightly stricter than the actual clinical limit to account for finite sampling resolution.

Priority	Volume	Type	Goal	Sufficient
Constraint	PTV	Max	$D_p \cdot 1.02$	
Constraint	PTV	Mean	$D_p \cdot 0.997$	
Constraint	Spinal canal	Max	47 Gy	
Constraint	Brachial plexus	Max	60 Gy	
Constraint	Shell PTV + 1 cm <sup>1</sup>	Max	$D_p$	
Constraint	Shell PTV + 7 cm <sup>1</sup>	Max	$D_p \cdot 0.75$	
Constraint	External ring <sup>2</sup>	Max	$D_p \cdot 0.8$	
1	PTV	↓ LTCP <sup>3</sup>	0.14/0.12/0.12	0.14/0.12/0.12
2	Lungs	↓ Mean	19 Gy	
3	Shell PTV + 3 mm <sup>1</sup>	↓ Max	$D_p$	$D_p$
4	Shell PTV + 1 cm <sup>1</sup>	↓ Max	$D_p \cdot 0.9$	$D_p \cdot 0.9$
5	Shell PTV + 7 cm <sup>1</sup>	↓ Max	$D_p \cdot 0.65$	
6	Lungs	↓ Mean	13 Gy	
7	Heart	↓ Mean	13 Gy	
8	Esophagus	↓ Mean	18 Gy	
9	Shell PTV + 3 cm <sup>1</sup>	↓ Max	$D_p \cdot 0.75$	
10	Shell PTV + 7 cm <sup>1</sup>	↓ Max	$D_p \cdot 0.55$	
11	Lungs	↓ Mean	0 Gy	
12	Heart	↓ Mean	0 Gy	
13	Esophagus	↓ Mean	0 Gy	

<sup>1</sup> Shells consist of all pixels located at the specified distance from the PTV. <sup>2</sup> Ring structure extending 2 cm inside the patient surface, subtracting PTV + 4 cm. <sup>3</sup> Logarithmic tumor control probability (LTCP) as defined in [10], using prescription  $D_p \cdot 0.95$  and  $\alpha = 0.85/0.8/0.8$ .

### 2.2.2. Generation of the Final iCE Plan Based on an Initial Erasmus-iCycle FMO Plan

The Erasmus-iCycle FMO plan was used to create a patient-specific objective template for automated generation of the final deliverable plan in Eclipse. This was performed automatically by a script that moved information from the OAR DVHs in .csv format into an objective template in .xml format (see Supplementary Materials). For each OAR involved, a line objective was created. Line objectives are defined by a collection of dose-volume pairs and limit the dose for all volume levels [29]. The distance between dose-volume points defining the line was set to 0.7 Gy. For the PTV objectives, the same fixed settings as in the clinical plans were used. Priorities and normal tissue objective settings were kept constant after tuning based on the first five patients. Table 3 shows the final template that was used for all of the patients.

**Table 3.** Applied Eclipse objective template. p.s. = patient specific, defined based on Erasmus-iCycle DVHs.

Volume	Type	Dose [Gy]	Priority
PTV_60/66/70	Min	59.5/65.5/69.5	130
	Max	60.5/66.5/70.5	130
Lungs	Line	p.s.	80
Heart	Line	p.s.	80
Esophagus	Line	p.s.	60
Spinal canal	Max	48	100
	Line	p.s.	40
Brachial plexus	Max	62	100
	Line	p.s.	40
Patient body	NTO <sup>1</sup>	-	100

<sup>1</sup> NTO = normal tissue objective, with the following fixed parameters: distance from target border 0.5 cm, start dose 105%, end dose 60% and fall-off 0.15 [30].

The generated objective templates as well as the optimized beam angles from Erasmus-iCycle were used for automated IMRT plan optimization in Eclipse, with no manual fine-tuning. The applied Eclipse version was the same as the version used for clinical planning. The final iCE plans were visually inspected to ensure that the high-dose conformity and the dose to undefined normal tissue was acceptable and comparable to the CLIN plans.

### 2.3. Comparison of iCE and CLIN Plans

For each patient, a 6-beam iCE plan (same beam number as clinically used) was generated, and compared to the corresponding CLIN plan using relevant dose-volume metrics for the target and OARs. The mean dose to the lungs, heart and esophagus are commonly reported parameters related to toxicity, and were therefore used for evaluation of per-patient differences. To separately assess the benefit of BAO in iCE, a second iCE plan (iCE\_noBAO) was generated for each patient, using the same beam angles as the CLIN plan, i.e., BAO in iCE was switched off.

### 2.4. Planning Times

The manual planning time was estimated from discussions with three treatment planners involved in clinical LA-NSCLC planning. The hands-on time in iCE planning, related to starting autoplanning and transfer of data between systems, was recorded.

### 2.5. Dosimetric QA of Plan Deliverability

For 10 randomly selected patients, the deliverability of the iCE plans was evaluated following the current clinical quality assurance (QA) procedure for this diagnosis at HUH. Electronic Portal Imaging Device measurements were performed, followed by analysis in the Portal Dosimetry system in Eclipse. A gamma passing rate of 95%, with a global criterion of 3%/3 mm, was required. In addition, the number of monitor units (MUs) in CLIN and iCE plans were compared.

### 2.6. 6-Beam vs. 4- and 8-Beam iCE

In addition to the 6-beam plans, iCE was also used to generate plans with 4 and 8 beams, to validate the clinical use of 6 beams for all patients. Relevant target and OAR dose-volume metrics were compared for the different numbers of beams.

### 2.7. Statistical Analysis

The two-tailed Wilcoxon signed-rank test was used for the statistical testing of dose-volume parameters for CLIN vs. iCE and iCE\_noBAO plans, and 6-beam vs. 4- and 8-beam plans.  $p$ -values  $\leq 0.05$  were considered as statistically significant.

## 3. Results

### 3.1. Patients

Among the 26 included patients, 21 had both a primary tumor and lymph nodes in the target volume, one had only lymph nodes and four had only a primary tumor. The distribution of stages, primary tumor locations, dose prescriptions and timing of the chemotherapy are summarized in Table 4. The average PTV volume was 395 cm<sup>3</sup> (range 138–1715 cm<sup>3</sup>).

**Table 4.** Patient and treatment characteristics.

Characteristic	Number of Patients
<b>Stage</b>	
IIB	2
IIIA	11
IIIB	10
IIIC	2
IVA	1
<b>Primary tumor location (lobe)</b>	
Right upper	10
Right upper + middle	1
Right lower	4
Left upper	4
Left lower	6
<b>Prescribed dose</b>	
60 Gy	10
66 Gy	15
70 Gy	1
<b>Chemotherapy</b>	
Concurrent	25
Sequential	1

### 3.2. Comparison of iCE and CLIN Plans

Overall, the iCE plans were clearly superior to the CLIN plans (Table 5, Figure 1). While the target coverage and lung dose were similar, the median heart  $D_{\text{mean}}$  was reduced from 9.0 Gy to 8.1 Gy ( $p = 0.02$ ), the median esophagus  $D_{\text{mean}}$  from 20.3 Gy to 18.5 Gy ( $p = 0.02$ ), the median heart  $V_{30\text{Gy}}$  from 11.0% to 6.2% ( $p = 0.002$ ) and the median esophagus  $V_{20\text{Gy}}$  from 38.4% to 36.8% ( $p = 0.008$ ) for iCE compared with CLIN. The maximum dose to the brachial plexus and patient body followed the clinic's requirements for all plans. The maximum dose to the spinal canal slightly exceeded the limit for two patients in both the CLIN and iCE plans, but these violations were located in very small volumes at the edge of the contour and were therefore found to be clinically acceptable.

**Table 5.** Dose-volume metrics for CLIN compared with iCE and iCE\_noBAO plans. Median value and interquartile range (IQR) is given, along with  $p$ -values for difference with regard to CLIN. Significant differences from CLIN are marked with \*.

Dose Metric	CLIN		iCE		$p$	iCE_noBAO		
	Median	IQR	Median	IQR		Median	IQR	$p$
PTV $V_{95\%}$ [%]	99.0	0.9	99.2	0.5	0.1	99.3	0.5	0.2
Lungs $D_{\text{mean}}$ [Gy]	14.7	4.2	14.2	4.7	0.3	14.6	4.4	0.4
Lungs $V_{5\text{Gy}}$ [%]	55.8	11.7	54.7	10.9	0.6	57.4	12.7	0.1
Lungs $V_{20\text{Gy}}$ [%]	25.0	6.7	24.4	7.9	0.5	24.3	7.0	0.2
Heart $D_{\text{mean}}$ [Gy]	9.0	7.1	8.1	5.9	0.02 *	8.3	6.7	0.07
Heart $V_{5\text{Gy}}$ [%]	34.0	33.1	31.8	30.9	0.7	33.2	31.6	0.9
Heart $V_{30\text{Gy}}$ [%]	11.0	9.5	6.2	6.5	0.002 *	8.8	8.4	0.002 *
Esophagus $D_{\text{mean}}$ [Gy]	20.3	8.2	18.5	9.2	0.02 *	18.9	9.1	0.05 *
Esophagus $V_{20\text{Gy}}$ [%]	38.4	14.3	36.8	17.7	0.008 *	35.4	16.4	0.08
Esophagus $V_{60\text{Gy}}$ [%]	5.1	14.3	4.9	12.8	1.0	4.7	13.2	0.05 * <sup>1</sup>

<sup>1</sup> Although the median value is lower, this parameter was significantly *increased* with iCE\_noBAO compared to CLIN (the value was higher in iCE\_noBAO for 16 patients, higher in CLIN for 9 patients and equal for 1 patient).

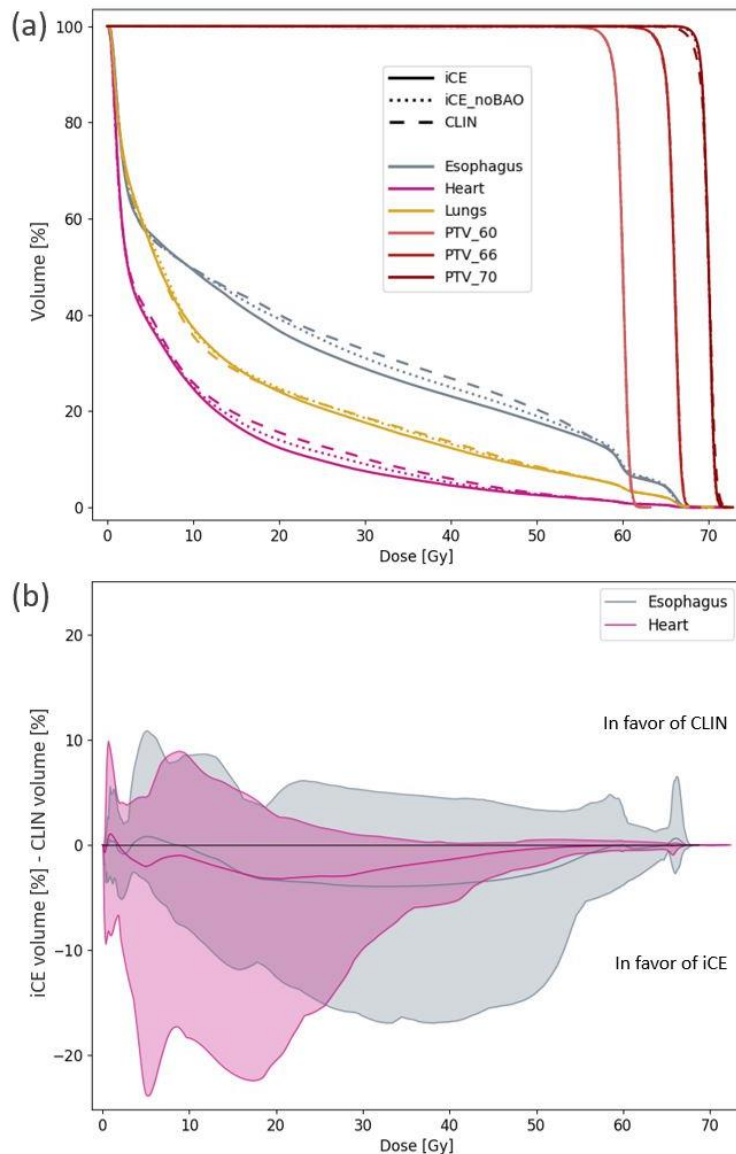


**Figure 1.** (a) Population average DVHs for PTV and OARs for CLIN, iCE and iCE\_noBAO plans. 10 patients had PTV\_60, 15 had PTV\_66 and 1 had PTV\_70. (b) Average DVH differences between CLIN and iCE plans for heart and esophagus (central bold lines) with 95% confidence intervals (shaded areas). For lungs, the differences were small and clinically insignificant.

The iCE plans spared the heart and esophagus for most dose levels as compared to CLIN (Figure 1b). The 95% confidence interval shows the large advantage of using iCE for some patients, with reductions of more than 15 percentage points in the heart volume receiving 5–25 Gy, and the esophagus volume receiving 25–50 Gy. The potential for substantial OAR sparing with iCE for individual patients is also evident in Figure 2, which shows reductions of more than 5 Gy in the  $D_{\text{mean}}$  of both the heart and esophagus compared

to CLIN. iCE reduced the heart  $D_{mean}$  for 19/26 patients and the esophagus  $D_{mean}$  for 17/26 patients. The differences in the mean lung dose were small (Figures 1a and 2).

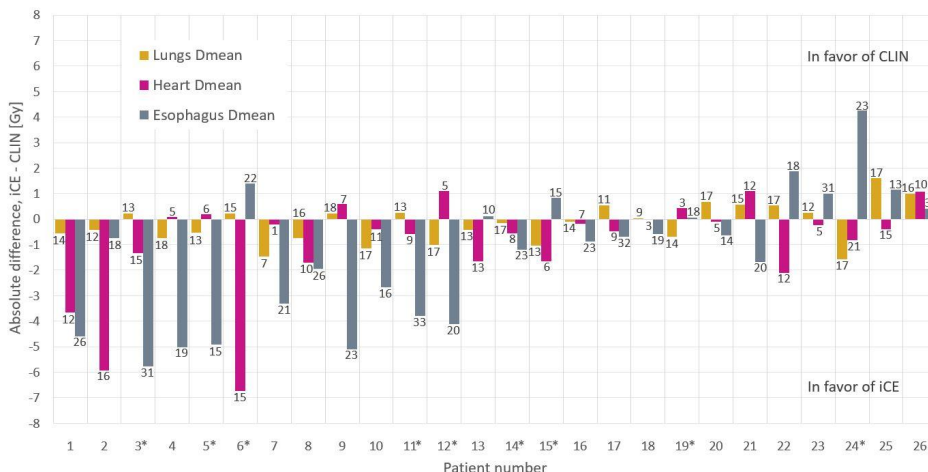


**Figure 2.** Differences in OAR mean doses between CLIN and iCE plans per patient. The numbers on the bars indicate the  $D_{mean}$  values [Gy] in the CLIN plans. The patients are sorted according to the sum of differences for all OARs. Patients marked with \* were used in wish-list tuning.

In general, the beam configurations used in the CLIN plans had most weight on the anterior-posterior direction, with little variation in the angles chosen for each patient. In contrast, the optimized beam angles in the iCE plans were well dispersed across the candidate beam space, revealing a large difference in optimal angles between patients (Figure 3). In Figure 4a,b, the optimized beam configuration in the iCE plan for patient 1 is compared with the configuration in the CLIN plan. The clear differences between the setups result in considerable sparing of the heart and esophagus with iCE (see also Figure 2). Additional examples with different tumor locations are shown in the Appendix A (Figures A1 and A2).

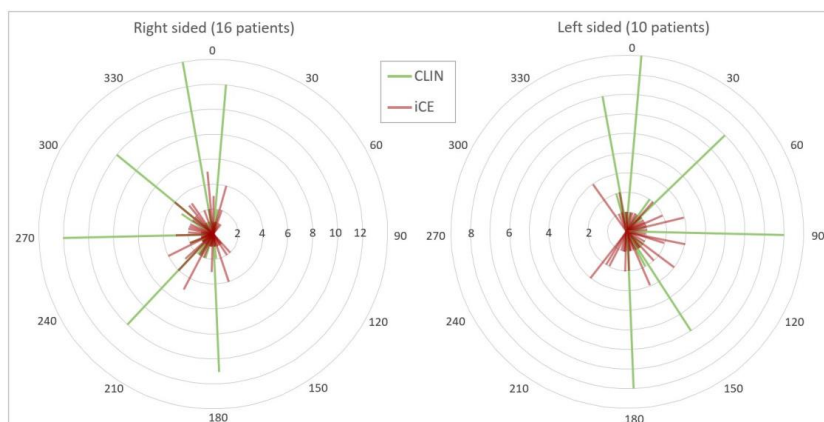


**Figure 3.** Selected beam angles in the CLIN plans (green) and optimized beam angles in the iCE plans (red) for patients with right-sided and left-sided tumors. Angles are rounded to the nearest 5 degrees. The number of patients is shown on the radial axis, and the angular axis shows beam angle in degrees.

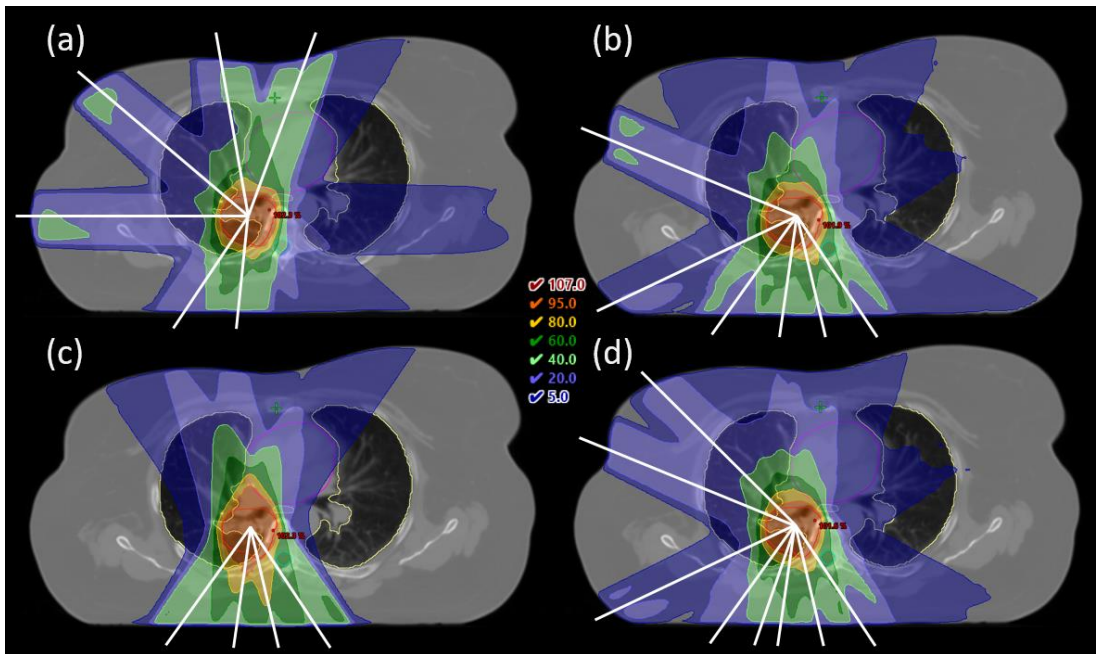


**Figure 4.** (a) CLIN plan with manually selected beam angles for patient 1. (b–d) iCE plans with 6, 4 and 8 optimized beam angles for the same patient. Dose is shown relative to the prescribed dose (66 Gy). Contours are the PTV (red), lungs (yellow), heart (magenta), esophagus (grey) and spinal cord (cyan), and beam angles are indicated by white lines.

When switching off BAO in iCE (iCE\_noBAO), the reductions compared to CLIN in heart  $V_{30\text{Gy}}$  and esophagus  $D_{\text{mean}}$  were smaller than with BAO, but remained statistically significant. Figure 1 and Table 5 illustrate that some OAR sparing is achieved with iCE\_noBAO compared to CLIN, and adding BAO in iCE results in a further improvement.

### 3.3. Planning Times

The manual planning time for the CLIN plans was usually between 2 and 4 h, although it could vary from less than an hour to a full day depending on the complexity of the case. This mainly comprised hands-on time, including adjustments of the beam configuration and optimization objectives during repeated rounds of optimization. For iCE, hands-on time was less than 10 min. The Erasmus-iCycle calculation time for automated generation of 6-beam plans was 1.5–3 h (7–25 min without BAO), and automated generation of the final deliverable plan with Eclipse took around 5 min.

### 3.4. Dosimetric QA of Plan Deliverability

All fields in all measured plans (in total 60 fields) passed the clinical requirement in the Portal Dosimetry analysis, with an average passing rate of 99.97% (range 99.0–100%). The average number of MUs in the iCE plans was 778 (range 474–1323), compared to 687 (range 406–1159) in the CLIN plans.

### 3.5. 6-Beam vs. 4- and 8-Beam iCE

While 6- and 8-beam iCE plans generally fulfilled the clinical dose constraints, not all 4-beam plans would have been acceptable due to a  $D_{\text{max}}$  in the spinal canal or patient body above the requirement (Table A1). High- and medium-dose conformity was also generally worse with 4 beams than with 6 or 8, as visible in Figures 4, A1 and A2. The target coverage was similar regardless of the number of beams. Reducing the number

of beams from 6 to 4 led to a median increase in  $D_{\text{mean}}$  of 0.7 Gy to the heart ( $p = 0.007$ ) and 1.2 Gy to the esophagus ( $p = 0.02$ ). Increasing the number of beams from 6 to 8 had a smaller, but still significant, benefit of 0.3 Gy to the heart ( $p = 0.02$ ) and 0.7 Gy to the esophagus ( $p < 0.001$ ) (Table 6 and Figure 5). The median  $D_{\text{mean}}$  for the lungs was similar for the different numbers of beams, but the DVH shows that 4-beam plans, on average, gave less low dose and more medium and high dose to the lungs compared with the 6- and 8-beam plans.

**Table 6.** Median differences in  $D_{\text{mean}}$  with range for OARs in 4- and 8-beam iCE plans compared to 6-beam iCE plans, all with optimized beam angles.  $p$ -values for comparison with 6-beam plans are given, and significant differences are marked with \*.

Dose Metric	Difference, 4 vs. 6 Beams			Difference, 8 vs. 6 Beams		
	Median	Range	$p$	Median	Range	$p$
Lungs $D_{\text{mean}}$ [Gy]	0.2	−2.5, 2.3	0.5	−0.2	−0.8, 0.5	0.004 *
Heart $D_{\text{mean}}$ [Gy]	0.7	−2.3, 4.0	0.007 *	−0.3	−3.9, 1.5	0.02 *
Esophagus $D_{\text{mean}}$ [Gy]	1.2	−4.2, 6.8	0.02 *	−0.7	−2.8, 2.9	<0.001 *

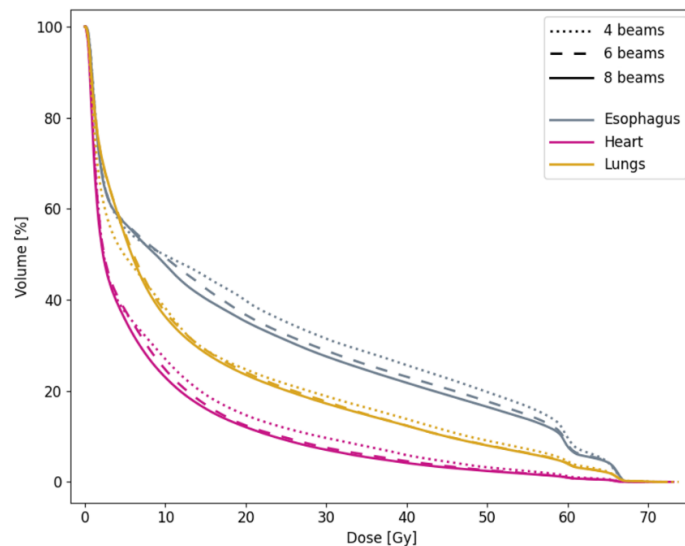


**Figure 5.** Population average DVHs for OARs in 4-, 6- and 8-beam iCE plans with optimized beam angles.

While the OAR doses overall decreased with an increasing number of beams, there was significant inter-patient variation (Tables 6 and A1). With 8 beams, for 15/26 patients the  $D_{\text{mean}}$  was reduced for all of the evaluated OARs compared to 6 beams, while for the remainder of patients, the dose was increased for one of the OARs. Around half the patients had a reduced lung  $D_{\text{mean}}$  with 4 beams compared to 6 beams, but this came at the cost of a higher dose to the heart and/or esophagus. For patient 1, less spreading of the low dose with 4 beams resulted in a sparing in the lung  $D_{\text{mean}}$  of 2.5 Gy compared to 6 beams (Figure 4b–d). However, this was achieved at the cost of increased heart and esophagus  $D_{\text{mean}}$  of 1.8 Gy and 3.3 Gy respectively, and worse high-dose conformity. In the 8-beam plan, the lung  $D_{\text{mean}}$  was slightly higher than with 6 beams, while sparing of the heart and esophagus was improved. For some of the patients, changing the number of



beams had little impact on the OAR doses; three patients had a change in the  $D_{\text{mean}}$  of less than 1 Gy for all OARs, both when reducing and when increasing the number of beams.

#### 4. Discussion

The novel iCE system for automated multi-criterial treatment planning with integrated BAO was developed, and used to investigate opportunities for OAR sparing in LA-NSCLC patients, and to systematically investigate the impact of beam angles on the radiotherapy dose. Compared to clinical plans, significant reductions in heart  $D_{\text{mean}}$  and  $V_{30\text{Gy}}$  and esophagus  $D_{\text{mean}}$  and  $V_{20\text{Gy}}$  were achieved with iCE. When using iCE with integrated patient-specific BAO, OAR sparing was found to be superior compared to using iCE for clinically applied beam angles. Increasing the number of optimized beams can improve OAR sparing. On average, differences in OAR sparing were found to be larger between 4 and 6 beams than between 6 and 8. The impact of the beam number varied largely between patients, and for some patients, changing the number of beams did not have a clinically relevant impact on the dose to any OAR.

While the reductions with iCE compared to CLIN in median  $D_{\text{mean}}$  for OARs were 0.5–1.8 Gy, a substantial sparing of >5 Gy was seen for the heart and esophagus for individual patients. This confirms one of the main strengths of automated planning; the ability to achieve a more homogeneous plan quality by avoiding occasional highly suboptimal plans. Bradley et al. reported an association between increased heart  $V_{30\text{Gy}}$  and increased risk of death, and Dess et al. found that mean heart dose,  $V_{5\text{Gy}}$  and  $V_{30\text{Gy}}$  were associated with grade  $\geq 3$  cardiac events [31,32]. Wijsman et al. reported on a correlation between mean esophagus dose and grade  $\geq 2$  acute esophageal toxicity [33]. These correlations suggest that the observed reductions in heart  $D_{\text{mean}}$  and  $V_{30\text{Gy}}$  and esophagus  $D_{\text{mean}}$  with iCE compared to CLIN are of clinical importance. Only minor differences were observed for lung dose, possibly because the lungs received the most attention in clinical planning. The dose to the spinal canal and brachial plexus were not studied in detail, as reductions below the maximum dose constraints are not considered a priority. An additional advantage of iCE compared to manual planning is the dramatic decrease in hands-on planning time, as the trial-and-error process of finding objectives and beam angles manually is avoided.

A previous study using Erasmus-iCycle for LA-NSCLC found reductions in the average  $D_{\text{mean}}$  of the lungs, heart and esophagus of 0.9, 1.5 and 3.6 Gy for automatically generated VMAT plans compared to manually created IMRT plans [8]. Although not directly comparable to our results, as the dose prescription, clinical priorities, delivery technique and TPS differed, the potential for reducing OAR doses for most patients with automated planning was found in both studies. The same has been found for other autoplanning strategies, including knowledge-based planning in Eclipse and multi-criteria optimization in RayStation (RaySearch Laboratories, Stockholm, Sweden) [9,23]. These findings highlight the potential of improving the plan quality in LA-NSCLC by increasing the availability, integration and utilization of autoplanning systems.

None of the published studies on automated planning for LA-NSCLC included integrated BAO to systematically investigate the impact of beam angles on plan quality, as has been performed in this study. Fixed-beam IMRT has the potential to reduce low dose to the lungs compared to VMAT, but exploiting this requires individual selection of appropriate beam angles [4]. LA-NSCLC is a heterogeneous patient group, and the position of the tumor in relation to OARs strongly affects which beam angles are most beneficial. The beam configurations in the CLIN plans, based on a template with emphasis on the anterior-posterior direction and a couple of additional lateral fields, were well suited for central tumors. For frontal and dorsal tumors, more oblique configurations, sometimes with opposing fields to cover nodal volumes, were selected by iCE and could spare dose to the heart, esophagus and/or contralateral lung for specific patients. Clearly, beam angles should be optimized individually in IMRT for LA-NSCLC.

In general, 6-beam plans appear to be a reasonable choice for this patient group. In some situations, reducing the number of beams in a treatment plan might be desirable, e.g.,

when the treatment time is of particular concern due to large target volume, split fields, DIBH treatment or poor condition of the patient. Similarly, increasing the number of beams might be appropriate in some situations, e.g., if OAR doses are above constraints. With the iCE method, creating several treatment plans with different numbers of optimized beams can be performed automatically, allowing for individual assessment of alternative plans. Plans with different numbers of beams can be created in a single round of optimization in Erasmus-iCycle, only the reconstruction in Eclipse must be done separately. Note that not all of the 4-beam iCE plans would be clinically acceptable. The wish-list constraints for the  $D_{\max}$  in the spinal canal and patient body as well as the high dose conformity were always achieved by default in Erasmus-iCycle. However, Eclipse struggled to reproduce the 4-beam dose distribution for some patients, and as hard constraints are not applied in Eclipse optimization, unacceptable plans could occur.

Increasing the number of beams on average improved OAR sparing, but the effect varied between patients. This is not surprising given the large heterogeneity in the anatomy of the LA-NSCLC patients. While the reasons behind the patient-specific differences were not investigated in detail, they appeared to be related to the OAR doses. Patients with high OAR doses had a greater benefit of increasing the number of beams than patients with low OAR doses. No impact of the size or location of the tumor was observed.

The average number of MUs was higher in the iCE plans than the CLIN plans (778 vs. 687). This could possibly be related to choices in the collimator angles, which were fixed at  $2^\circ$  in iCE plans, while in the CLIN plans, the collimator angle for each field was tuned to narrow the field size in the X direction, leading to larger field openings and fewer MUs. In our clinic, the enhanced MUs with iCE were not a concern, given the excellent deliverability of the plans. No restriction on the number of MUs was applied in the optimization of CLIN or iCE plans. Nonetheless, if desired, adjusting the collimator with regard to the optimized beam angles is a simple operation.

Different systems for automated treatment planning have different characteristics, advantages and limitations [7]. Advantages of Erasmus-iCycle are that configuration with a high-quality wish-list will result in optimal dose distributions according to the clinic's priorities, and that few (or even zero) example plans are needed for the wish-list configuration. In many studies, Erasmus-iCycle plans proved superior to the example plans used for configuration [13,17,19,34,35]. A limitation is that the generated dose distributions are not directly deliverable. Therefore, translations into segmented treatment plans must be performed. In this study, the translations were performed by the Eclipse TPS, with use of line objectives that offer a simple way of controlling the entire dose-volume range simultaneously. It also makes the configuration for new treatment sites simple, as the only tuning required for plan recreation in Eclipse is of the priorities and normal tissue objective.

RapidPlan is a tool for automated planning already integrated in Eclipse, using so-called knowledge-based planning. Comparing the quality of iCE and RapidPlan plans was not within the scope of this study, in part because RapidPlan does not feature BAO. Studies have shown the dependence of the output plan quality on the quality of plans in the RapidPlan library [36,37]. In future work, we plan to explore the possibility of building a RapidPlan library containing iCE plans.

A limitation of the current study is the total number of investigated patients. However, all patients had LA-NSCLC and they were prospectively included. Moreover, there was a large variation in the tumor location and OAR dose-volume parameters among these LA-NSCLC patients. In order to strengthen the statistics, some patients were used for both Erasmus-iCycle wish-list tuning and for comparisons between CLIN and iCE. This is not a concern in the same way as for library-based methods, as the wish-list is based on the clinical protocol and priorities and not directly on the test patients used for guiding the wish-list creation.

Furthermore, some information from the clinical planning (choice of FB vs. DIBH technique and 60 Gy vs. 66 Gy prescription) was transferred to the automated planning, as required for fair comparison. These properties are sometimes changed during the

planning process in response to the obtained OAR doses. With automated planning, several plans can be created with little additional work to find the most suitable option for each individual patient.

This study has been evaluated using the RATING criteria for treatment planning studies and a score of 96% was achieved [38].

## 5. Conclusions

The novel iCE system for automated multi-criterial IMRT treatment planning with integrated BAO was developed, and applied to optimize OAR sparing and to systematically investigate the impact of beam angles on plan quality for LA-NSCLC patients. A potential for improved sparing of the heart and esophagus was observed for most patients, with significant reductions in heart  $D_{\text{mean}}$  and  $V_{30\text{Gy}}$  and esophagus  $D_{\text{mean}}$  and  $V_{20\text{Gy}}$  with iCE compared to CLIN. Due to the automation, iCE reduced the hands-on planning time to the level of minutes. The dosimetric implications of increasing or reducing the number of treatment beams were highly patient-specific, but overall, increasing the number of beams improved OAR sparing. Due to the low workload, iCE could be used to generate a set of plans with different beam numbers for each patient and then select the best plan for the individual patient. Automated multi-criterial treatment planning with integrated BAO has great potential to further individualize and enhance radiotherapy for LA-NSCLC patients.

**Supplementary Materials:** The following are available online at <https://www.mdpi.com/article/10.3390/cancers13225683/s1>: Eclipse objective template: emptyObjectiveTemplate.xml and script for transferring patient-specific values from DVHs to objective templates: addObjectives.py.

**Author Contributions:** Conceptualization, K.F., L.B.H., B.J.M.H., H.E.S.P., S.B. and L.R.; methodology, K.F., L.B.H., B.J.M.H., H.E.S.P., S.B. and L.R.; software, K.F., H.E.S.P., S.B. and L.R.; validation, K.F.; formal analysis, K.F. and L.B.H.; investigation, K.F., L.B.H., I.M.S., T.H.S. and L.R.; resources, L.B.H., B.J.M.H., I.M.S. and T.H.S.; data curation, K.F.; writing—original draft preparation, K.F.; writing—review and editing, K.F., L.B.H., B.J.M.H., H.E.S.P., I.M.S., T.H.S., S.B. and L.R.; visualization, K.F. and H.E.S.P.; supervision, L.B.H., B.J.M.H., H.E.S.P. and L.R.; project administration, L.B.H.; funding acquisition, K.F. and L.B.H. All authors have read and agreed to the published version of the manuscript.

**Funding:** This research received funding from Helse Vest RHF (grant number F-12505) and the Trond Mohn Foundation (grant number BFS2017TMT07).

**Institutional Review Board Statement:** The study was conducted according to the guidelines of the Declaration of Helsinki, and approved by the regional committee for medical and health research ethics in Western Norway (protocol code 2019/749, 21.06.2019).

**Informed Consent Statement:** Informed consent was obtained from all subjects involved in the study.

**Data Availability Statement:** The data presented in this study are available on request from the corresponding author. The data are not publicly available due to privacy reasons as they are part of an ongoing study.

**Acknowledgments:** The authors would like to thank Marcin Sikora for assistance with QA measurements.

**Conflicts of Interest:** B.J.M.H., S.B. and L.R.: Erasmus MC Cancer Institute has research collaborations with Elekta AB (Stockholm, Sweden), Accuray, Inc (Sunnyvale, CA, USA) and Varian Medical Systems, Inc (Palo Alto, CA, USA). The other authors declare no conflict of interest. The funders had no role in the design of the study; in the collection, analyses, or interpretation of data; in the writing of the manuscript, or in the decision to publish the results.

## Appendix A. Beam Configurations for Example Patients

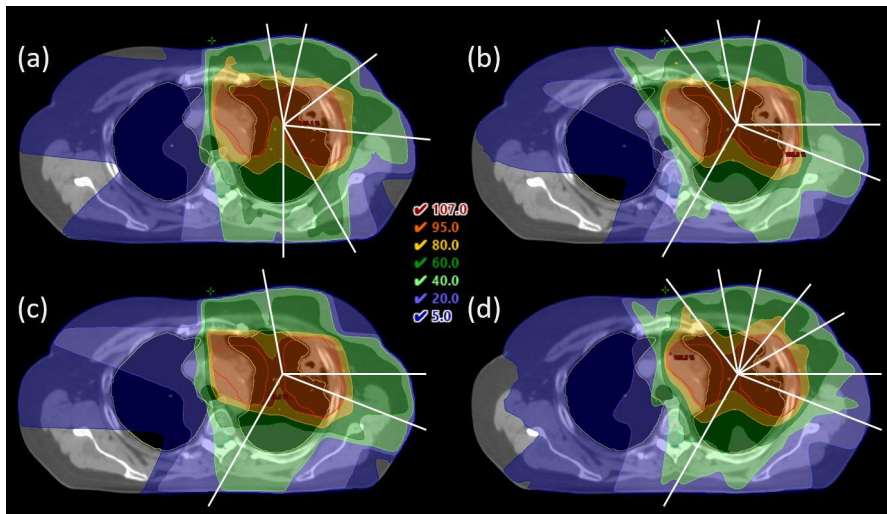


**Figure A1.** (a) CLIN plan with manually selected beam angles for patient 4, with a frontal tumor and lymph nodes. (b–d) iCE plans with 6, 4 and 8 optimized beam angles for the same patient. Dose is shown relative to the prescribed dose (66 Gy). Contours are the PTV (red), lungs (yellow), esophagus (grey) and spinal cord (cyan), and beam angles are indicated by white lines. For this patient, the optimized beam angles in the 6- and 8-beam plans enabled sparing of the esophagus.

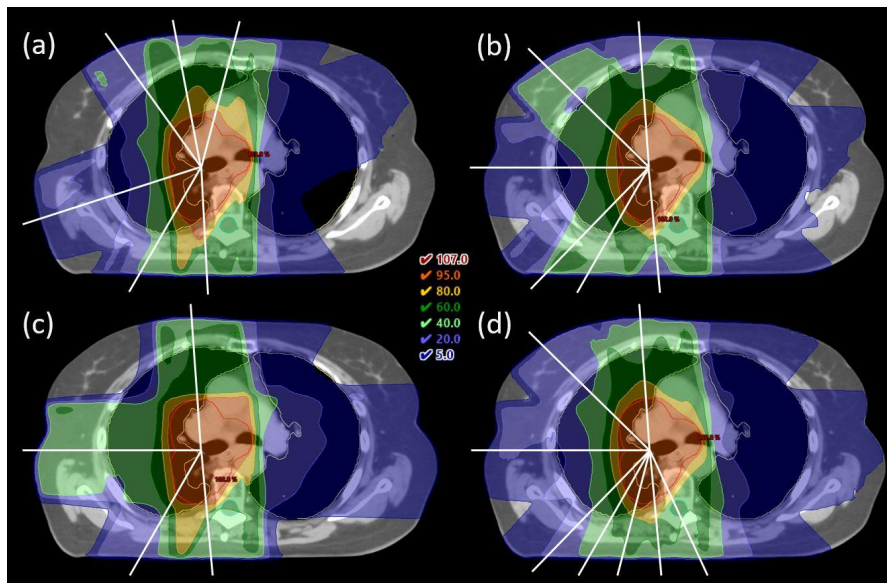


**Figure A2.** (a) CLIN plan with manually selected beam angles for patient 25, with a centrally located tumor. (b–d) iCE plans with 6, 4 and 8 optimized beam angles for the same patient. Dose is shown relative to the prescribed dose (66 Gy). Contours are the PTV (red), lungs (yellow), esophagus (grey) and spinal cord (cyan), and beam angles are indicated by white lines. For this patient, the distribution of high dose in the CLIN plan was not as conformal as desired. The 6-beam iCE plan has slightly higher lung and esophagus  $D_{\text{mean}}$  and better high dose conformity.

## Appendix B. Impact of Applied Number of Beams per Patient

**Table A1.** Difference per patient in  $D_{\text{mean}}$  for OARs in 4- and 8-beam iCE plans compared to 6-beam iCE plans, all with optimized beam angles. The colors indicate if the dose was increased (red), reduced (green) or equal (yellow) compared to the 6-beam plan. For patients marked with \*, the  $D_{\text{max}}$  requirement for the spinal canal or patient body was not met in the 4-beam plan only.

Patient	$D_{\text{mean}}$ Difference [Gy], 4 vs. 6 Beams			$D_{\text{mean}}$ Difference [Gy], 8 vs. 6 Beams		
	Lungs	Heart	Esophagus	Lungs	Heart	Esophagus
1	−2.5	1.8	3.3	0.5	−1.1	−2.3
2 *	0.6	−0.8	1.2	−0.3	1.5	−1.5
3 *	−2.0	0.6	6.8	0.3	−0.1	−2.8
4	0.7	0.8	4.6	−0.2	−0.8	2.9
5	0.4	1.3	2.3	−0.3	−0.9	−0.4
6	1.3	2.6	2.4	−0.4	1.1	−0.9
7 *	−0.6	0.0	−0.9	−0.4	0.0	−0.4
8	1.2	1.7	−0.1	−0.4	−0.5	−1.2
9	−0.1	−0.8	4.4	−0.2	−1.5	−0.1
10	−0.5	1.8	−1.4	0.0	−1.1	−0.2
11 *	−1.1	0.6	4.8	0.4	−0.4	−2.5
12	0.3	0.6	0.7	−0.4	−0.3	−1.4
13	0.9	0.9	3.4	−0.3	0.4	−1.4
14	2.0	3.2	−0.9	−0.6	0.0	−1.1
15 *	1.2	1.6	−2.2	−0.2	−0.1	−0.6
16	0.8	0.1	1.6	−0.2	−1.0	−1.8
17	−0.5	1.1	1.1	0.0	0.1	−0.3
18	−0.8	0.6	−0.8	−0.6	−0.5	−0.9
19	−0.3	0.3	0.1	0.0	−0.4	−0.2
20	−0.1	4.0	−4.2	−0.1	−0.2	−0.8
21 *	0.0	−2.3	4.5	−0.6	−3.9	0.3
22 *	0.8	−0.3	1.3	−0.8	−0.1	−0.6
23 *	−0.2	0.2	1.5	−0.2	−0.3	−0.5
24	1.8	3.5	−1.0	−0.2	−0.9	−0.9
25	2.3	1.9	0.0	0.2	−1.1	−0.3
26 *	−2.0	−1.8	−0.5	−0.4	0.7	−0.4

## References

- Bradley, J.D.; Hu, C.; Komaki, R.R.; Masters, G.A.; Blumenschein, G.R.; Schild, S.E.; Bogart, J.A.; Forster, K.M.; Magliocco, A.M.; Kavadi, V.S.; et al. Long-Term Results of NRG Oncology RTOG 0617: Standard- Versus High-Dose Chemoradiotherapy With or Without Cetuximab for Unresectable Stage III Non-Small-Cell Lung Cancer. *J. Clin. Oncol.* **2020**, *38*, 706–714. [[CrossRef](#)] [[PubMed](#)]
- Chun, S.G.; Hu, C.; Choy, H.; Komaki, R.U.; Timmerman, R.D.; Schild, S.E.; Bogart, J.A.; Dobelbower, M.C.; Bosch, W.; Galvin, J.M.; et al. Impact of Intensity-Modulated Radiation Therapy Technique for Locally Advanced Non-Small-Cell Lung Cancer: A Secondary Analysis of the NRG Oncology RTOG 0617 Randomized Clinical Trial. *J. Clin. Oncol.* **2017**, *35*, 56–62. [[CrossRef](#)] [[PubMed](#)]
- Ma, L.; Men, Y.; Feng, L.; Kang, J.; Sun, X.; Yuan, M.; Jiang, W.; Hui, Z. A Current Review of Dose-Escalated Radiotherapy in Locally Advanced Non-Small Cell Lung Cancer. *Radiol. Oncol.* **2019**, *53*, 6–14. [[CrossRef](#)] [[PubMed](#)]
- Hoffmann, L.; Knap, M.M.; Alber, M.; Møller, D.S. Optimal Beam Angle Selection and Knowledge-Based Planning Significantly Reduces Radiotherapy Dose to Organs at Risk for Lung Cancer Patients. *Acta Oncol.* **2021**, *60*, 293–299. [[CrossRef](#)]
- Nelms, B.E.; Robinson, G.; Markham, J.; Velasco, K.; Boyd, S.; Narayan, S.; Wheeler, J.; Sobczak, M.L. Variation in External Beam Treatment Plan Quality: An Inter-Institutional Study of Planners and Planning Systems. *Pract. Radiat. Oncol.* **2012**, *2*, 296–305. [[CrossRef](#)]
- Berry, S.L.; Boczkowski, A.; Ma, R.; Mechalakos, J.; Hunt, M. Interobserver Variability in Radiation Therapy Plan Output: Results of a Single-Institution Study. *Pract. Radiat. Oncol.* **2016**, *6*, 442–449. [[CrossRef](#)] [[PubMed](#)]
- Hussein, M.; Heijmen, B.J.M.; Verellen, D.; Nisbet, A. Automation in Intensity Modulated Radiotherapy Treatment Planning—A Review of Recent Innovations. *Br. J. Radiol.* **2018**, *91*, 20180270. [[CrossRef](#)] [[PubMed](#)]
- Della Gala, G.; Dirx, M.L.P.; Hoekstra, N.; Fransen, D.; Lanconelli, N.; van de Pol, M.; Heijmen, B.J.M.; Petit, S.F. Fully Automated VMAT Treatment Planning for Advanced-Stage NSCLC Patients. *Strahlenther. Onkol.* **2017**, *193*, 402–409. [[CrossRef](#)] [[PubMed](#)]
- Kamran, S.C.; Mueller, B.S.; Paetzold, P.; Dunlap, J.; Niemierko, A.; Bortfeld, T.; Willers, H.; Craft, D. Multi-Criteria Optimization Achieves Superior Normal Tissue Sparing in a Planning Study of Intensity-Modulated Radiation Therapy for RTOG 1308-Eligible Non-Small Cell Lung Cancer Patients. *Radiother. Oncol.* **2016**, *118*, 515–520. [[CrossRef](#)]

10. Breedveld, S.; Storchi, P.R.M.; Voet, P.W.J.; Heijmen, B.J.M. ICycle: Integrated, Multicriterial Beam Angle, and Profile Optimization for Generation of Coplanar and Noncoplanar IMRT Plans. *Med. Phys.* **2012**, *39*, 951–963. [[CrossRef](#)]
11. Rossi, L.; Breedveld, S.; Heijmen, B.J.M.; Voet, P.W.J.; Lanconelli, N.; Aluwini, S. On the Beam Direction Search Space in Computerized Non-Coplanar Beam Angle Optimization for IMRT—Prostate SBRT. *Phys. Med. Biol.* **2012**, *57*, 5441–5458. [[CrossRef](#)]
12. Sharfo, A.W.M.; Dirkx, M.L.P.; Breedveld, S.; Romero, A.M.; Heijmen, B.J.M. VMAT plus a Few Computer-Optimized Non-Coplanar IMRT Beams (VMAT+) Tested for Liver SBRT. *Radiother. Oncol.* **2017**, *123*, 49–56. [[CrossRef](#)] [[PubMed](#)]
13. Rossi, L.; Sharfo, A.W.; Aluwini, S.; Dirkx, M.; Breedveld, S.; Heijmen, B. First Fully Automated Planning Solution for Robotic Radiosurgery—Comparison with Automatically Planned Volumetric Arc Therapy for Prostate Cancer. *Acta Oncol.* **2018**, *57*, 1490–1498. [[CrossRef](#)]
14. Sharfo, A.W.M.; Rossi, L.; Dirkx, M.L.P.; Breedveld, S.; Aluwini, S.; Heijmen, B.J.M. Complementing Prostate SBRT VMAT With a Two-Beam Non-Coplanar IMRT Class Solution to Enhance Rectum and Bladder Sparing With Minimum Increase in Treatment Time. *Front. Oncol.* **2021**, *11*, 620978. [[CrossRef](#)] [[PubMed](#)]
15. Rossi, L.; Cambraia Lopes, P.; Marques Leitão, J.; Janus, C.; van de Pol, M.; Breedveld, S.; Penninkhof, J.; Heijmen, B.J.M. On the Importance of Individualized, Non-Coplanar Beam Configurations in Mediastinal Lymphoma Radiotherapy, Optimized With Automated Planning. *Front. Oncol.* **2021**, *11*, 619929. [[CrossRef](#)]
16. Schipaanboord, B.W.K.; Giżyńska, M.K.; Rossi, L.; Vries, K.C.; Heijmen, B.J.M.; Breedveld, S. Fully Automated Treatment Planning for MLC-based Robotic Radiotherapy. *Med. Phys.* **2021**, *48*, 4139–4147. [[CrossRef](#)]
17. Voet, P.W.J.; Dirkx, M.L.P.; Breedveld, S.; Al-Mamgani, A.; Incrocci, L.; Heijmen, B.J.M. Fully Automated Volumetric Modulated Arc Therapy Plan Generation for Prostate Cancer Patients. *Int. J. Radiat. Oncol.* **2014**, *88*, 1175–1179. [[CrossRef](#)]
18. Buschmann, M.; Sharfo, A.W.M.; Penninkhof, J.; Seppenwoolde, Y.; Goldner, G.; Georg, D.; Breedveld, S.; Heijmen, B.J.M. Automated Volumetric Modulated Arc Therapy Planning for Whole Pelvic Prostate Radiotherapy. *Strahlenther. Onkol.* **2018**, *194*, 333–342. [[CrossRef](#)] [[PubMed](#)]
19. Sharfo, A.W.M.; Breedveld, S.; Voet, P.W.J.; Heijkoop, S.T.; Mens, J.-W.M.; Hoogeman, M.S.; Heijmen, B.J.M. Validation of Fully Automated VMAT Plan Generation for Library-Based Plan-of-the-Day Cervical Cancer Radiotherapy. *PLoS ONE* **2016**, *11*, e0169202. [[CrossRef](#)]
20. Buerge, D.; Sharfo, A.W.M.; Heijmen, B.J.M.; Voet, P.W.J.; Breedveld, S.; Wenz, F.; Lohr, F.; Stieler, F. Fully Automated Treatment Planning of Spinal Metastases—A Comparison to Manual Planning of Volumetric Modulated Arc Therapy for Conventionally Fractionated Irradiation. *Radiat. Oncol.* **2017**, *12*, 33. [[CrossRef](#)]
21. Voet, P.W.J.; Breedveld, S.; Dirkx, M.L.P.; Levendag, P.C.; Heijmen, B.J.M. Integrated Multicriterial Optimization of Beam Angles and Intensity Profiles for Coplanar and Noncoplanar Head and Neck IMRT and Implications for VMAT. *Med. Phys.* **2012**, *39*, 4858–4865. [[CrossRef](#)] [[PubMed](#)]
22. Bijman, R.; Sharfo, A.W.; Rossi, L.; Breedveld, S.; Heijmen, B. Pre-Clinical Validation of a Novel System for Fully-Automated Treatment Planning. *Radiother. Oncol.* **2021**, *158*, 253–261. [[CrossRef](#)]
23. Fogliata, A.; Belosi, F.; Clivio, A.; Navarria, P.; Nicolini, G.; Scorsetti, M.; Vanetti, E.; Cozzi, L. On the Pre-Clinical Validation of a Commercial Model-Based Optimisation Engine: Application to Volumetric Modulated Arc Therapy for Patients with Lung or Prostate Cancer. *Radiother. Oncol.* **2014**, *113*, 385–391. [[CrossRef](#)] [[PubMed](#)]
24. Yuan, L.; Zhu, W.; Ge, Y.; Jiang, Y.; Sheng, Y.; Yin, F.-F.; Wu, Q.J. Lung IMRT Planning with Automatic Determination of Beam Angle Configurations. *Phys. Med. Biol.* **2018**, *63*, 135024. [[CrossRef](#)] [[PubMed](#)]
25. Amit, G.; Purdie, T.G.; Levinshtein, A.; Hope, A.J.; Lindsay, P.; Marshall, A.; Jaffray, D.A.; Pekar, V. Automatic Learning-Based Beam Angle Selection for Thoracic IMRT. *Med. Phys.* **2015**, *42*, 1992–2005. [[CrossRef](#)] [[PubMed](#)]
26. Nestle, U.; De Ruyscher, D.; Ricardi, U.; Geets, X.; Belderbos, J.; Pöttgen, C.; Dziaduszkó, R.; Peeters, S.; Lievens, Y.; Hurkmans, C.; et al. ESTRO ACROP Guidelines for Target Volume Definition in the Treatment of Locally Advanced Non-Small Cell Lung Cancer. *Radiother. Oncol.* **2018**, *127*, 1–5. [[CrossRef](#)] [[PubMed](#)]
27. Kong, F.-M.; Ritter, T.; Quint, D.J.; Senan, S.; Gaspar, L.E.; Komaki, R.U.; Hurkmans, C.W.; Timmerman, R.; Bezjak, A.; Bradley, J.D.; et al. Consideration of Dose Limits for Organs at Risk of Thoracic Radiotherapy: Atlas for Lung, Proximal Bronchial Tree, Esophagus, Spinal Cord, Ribs, and Brachial Plexus. *Int. J. Radiat. Oncol.* **2011**, *81*, 1442–1457. [[CrossRef](#)] [[PubMed](#)]
28. Heijmen, B.; Voet, P.; Fransen, D.; Penninkhof, J.; Milder, M.; Akhlat, H.; Bonomo, P.; Casati, M.; Georg, D.; Goldner, G.; et al. Fully Automated, Multi-Criterial Planning for Volumetric Modulated Arc Therapy—An International Multi-Center Validation for Prostate Cancer. *Radiother. Oncol.* **2018**, *128*, 343–348. [[CrossRef](#)] [[PubMed](#)]
29. Cozzi, L.; Vanderstraeten, R.; Fogliata, A.; Chang, F.-L.; Wang, P.-M. The Role of a Knowledge Based Dose–Volume Histogram Predictive Model in the Optimisation of Intensity-Modulated Proton Plans for Hepatocellular Carcinoma Patients: Training and Validation of a Novel Commercial System. *Strahlenther. Onkol.* **2021**, *197*, 332–342. [[CrossRef](#)] [[PubMed](#)]
30. Varian Medical Systems, Inc. *Eclipse Photon and Electron Reference Guide*; Varian Medical Systems, Inc.: Palo Alto, CA, USA, 2017.
31. Bradley, J.D.; Paulus, R.; Komaki, R.; Masters, G.; Blumenschein, G.; Schild, S.; Bogart, J.; Hu, C.; Forster, K.; Magliocco, A.; et al. Standard-Dose versus High-Dose Conformal Radiotherapy with Concurrent and Consolidation Carboplatin plus Paclitaxel with or without Cetuximab for Patients with Stage IIIA or IIIB Non-Small-Cell Lung Cancer (RTOG 0617): A Randomised, Two-by-Two Factorial Phase 3 Study. *Lancet Oncol.* **2015**, *16*, 187–199. [[CrossRef](#)] [[PubMed](#)]

32. Dess, R.T.; Sun, Y.; Matuszak, M.M.; Sun, G.; Soni, P.D.; Bazzi, L.; Murthy, V.L.; Hearn, J.W.D.; Kong, F.-M.; Kalemkerian, G.P.; et al. Cardiac Events After Radiation Therapy: Combined Analysis of Prospective Multicenter Trials for Locally Advanced Non-Small-Cell Lung Cancer. *J. Clin. Oncol.* **2017**, *35*, 1395–1402. [[CrossRef](#)]
33. Wijsman, R.; Dankers, F.; Troost, E.G.C.; Hoffmann, A.L.; van der Heijden, E.H.F.M.; de Geus-Oei, L.-F.; Bussink, J. Multivariable Normal-Tissue Complication Modeling of Acute Esophageal Toxicity in Advanced Stage Non-Small Cell Lung Cancer Patients Treated with Intensity-Modulated (Chemo-)Radiotherapy. *Radiother. Oncol.* **2015**, *117*, 49–54. [[CrossRef](#)] [[PubMed](#)]
34. Bijman, R.; Rossi, L.; Janssen, T.; de Ruyter, P.; Carbaat, C.; van Triest, B.; Breedveld, S.; Sonke, J.-J.; Heijmen, B. First System for Fully-Automated Multi-Criterial Treatment Planning for a High-Magnetic Field MR-Linac Applied to Rectal Cancer. *Acta Oncol.* **2020**, *59*, 926–932. [[CrossRef](#)] [[PubMed](#)]
35. Rossi, L.; Méndez Romero, A.; Milder, M.; de Klerck, E.; Breedveld, S.; Heijmen, B. Individualized Automated Planning for Dose Bath Reduction in Robotic Radiosurgery for Benign Tumors. *PLoS ONE* **2019**, *14*, e0210279. [[CrossRef](#)] [[PubMed](#)]
36. Hundvin, J.A.; Fjellanger, K.; Pettersen, H.E.S.; Nygaard, B.; Revheim, K.; Sulen, T.H.; Ekanger, C.; Hysing, L.B. Clinical Iterative Model Development Improves Knowledge-Based Plan Quality for High-Risk Prostate Cancer with Four Integrated Dose Levels. *Acta Oncol.* **2021**, *60*, 237–244. [[CrossRef](#)] [[PubMed](#)]
37. Fogliata, A.; Cozzi, L.; Reggiori, G.; Stravato, A.; Lobefalo, F.; Franzese, C.; Franceschini, D.; Tomatis, S.; Scorsetti, M. RapidPlan Knowledge Based Planning: Iterative Learning Process and Model Ability to Steer Planning Strategies. *Radiat. Oncol.* **2019**, *14*, 187. [[CrossRef](#)] [[PubMed](#)]
38. Hansen, C.R.; Crijns, W.; Hussein, M.; Rossi, L.; Gallego, P.; Verbakel, W.; Unkelbach, J.; Thwaites, D.; Heijmen, B. Radiotherapy Treatment Planning Study Guidelines (RATING): A Framework for Setting up and Reporting on Scientific Treatment Planning Studies. *Radiother. Oncol.* **2020**, *153*, 67–78. [[CrossRef](#)]







# Improving knowledge-based treatment planning for lung cancer radiotherapy with automatic multi-criteria optimized training plans

Kristine Fjellanger, Marte Hordnes, Inger Marie Sandvik, Turid Husevåg Sulen, Ben J. M. Heijmen, Sebastiaan Breedveld, Linda Rossi, Helge Egil Seime Pettersen & Liv Bolstad Hysing

To cite this article: Kristine Fjellanger, Marte Hordnes, Inger Marie Sandvik, Turid Husevåg Sulen, Ben J. M. Heijmen, Sebastiaan Breedveld, Linda Rossi, Helge Egil Seime Pettersen & Liv Bolstad Hysing (2023) Improving knowledge-based treatment planning for lung cancer radiotherapy with automatic multi-criteria optimized training plans, Acta Oncologica, 62:10, 1194-1200, DOI: [10.1080/0284186X.2023.2238882](https://doi.org/10.1080/0284186X.2023.2238882)

To link to this article: <https://doi.org/10.1080/0284186X.2023.2238882>



© 2023 The Author(s). Published by Informa UK Limited, trading as Taylor & Francis Group.



[View supplementary material](#)



Published online: 17 Aug 2023.



[Submit your article to this journal](#)



Article views: 490



[View related articles](#)






[View Crossmark data](#)



[Citing articles: 1 View citing articles](#)

## Improving knowledge-based treatment planning for lung cancer radiotherapy with automatic multi-criteria optimized training plans

Kristine Fjellanger<sup>a,b</sup> , Marte Hordnes<sup>b</sup>, Inger Marie Sandvik<sup>a</sup>, Turid Husevåg Sulen<sup>a</sup>, Ben J. M. Heijmen<sup>c</sup>, Sebastiaan Breedveld<sup>c</sup>, Linda Rossi<sup>c</sup>, Helge Egil Seime Pettersen<sup>a</sup>  and Liv Bolstad Hysing<sup>a,b</sup> 

<sup>a</sup>Department of Oncology and Medical Physics, Haukeland University Hospital, Bergen, Norway; <sup>b</sup>Institute of Physics and Technology, University of Bergen, Bergen, Norway; <sup>c</sup>Department of Radiotherapy, Erasmus MC Cancer Institute, Erasmus University Medical Center, Rotterdam, Netherlands

### ABSTRACT

**Background:** Knowledge-based planning (KBP) is a method for automated radiotherapy treatment planning where appropriate optimization objectives for new patients are predicted based on a library of training plans. KBP can save time and improve organ at-risk sparing and inter-patient consistency compared to manual planning, but its performance depends on the quality of the training plans. We used another system for automated planning, which generates multi-criteria optimized (MCO) plans based on a wish list, to create training plans for the KBP model, to allow seamless integration of knowledge from a new system into clinical routine. Model performance was compared for KBP models trained with manually created and automatic MCO treatment plans.

**Material and Methods:** Two RapidPlan models with the same 30 locally advanced non-small cell lung cancer patients included were created, one containing manually created clinical plans (RP\_CLIN) and one containing fully automatic multi-criteria optimized plans (RP\_MCO). For 15 validation patients, model performance was compared in terms of dose-volume parameters and normal tissue complication probabilities, and an oncologist performed a blind comparison of the clinical (CLIN), RP\_CLIN, and RP\_MCO plans.

**Results:** The heart and esophagus doses were lower for RP\_MCO compared to RP\_CLIN, resulting in an average reduction in the risk of 2-year mortality by 0.9 percentage points and the risk of acute esophageal toxicity by 1.6 percentage points with RP\_MCO. The oncologist preferred the RP\_MCO plan for 8 patients and the CLIN plan for 7 patients, while the RP\_CLIN plan was not preferred for any patients.

**Conclusion:** RP\_MCO improved OAR sparing compared to RP\_CLIN and was selected for implementation in the clinic. Training a KBP model with clinical plans may lead to suboptimal output plans, and making an extra effort to optimize the library plans in the KBP model creation phase can improve the plan quality for many future patients.

### ARTICLE HISTORY

Received 17 April 2023  
Accepted 4 July 2023

### KEYWORDS

Automated treatment planning; knowledge-based planning; multi-criteria optimization (MCO); RapidPlan; Erasmus-iCycle; iCE; locally advanced non-small cell lung cancer (NSCLC); radiotherapy

## Background


Manual treatment planning for intensity-modulated radiotherapy (IMRT) of locally advanced non-small cell lung cancer (LA-NSCLC) can be complex and time-consuming, and plan quality may depend on the experience and skills of the treatment planner and the available time. In recent years, systems for automated treatment planning have been introduced that can reduce planning time and improve plan quality and inter-patient consistency, and they are becoming more and more widespread [1].

Automatic multi-criteria optimization (MCO), where Pareto-optimal plans are created with no user intervention according to a treatment site-specific wish-list, has shown a potential to increase the sparing of organs at risk (OARs) compared to manual planning, also for NSCLC [2–4]. The clinical availability of such systems is however limited. In

knowledge-based planning (KBP), the achievable dose for each patient is predicted using a library of previous plans, in order to automatically set suitable planning objectives for plan generation. KBP can automatically generate plans with similar or even better quality compared to manual plans [5–11], but the quality of the output plans depends on the quality of the plans in the library [12–16]. The commercially available RapidPlan system for KBP (Varian Medical Systems, Palo Alto, USA) has been implemented in many centers.

Once a KBP model is implemented in the clinic, it will likely be used to create treatment plans for a number of future patients. Therefore, the strategy selected for the model creation phase is of great importance, as it consistently will affect the plan quality for all these patients. In this study, we investigate if automatic MCO could be used to improve training of our clinically available KBP system, and

**CONTACT** Kristine Fjellanger  [kristine.fjellanger@helse-bergen.no](mailto:kristine.fjellanger@helse-bergen.no)  Department of Oncology and Medical Physics, Haukeland University Hospital, Bergen, Norway; Institute of Physics and Technology, University of Bergen, Bergen, Norway

 Supplemental data for this article can be accessed online at <https://doi.org/10.1080/0284186X.2023.2238882>.

© 2023 The Author(s). Published by Informa UK Limited, trading as Taylor & Francis Group.

This is an Open Access article distributed under the terms of the Creative Commons Attribution License (<http://creativecommons.org/licenses/by/4.0/>), which permits unrestricted use, distribution, and reproduction in any medium, provided the original work is properly cited. The terms on which this article has been published allow the posting of the Accepted Manuscript in a repository by the author(s) or with their consent.

thereby indirectly enhance plan quality in a clinic without routine access to automatic MCO. To this purpose, plans generated with a KBP model trained with automatic MCO plans were compared to plans for the same patients generated with a KBP model trained with previous clinical plans. The final aim was to select a KBP model for clinical implementation.

**Material and methods**

**Patients and clinical treatment planning**

Forty-five consecutive patients with inoperable non-small cell lung cancer (stage IB-IVA, mainly stage III) were prospectively included in this study. All patients received radiotherapy according to the protocol for LA-NSCLC and concurrent or sequential chemotherapy at Haukeland University Hospital between October 2019 and November 2022. The study was approved by the Regional Committee for Medical and Health Research Ethics in Western Norway (protocol code 2019/749) and all participants gave informed consent.

The imaging and delineation procedures have been described in detail in previous work [17]. The clinical plans (CLIN) were manually created by experienced treatment planners in Eclipse version 15.6 or 16.1 (Varian Medical Systems, Palo Alto, USA) using the Photon Optimizer algorithm for optimization and the Acuros External Beam algorithm for dose calculation. Most plans had 6 coplanar IMRT beams with beam angles based on a template that was individually adapted, four patients had 5-field IMRT plans and two had VMAT plans. According to national guidelines, the prescribed dose was 60 or 66 Gy for concurrent chemo-radiation (depending on lung function, lung dose, and proximity of the brachial plexus to the PTV) and 70 Gy when chemo- and radiotherapy were delivered sequentially, all in 2 Gy fractions. The plans were normalized to the median dose in the PTV. Dose constraints applied for planning are shown in Table 1.

**iCE treatment planning**

In addition to the CLIN plan, an automatically generated MCO treatment plan from the novel in-house iCE system was available for each patient. In iCE, an initial Pareto-optimal fluence-map optimized treatment plan with optimized beam angles is generated in Erasmus-iCycle [18]. This is a fully automatic process based on a wish-list containing constraints

and objectives with ascribed priorities, tuned to reflect the clinical priorities for this patient group in the treating center. The objectives are first optimized in turn according to their priorities, keeping the achieved values as constraints in following optimizations. In a second round, objectives that can be optimized further than their defined goal are optimized as far as possible within constraints, starting with the highest priority objective.

In the second step of iCE, the dose distribution from Erasmus-iCycle is automatically reconstructed in Eclipse, using patient-specific line objectives that limit the dose for all volume levels for OARs. This results in a deliverable plan created without manual intervention. A detailed description of iCE and the applied wish-list can be found elsewhere [2]. In a previous study, iCE reduced the median  $D_{mean}$  for the heart and esophagus by 9–10% compared to manual planning for LA-NSCLC patients, while maintaining similar PTV coverage and lung dose [2].

**RapidPlan model creation**

Of the first 40 included patients, 30 were randomly selected for training of KBP prediction models. The remaining 10 patients and the last 5 included study patients (15 in total) were used for comparison of MCO-based KBP with CLIN-based KBP (next section).

First, a RapidPlan (RP) model containing the CLIN plans (RP\_CLIN) of the 30 training patients was created. The model featured line objectives generated from predicted DVHs for the lungs, heart, and esophagus, complemented with maximum and minimum dose objectives for the PTV and maximum dose objectives for the spinal canal and brachial plexus. The PTV objectives and normal tissue objective (NTO, see Table 2) were tuned using three of the training patients, with the goal of achieving similar target coverage as in the CLIN plans.

A second model, containing the multi-criteria optimized iCE plans for the same patients (RP\_MCO) was then created. The optimization objectives were re-tuned using the same approach as above. The objectives in both models are summarized in Table 2. A detailed description of RapidPlan functionality can be found elsewhere [5].

**Table 2.** Objectives in the RapidPlan models.

Structure	Type	Volume	Dose	Priority RP_CLIN/RP_MCO
PTV	Upper	0%	100.8%	130/140
	Lower	100%	99.2%	130/140
Lungs	Line	Generated	Generated	Generated
Heart	Line	Generated	Generated	Generated
Esophagus	Line	Generated	Generated	Generated
Spinal canal	Upper	0%	48 Gy	Generated
Brachial plexus	Upper	0%	60 Gy	100
Patient body	NTO	–	–	100

NTO: normal tissue objective, with the following fixed parameters: distance from target border 0.5 cm, start dose 105%, end dose 60% and fall-off 0.15 [19]. For line objectives, the ‘preferring OAR’ option was used. Only 11 of the patients had the brachial plexus delineated, and a fixed objective had to be used as this is too few structures to train a prediction model. The PTV dose levels of 100.8% and 99.2% were applied in RapidPlan to facilitate a common model for the different prescriptions (in the manually created plans, the dose level for the PTV objectives were set 0.5 Gy above/below the prescribed dose).

**Table 1.** Planning dose constraints for the PTV, OARs and normal tissue.

Volume	Dose constraint
PTV	$V_{95\%} > 98\%$
Lungs	$V_{5Gy} < 65\%$
	$V_{20Gy} < 35\%$
	$D_{mean} < 20$ Gy
Heart	$V_{30Gy} < 40\%$
Esophagus	$D_{mean} < 34$ Gy
Spinal canal	$D_{max} < 50$ Gy
Brachial plexus	$D_{max} < 66$ Gy
Patient body	$D_{max} < D_p \cdot 1.07$

$D_p$ : prescribed dose. In cases where fulfilling all constraints was impossible, the responsible oncologist decided whether target coverage or OAR constraints should be compromised.

### Comparison of RapidPlan models

For each of the 15 patients not used in the model building, one plan was automatically generated with the RP\_CLIN prediction model and one with the RP\_MCO model, with no manual interventions. The same beam configuration as in the CLIN plan was used in the RP plans for each patient. Relevant dose-volume parameters for the PTV and OARs were compared. To illustrate the clinical difference, normal tissue complication probabilities (NTCPs) for radiation pneumonitis (RP) grade  $\geq 2$ , 2-year mortality, and acute esophageal toxicity (AET) grade  $\geq 2$  were calculated using validated models described in detail in the [Supplementary materials \[20–23\]](#). Goodness of fit statistics ( $R^2$  and  $\chi^2$ ) reported for each model in the model configuration workspace was also evaluated.

### Comparison with clinical plans

The responsible oncologist evaluated the CLIN, RP\_CLIN, and RP\_MCO plans and selected the preferred plan for each patient, while blinded to the technique. Based on the oncologist's preference and the quantitative analysis above, the best RP model for clinical use was selected and validated against the CLIN plans using relevant dose-volume parameters.

### Statistical analysis

The two-tailed Wilcoxon signed-rank test was used for statistical testing of dose-volume parameters for RP\_MCO plans vs. RP\_CLIN and CLIN plans.

## Results

### Comparison of RapidPlan models

The dose to the heart and esophagus was lower in RP\_MCO plans than RP\_CLIN plans ([Table 3](#), [Figures 1](#) and [S1](#)). The lungs  $V_{5Gy}$  was also slightly reduced, while the target coverage was similar. The clinical impact for individual patients is illustrated in [Figure 2](#), showing a modest but consistent reduction in the risk of 2-year mortality and AET with

RP\_MCO compared to RP\_CLIN. On average, RP\_MCO plans reduced the risk of 2-year mortality by 0.9 percentage points (pp) ( $p < 0.001$ ), and the risk of AET by 1.6 pp ( $p < 0.001$ ) ([Table 3](#)).

The  $R^2$  values were similar, indicating a similar determination capability of the regression models in RP\_CLIN and RP\_MCO, and the  $\chi^2$  values were slightly improved with RP\_MCO, indicating a better fit between original and estimated values ([Table S2](#)).

### Comparison with clinical plans

In blinded evaluations, the oncologist preferred the RP\_MCO plan for 8 and the CLIN plan for 7 out of 15 patients. The RP\_CLIN plan was not preferred for any of the patients ([Figure 3](#)). Lower dose to the heart and esophagus were the main reasons for choosing the RP\_MCO plan, and lower lung dose was the main reason for choosing the CLIN plan. The oncologist also noted that the  $D_{max}$  to the spinal canal was above or very close to the constraint in one or more plans for 5 of the patients.

As the reported results clearly showed an advantage of RP\_MCO compared to RP\_CLIN, the RP\_MCO model was selected for clinical implementation, and the RP\_MCO plans were compared to the CLIN plans also in terms of dosimetric parameters and NTCP. Dosimetric parameters for the heart and esophagus were lower in the RP\_MCO plans than the CLIN plans, while the lung dose and spinal canal  $D_{max}$  were higher ([Table S3](#)). As a result, the average NTCP for RP was 1 pp higher with RP\_MCO than CLIN ( $p = 0.04$ ), for 2-year mortality it was 0.4 pp lower ( $p = 0.04$ ) and for AET it was 2.3 pp lower ( $p = 0.003$ ).

## Discussion

To our knowledge, this is the first study to compare the performance of KBP models trained with manual plans vs. generated plans from a different autoplanning system. Training RapidPlan with automatic MCO plans gave better model performance than training with clinical plans. RP\_MCO improved the sparing of the heart and esophagus compared to RP\_CLIN, resulting in a reduction in the average NTCPs for

**Table 3.** Comparison of dose-volume parameters and NTCPs for RP\_CLIN and RP\_MCO plans.

Metric	RP_CLIN			RP_MCO			p-value
	Average	Median	10 <sup>th</sup> –90 <sup>th</sup> percentile	Avg	Median	10 <sup>th</sup> –90 <sup>th</sup> percentile	
PTV $V_{95\%}$ [%]	98.9	99.4	96.6–99.8	98.9	99.3	97.1–99.8	0.9
Lungs $D_{mean}$ [Gy]	13.6	14.1	10.1–16.6	13.5	13.9	10.2–16.5	0.8
Lungs $V_{5Gy}$ [%]	54.5	56.2	39.2–66.8	53.9	55.1	39.0–66.5	0.009
Lungs $V_{20Gy}$ [%]	23.5	22.4	15.8–31.3	23.4	21.7	15.6–32.0	0.5
Heart $D_{mean}$ [Gy]	9.4	7.8	2.8–22.7	8.3	7.7	2.4–18.3	<0.001
Heart $V_{5Gy}$ [%]	40.1	31.9	10.9–92.0	38.3	29.7	9.9–87.2	0.002
Heart $V_{30Gy}$ [%]	8.1	5.7	1.3–15.5	7.6	4.9	0.7–19.9	0.02
Esophagus $D_{mean}$ [Gy]	19.3	17.9	6.4–32.1	18.3	17.6	6.0–30.5	<0.001
Esophagus $V_{20Gy}$ [%]	33.7	31.2	11.5–59.4	31.2	27.6	7.5–55.8	0.001
Esophagus $V_{60Gy}$ [%]	10.2	7.3	0.0–24.3	9.2	4.9	0.0–23.7	0.009
Spinal canal $D_{max}$ [Gy]	44.5	49.1	28.9–50.4	44.8	48.7	29.9–50.8	0.4
NTCP RP [%]	22.2	22.9	6.6–36.3	22.2	21.8	6.2–37.9	0.9
NTCP 2-year mortality [%]	48.4	43.4	34.7–75.9	47.5	42.2	34.1–73.4	<0.001
NTCP AET [%]	35.3	35.6	10.2–57.3	33.7	35.0	9.2–55.2	<0.001

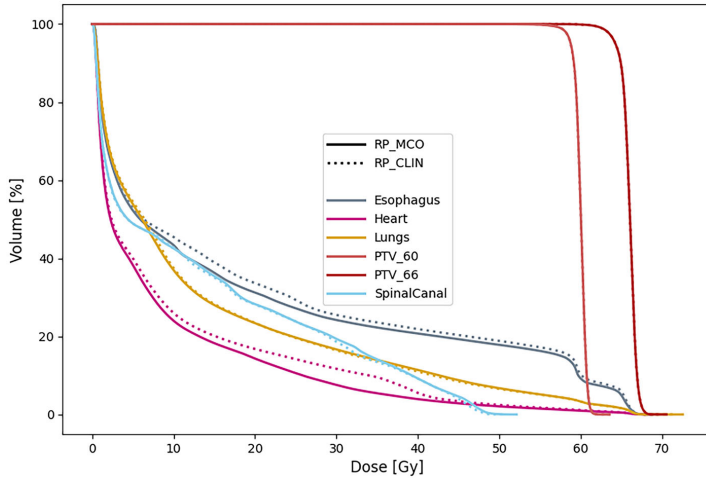


**Figure 1.** Population average DVHs for PTV and OARs for RP\_CLIN and RP\_MCO plans. Three patients had PTV\_60 and 12 had PTV\_66. For DVHs with confidence intervals, see Figure S1 in the Supplementary materials.

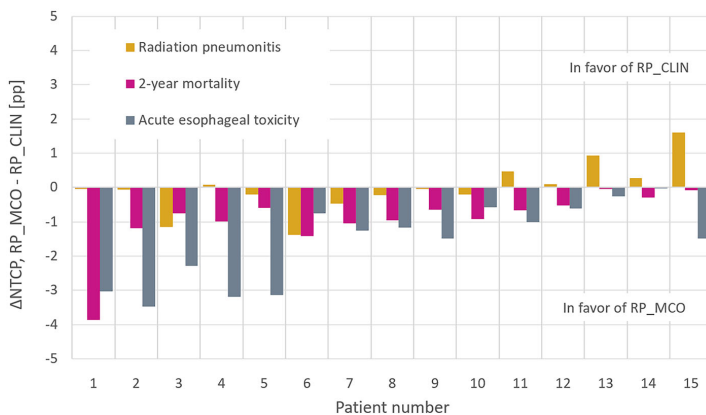


**Figure 2.** Differences in NTCPs between RP\_CLIN and RP\_MCO plans per patient. The patients are sorted according to the sum of differences for the three NTCPs.

2-year mortality and acute esophageal toxicity. The difference in performance between the models can be explained by the difference in the dose distributions of the training plans [2]. In line with previous studies, this demonstrates that improving the quality of the library improves the model performance [12–16,24–26].

The most common approach for creating a new RP model for the clinic is to build a library with manually created, clinically used plans for a group of relevant patients [5–9]. Although these plans have been approved for treatment and meet the clinical goals, they are usually not optimal. The treatment planners work under time pressure with limited time for testing different planning strategies, and generally do not know when a treatment plan cannot be further improved.

Some studies have explored different strategies for optimizing KBP model training. Iterative approaches where an initial RP model was used to generate plans for new

patients that were included in a second RP model improved OAR sparing in the output plans [12,24,25], while re-optimization with RP for the patients included in the original model gave a modest improvement for some OARs but also induces a risk of overfitting [13,14,26,27]. Others have selected the plans with the best OAR sparing from the original training set for use in the final model, or in an intermediate model for re-optimization of the training plans [28–30]. In a recent study, periodical updates to a RP model were performed in order to increase the number of training patients, and increase the mean plan quality in the training set [15]. Most of these approaches improved the quality of the resulting RP plans, illustrating the potential of optimized training. However, they still depend on the quality of the plans in the original model, and some approaches are not applicable when introducing a RP model for a new treatment site, or require extra work and a new validation at a later time.

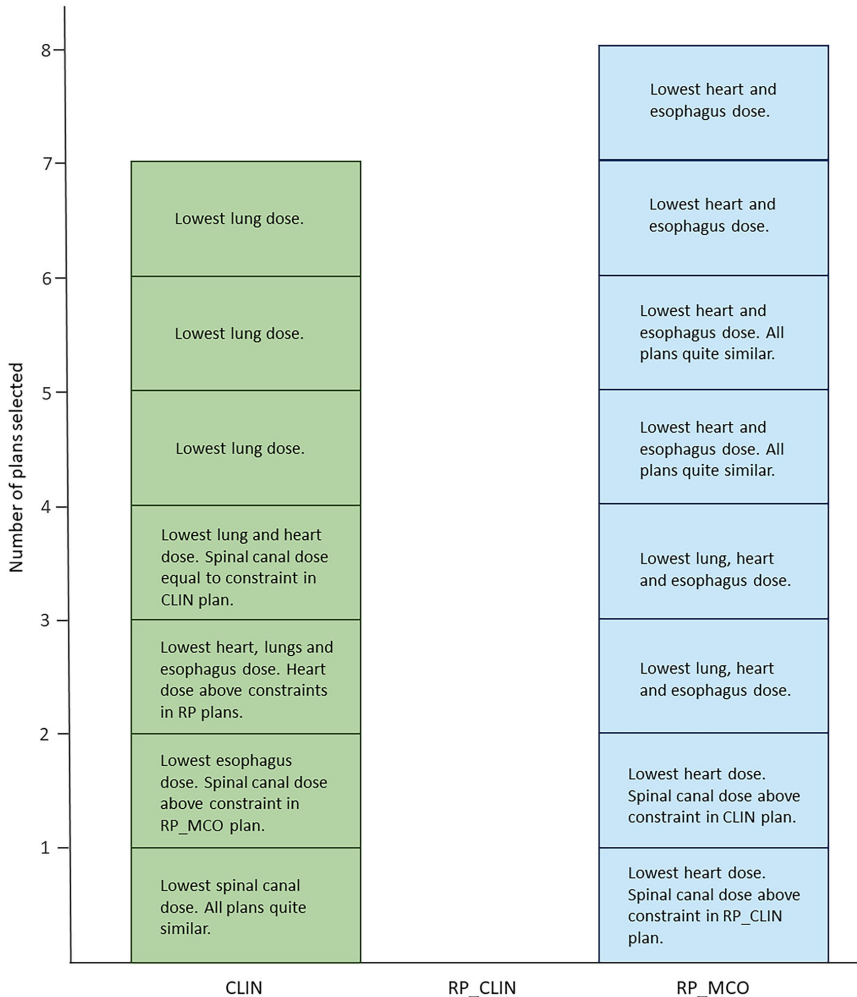


**Figure 3.** Oncologist’s choice in blinded comparison of CLIN, RP\_CLIN and RP\_MCO plans for the 15 patients. The justification for the choice for each patient is given inside the boxes.

RapidPlan has previously been combined with manual MCO-based trade-off exploration (TO) for head and neck and prostate SBRT [16,31]. The best results were achieved when both populating the model with training plans manually optimized with TO and then further individually optimizing the output plans once more with TO. This requires manual work for every patient and is dependent on the judgment of the treatment planner. Only optimizing the training plans with manual TO would be more efficient and also improved the model performance compared to using clinical plans for training [16]. Another study used 20 plans from Pinnacle Auto-Planning to train a RP model, and found similar plan quality for RP and Auto-Planning validation plans [32]. In the current study, we have demonstrated how an automatic MCO system can be used to optimally train a KBP model, for

seamless integration of knowledge from an independent system into clinical routine.

As the NTCP benefit of training RP with MCO plans instead of CLIN plans is modest, it could be questioned whether it is worth the extra effort. It should however be taken into consideration that this is a one-time effort, which leads to reduced OAR doses for many future patients. In addition, mortality in particular is a complication of paramount severity and any reduction in the risk could be of importance.

Both in manual planning and KBP of LA-NSCLC, achieving a maximum dose to the spinal canal below the constraint can be a challenge. Also in this study, the dose was slightly above the constraint for a few patients, and the  $D_{max}$  was higher in RP plans than CLIN plans. The model objectives for

the spinal canal could be set stricter in order to automatically generate plans that are always within the constraint. However, setting the right model objectives is a fine balance, and this would limit the possibility to optimize the other objectives. For clinical implementation, we decided to use the RP\_MCO model, and manually tune the spinal canal dose for the occasional patient where it is needed.

Although there were some differences in dose-volume parameters and NTCPs between the CLIN and RP\_MCO plans, these were quite small and it varied which technique was the best. The blinded evaluation also showed that the quality of the plans was similar. Therefore, the implementation of the RP\_MCO model is not expected to cause any major difference in the overall plan quality for this patient group. However, we do anticipate a reduction in planning time and more homogeneous plan quality. In addition, the complex manual planning has been performed by a few highly experienced treatment planners, while with RP, also less experienced planners can take part in the planning for this patient group.

A limitation of this study was the number of patients available for validation. In preparation for this study, we compared RP models with 20, 25, 30, 35, and 40 patients in the library, and concluded that 30 patients gave sufficient model quality and that further increasing the number of patients did not improve the model performance. This left 15 patients for open-loop validation. In addition, we have only evaluated planned and not delivered dose. However, we find it likely that uncertainties will affect the delivery of the different plans in a similar way, and that the differences found in this study will remain during treatment.

Beam angle optimization was included in the automatic MCO planning, but not available clinically. Therefore the manually selected beam angles from the clinical plan for each patient were used also in the RP plans in this study. With RP in clinical use, the planning will be quick and automated, making it easier for the treatment planner to try different options for beam placement.

Sharing of RP models between centers can be challenging due to differences in delineation, prescription, and planning techniques and strategies. Still, studies have shown that this could be feasible in some circumstances. Further work with homogenization of planning routines would be desirable in several respects, and could for instance allow centers without access to automatic MCO to incorporate KBP models from other centers with MCO training plans.

To conclude, the RapidPlan model based on automatically generated MCO plans reduced the dose to the heart and esophagus compared to the model based on clinical plans. The RP\_MCO model was implemented in the clinic, with manual tuning of the spinal canal dose when necessary, and is expected to save time in the clinical routine. Training a knowledge-based planning model with clinical plans may not be optimal in order to minimize OAR doses, and making an extra effort to optimize the library plans in the KBP model creation phase can improve the plan quality for many future patients.

This study has been evaluated using the RATING criteria for treatment planning studies and a score of 94% was achieved [33].

## Acknowledgements

The authors acknowledge Aurora Maria Baadsvik, Miriam Paetzel, Eileen Vie and Eili Helene Holm for participation in the clinical implementation of the RapidPlan model.

## Disclosure statement

B.H., S.B. and L.R.: Erasmus MC Cancer Institute has research collaborations with Elekta AB (Stockholm, Sweden), Accuray, Inc (Sunnyvale, USA), and Varian Medical Systems, Inc (Palo Alto, USA). The other authors declare no conflict of interest. The funders had no role in the design of the study; in the collection, analyses, or interpretation of data; in the writing of the manuscript, or in the decision to publish the results.

## Funding

This work was supported by Helse Vest RHF under grant number F-12505 and the Trond Mohn Foundation under grant number BFS2017TMT07.

## ORCID

Kristine Fjellanger  <http://orcid.org/0000-0002-7376-0321>  
 Helge Egil Seime Pettersen  <http://orcid.org/0000-0003-4879-771X>  
 Liv Bolstad Hysing  <http://orcid.org/0000-0002-7593-7549>

## Data availability statement

The data presented in this study are available on request from the corresponding author. The data are not publicly available due to privacy reasons as they are part of an ongoing study.

## References

- [1] Hussein M, Heijmen BJM, Verellen D, et al. Automation in intensity modulated radiotherapy treatment planning—a review of recent innovations. *Br J Radiol.* 2018;91(1092):20180270. doi: 10.1259/bjr.20180270.
- [2] Fjellanger K, Hysing LB, Heijmen BJM, et al. Enhancing radiotherapy for locally advanced non-small cell lung cancer patients with iCE, a novel system for automated multi-criterial treatment planning including beam angle optimization. *Cancers.* 2021;13:5683. doi: 10.3390/cancers13225683.
- [3] Della Gala G, Dirkx MLP, Hoekstra N, et al. Fully automated VMAT treatment planning for advanced-stage NSCLC patients. *Strahlenther Onkol.* 2017;193(5):402–409. doi: 10.1007/s00066-017-1121-1.
- [4] Bijman R, Sharfo AW, Rossi L, et al. Pre-clinical validation of a novel system for fully-automated treatment planning. *Radiother Oncol.* 2021;158:253–261. doi: 10.1016/j.radonc.2021.03.003.
- [5] Fogliata A, Belosi F, Clivio A, et al. On the pre-clinical validation of a commercial model-based optimisation engine: application to volumetric modulated arc therapy for patients with lung or prostate cancer. *Radiother Oncol.* 2014;113(3):385–391. doi: 10.1016/j.radonc.2014.11.009.
- [6] Visak J, McGarry RC, Randall ME, et al. Development and clinical validation of a robust knowledge-based planning model for stereotactic body radiotherapy treatment of centrally located lung tumors. *J Appl Clin Med Phys.* 2021;22(1):146–155. doi: 10.1002/acm2.13120.



- [7] Hussein M, South CP, Barry MA, et al. Clinical validation and benchmarking of knowledge-based IMRT and VMAT treatment planning in pelvic anatomy. *Radiother Oncol.* 2016;120(3):473–479. doi: [10.1016/j.radonc.2016.06.022](https://doi.org/10.1016/j.radonc.2016.06.022).
- [8] Kubo K, Monzen H, Ishii K, et al. Dosimetric comparison of RapidPlan and manually optimized plans in volumetric modulated arc therapy for prostate cancer. *Phys Med.* 2017;44:199–204. doi: [10.1016/j.ejmp.2017.06.026](https://doi.org/10.1016/j.ejmp.2017.06.026).
- [9] Fogliata A, Reggiori G, Stravato A, et al. RapidPlan head and neck model: the objectives and possible clinical benefit. *Radiat Oncol.* 2017;12(1):73. doi: [10.1186/s13014-017-0808-x](https://doi.org/10.1186/s13014-017-0808-x).
- [10] Schubert C, Waletzko O, Weiss C, et al. Intercenter validation of a knowledge based model for automated planning of volumetric modulated arc therapy for prostate cancer. The experience of the german RapidPlan consortium. Zhang Q, editor. *PLOS One.* 2017; 12(5):e0178034. doi: [10.1371/journal.pone.0178034](https://doi.org/10.1371/journal.pone.0178034).
- [11] Kaderka R, Mundt RC, Li N, et al. Automated closed- and open-loop validation of knowledge-based planning routines across multiple disease sites. *Pract Radiat Oncol.* 2019;9(4):257–265. doi: [10.1016/j.pro.2019.02.010](https://doi.org/10.1016/j.pro.2019.02.010).
- [12] Hundvin JA, Fjellanger K, Pettersen HES, et al. Clinical iterative model development improves knowledge-based plan quality for high-risk prostate cancer with four integrated dose levels. *Acta Oncol.* 2021;60(2):237–244. doi: [10.1080/0284186X.2020.1828619](https://doi.org/10.1080/0284186X.2020.1828619).
- [13] Fogliata A, Cozzi L, Reggiori G, et al. RapidPlan knowledge based planning: iterative learning process and model ability to steer planning strategies. *Radiat Oncol.* 2019;14(1):187. doi: [10.1186/s13014-019-1403-0](https://doi.org/10.1186/s13014-019-1403-0).
- [14] Hoffmann L, Knap MM, Alber M, et al. Optimal beam angle selection and knowledge-based planning significantly reduces radiotherapy dose to organs at risk for lung cancer patients. *Acta Oncol.* 2021;60(3):293–299. doi: [10.1080/0284186X.2020.1856409](https://doi.org/10.1080/0284186X.2020.1856409).
- [15] Scaggion A, Fusella M, Cavinato S, et al. Updating a clinical knowledge-based planning prediction model for prostate radiotherapy. *Phys Med.* 2023;107:102542. doi: [10.1016/j.ejmp.2023.102542](https://doi.org/10.1016/j.ejmp.2023.102542).
- [16] Miguel-Chumacero E, Currie G, Johnston A, et al. Effectiveness of multi-criteria optimization-based trade-off exploration in combination with RapidPlan for head & neck radiotherapy planning. *Radiat Oncol.* 2018;13(1):229. doi: [10.1186/s13014-018-1175-y](https://doi.org/10.1186/s13014-018-1175-y).
- [17] Fjellanger K, Rossi L, Heijnen BJM, et al. Patient selection, inter-fraction plan robustness and reduction of toxicity risk with deep inspiration breath hold in intensity-modulated radiotherapy of locally advanced non-small cell lung cancer. *Front Oncol.* 2022; 12:966134. doi: [10.3389/fonc.2022.966134](https://doi.org/10.3389/fonc.2022.966134).
- [18] Breedveld S, Storchi PRM, Voet PWJ, et al. iCycle: integrated, multicriterial beam angle, and profile optimization for generation of coplanar and noncoplanar IMRT plans. *Med Phys.* 2012;39(2):951–963. doi: [10.1118/1.3676689](https://doi.org/10.1118/1.3676689).
- [19] Varian Medical Systems, Inc. Eclipse Photon and Electron Reference Guide [Internet]. Varian Medical Systems, Inc.; 2017. p 1020504-002-B.
- [20] Nederlandse Vereniging voor Radiotherapie en Oncologie. Landelijk Indicatie Protocol Protonen Therapie - Longcarcinoom [Internet]. 2019. Available from: [nvro.nl/images/documenten/rapporten/LIPP\\_longen\\_final\\_01122019.pdf](https://nvro.nl/images/documenten/rapporten/LIPP_longen_final_01122019.pdf).
- [21] Appelt AL, Vogelius IR, Farr KP, et al. Towards individualized dose constraints: adjusting the QUANTEC radiation pneumonitis model for clinical risk factors. *Acta Oncol.* 2014;53(5):605–612. doi: [10.3109/0284186X.2013.820341](https://doi.org/10.3109/0284186X.2013.820341).
- [22] Defraene G, Dankers FJWM, Price G, et al. Multifactorial risk factors for mortality after chemotherapy and radiotherapy for non-small cell lung cancer. *Radiother Oncol.* 2020;152:117–125. doi: [10.1016/j.radonc.2019.09.005](https://doi.org/10.1016/j.radonc.2019.09.005).
- [23] Wijsman R, Dankers F, Troost EGC, et al. Multivariable normal-tissue complication modeling of acute esophageal toxicity in advanced stage non-small cell lung cancer patients treated with intensity-modulated (chemo-)radiotherapy. *Radiother Oncol.* 2015;117(1):49–54. doi: [10.1016/j.radonc.2015.08.010](https://doi.org/10.1016/j.radonc.2015.08.010).
- [24] Nakamura K, Okuhata K, Tamura M, et al. An updating approach for knowledge-based planning models to improve plan quality and variability in volumetric-modulated arc therapy for prostate cancer. *J Appl Clin Med Phys.* 2021;22(9):113–122. doi: [10.1002/acm2.13353](https://doi.org/10.1002/acm2.13353).
- [25] Monzen H, Tamura M, Ueda Y, et al. Dosimetric evaluation with knowledge-based planning created at different periods in volumetric-modulated arc therapy for prostate cancer: a multi-institution study. *Radiol Phys Technol.* 2020;13(4):327–335. doi: [10.1007/s12194-020-00585-0](https://doi.org/10.1007/s12194-020-00585-0).
- [26] Kang Z, Fu L, Liu J, et al. A practical method to improve the performance of knowledge-based VMAT planning for endometrial and cervical cancer. *Acta Oncol.* 2022;61(8):1012–1018. doi: [10.1080/0284186X.2022.2093615](https://doi.org/10.1080/0284186X.2022.2093615).
- [27] Wang M, Li S, Huang Y, et al. An interactive plan and model evolution method for knowledge-based pelvic VMAT planning. *J Appl Clin Med Phys.* 2018;19(5):491–498. doi: [10.1002/acm2.12403](https://doi.org/10.1002/acm2.12403).
- [28] Li N, Carmona R, Sirak I, et al. Highly efficient training, refinement, and validation of a knowledge-based planning quality-control system for radiation therapy clinical trials. *Int J Radiat Oncol Biol Phys.* 2017;97(1):164–172. doi: [10.1016/j.ijrobp.2016.10.005](https://doi.org/10.1016/j.ijrobp.2016.10.005).
- [29] Chatterjee A, Serban M, Abdulkarim B, et al. Performance of knowledge-based radiation therapy planning for the glioblastoma disease Site. *Int J Radiat Oncol Biol Phys.* 2017;99(4):1021–1028. doi: [10.1016/j.ijrobp.2017.07.012](https://doi.org/10.1016/j.ijrobp.2017.07.012).
- [30] Chatterjee A, Serban M, Faria S, et al. Novel knowledge-based treatment planning model for hypofractionated radiotherapy of prostate cancer patients. *Phys Med.* 2020;69:36–43. doi: [10.1016/j.ejmp.2019.11.023](https://doi.org/10.1016/j.ejmp.2019.11.023).
- [31] Jayarathna S, Shen X, Chen RC, et al. The effect of integrating knowledge-based planning with multicriteria optimization in treatment planning for prostate SBRT. *J Appl Clin Med Phys.* 2023;24(6):e13940. doi: [10.1002/acm2.13940](https://doi.org/10.1002/acm2.13940).
- [32] Smith A, Granatowicz A, Stoltenberg C, et al. Can the student outperform the master? A plan comparison between pinnacle auto-planning and eclipse knowledge-based RapidPlan following a prostate-bed plan competition. *Technol Cancer Res Treat.* 2019; 18:1533033819851763. doi: [10.1177/1533033819851763](https://doi.org/10.1177/1533033819851763).
- [33] Hansen CR, Crijns W, Hussein M, et al. Radiotherapy treatment planning study guidelines (RATING): a framework for setting up and reporting on scientific treatment planning studies. *Radiother Oncol.* 2020;153:67–78. doi: [10.1016/j.radonc.2020.09.033](https://doi.org/10.1016/j.radonc.2020.09.033).

## Supplementary materials

### NTCP calculations

#### *Radiation pneumonitis (RP)*

The NTCP for RP grade  $\geq 2$  was calculated using a QUANTEC model refined by Appelt et al. [1,2]:

$$NTCP = \frac{1}{1+e^{-S}} \text{ with } S = -4.12 + 0.138 \cdot MLD - 0.3711 \cdot (\text{Former smoker}) - 0.478 \cdot (\text{Current smoker}) + 0.8198 \cdot (\text{Co - morbidity}) + 0.6259 \cdot (\text{Tumor location}) + 0.5068 \cdot (\text{Old age}) + 0.47 \cdot (\text{Sequential chemo}),$$

where MLD is the mean lung dose in Gy and the other parameters are assigned value 1 or 0 according to Table S1.

Table S1. Variables in the NTCP model for radiation pneumonitis.

<b>Variable</b>	<b>Value = 1</b>	<b>Value = 0</b>
Former smoker	Yes	Never smoked/active smoker
Current smoker	Yes	Never smoked/stopped smoking
Co-morbidity <sup>1</sup>	Yes	No
Tumor location	Middle/lower lobe	Upper lobe
Old age	$\geq 63$ years	$< 63$ years
Sequential chemo	Yes	No

<sup>1</sup> Chronic obstructive pulmonary disease or other pre-existing lung disease.

### ***2-year mortality***

The NTCP for 2-year mortality based on heart dose was calculated using a model developed by Defraene et al. and revised after external validation in several patient cohorts [2,3]:

$$NTCP = \frac{1}{1+e^{-S}} \text{ with } S = -1.3409 + 0.0590 \cdot \sqrt{GTV} + 0.2635 \cdot \sqrt{MHD},$$

where GTV is the combined GTV volume of the primary tumor and nodes in cm<sup>3</sup> and MHD is the mean heart dose in Gy.

### ***Acute esophageal toxicity (AET)***

The NTCP for AET grade  $\geq 2$  was calculated using a model developed by Wijsman et al. and revised after external validation in several patient cohorts [2,4]:

$$NTCP = \frac{1}{1+e^{-S}} \text{ with } S = -3.634 + 1.496 \cdot \ln(MED) - 0.0297 \cdot OTT,$$

where MED is the mean esophagus dose in Gy and OTT is the overall radiotherapy treatment time in days.

## Results

### *Goodness of fit statistics*

The goodness of fit statistics describe how well the RapidPlan model represents the data in the training set. The coefficient of determination,  $R^2$ , describes how well the regression model represents the training plan data.  $R^2$  has values between 0.0 and 1.0, and larger values indicate a better fit. The  $\chi^2$  measures the residuals between the original and estimated data, and values closer to 1.0 indicate a better regression model.

Table S2. Training statistics for the RapidPlan models.

OAR	RP_CLIN		RP_MCO	
	$R^2$	$\chi^2$	$R^2$	$\chi^2$
Lungs	0.85	1.18	0.84	1.11
Heart	0.79	1.12	0.80	1.05
Esophagus	0.73	1.06	0.74	1.06
Spinal canal	0.77	1.00	0.89	1.14

### *Comparison of RP\_MCO and CLIN plans*

Table S3. Comparison of dose-volume parameters and NTCPs for CLIN and RP\_MCO plans.

Dose metric	CLIN			RP_MCO			<i>p</i> -value
	Avg	Median	10 <sup>th</sup> -90 <sup>th</sup> percentile	Avg	Median	10 <sup>th</sup> -90 <sup>th</sup> percentile	
PTV V <sub>95%</sub> [%]	99.0	99.1	97.8-99.8	98.9	99.3	97.1-99.8	0.4
Lungs D <sub>mean</sub> [Gy]	13.2	13.8	9.7-16.1	13.5	13.9	10.2-16.5	0.2
Lungs V <sub>5Gy</sub> [%]	52.4	53.6	38.0-62.0	53.9	55.1	39.0-66.5	0.1
Lungs V <sub>20Gy</sub> [%]	22.4	21.8	16.6-29.0	23.4	21.7	15.6-32.0	0.05
Heart D <sub>mean</sub> [Gy]	8.5	7.9	2.7-17.0	8.3	7.7	2.4-18.3	0.06
Heart V <sub>5Gy</sub> [%]	39.0	30.1	10.3-92.2	38.3	29.7	9.9-87.2	0.4
Heart V <sub>30Gy</sub> [%]	11.7	5.9	1.0-39.1	7.6	4.9	0.7-19.9	<0.001
Esophagus D <sub>mean</sub> [Gy]	19.5	18.4	7.0-32.3	18.3	17.6	6.0-30.5	0.003
Esophagus V <sub>20Gy</sub> [%]	34.8	32.1	16.7-56.6	31.2	27.6	7.5-55.8	0.005
Esophagus V <sub>60Gy</sub> [%]	9.6	7.5	0.0-24.5	9.2	4.9	0.0-23.7	0.1
Spinal canal D <sub>max</sub> [Gy]	42.7	45.7	24.2-50.3	44.8	48.7	29.9-50.8	0.05
NTCP RP [%]	21.2	22.4	6.6-36.3	22.2	21.8	6.2-37.9	0.04
NTCP 2 year mortality [%]	47.9	42.1	34.3-72.1	47.5	42.2	34.1-73.4	0.04
NTCP AET [%]	36.0	36.1	11.4-56.7	33.7	35.0	9.2-55.2	0.003

Avg = average.

### Population average DVHs with confidence intervals

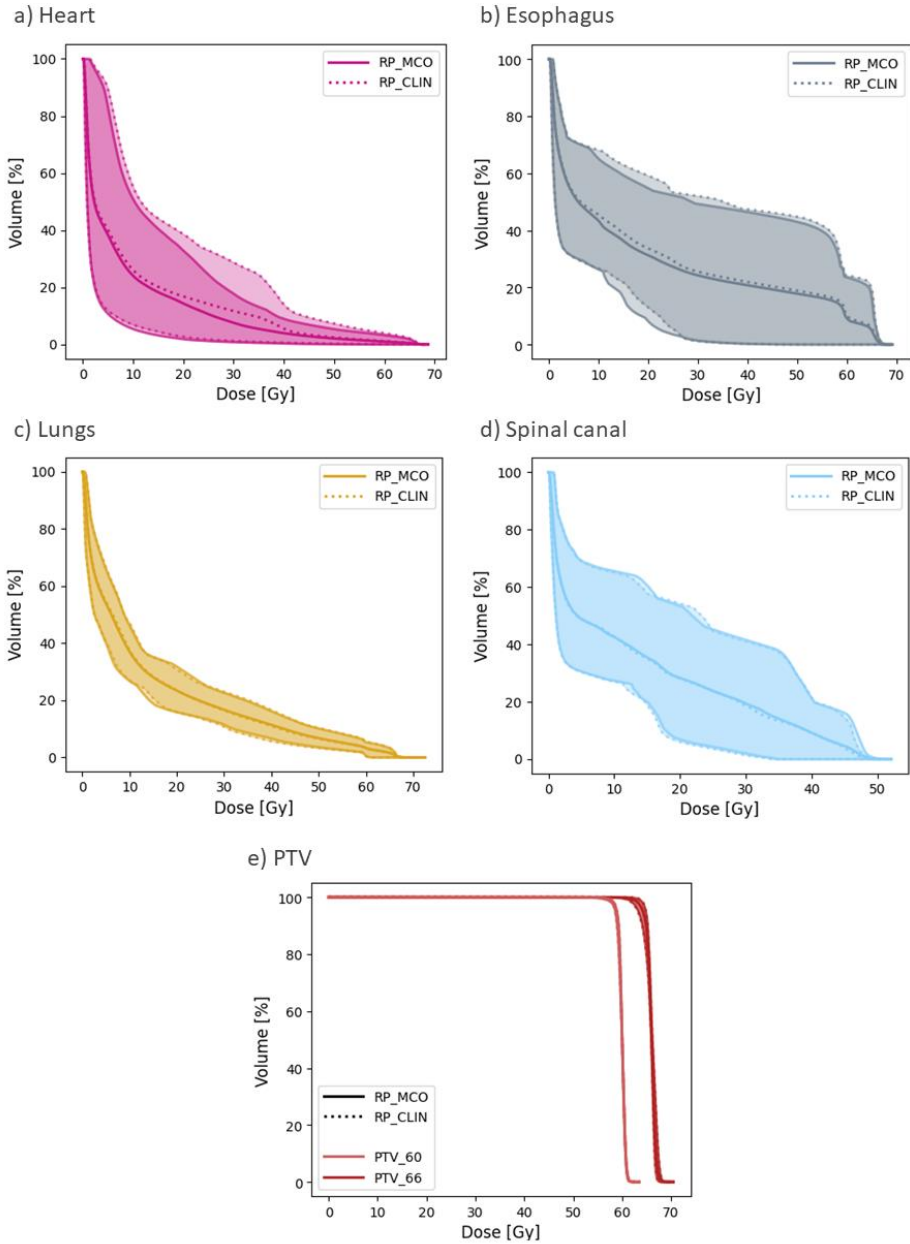


Figure S1. Population average DVHs for PTV and OARs for RP\_CLIN and RP\_MCO plans. The central lines show the average, and the shaded areas indicate the 90% confidence interval.

## References

- [1] Appelt AL, Vogelius IR, Farr KP, et al. Towards individualized dose constraints: Adjusting the QUANTEC radiation pneumonitis model for clinical risk factors. *Acta Oncologica*. 2014;53:605–612.
- [2] Nederlandse Vereniging voor Radiotherapie en Oncologie. Landelijk Indicatie Protocol Protonen Therapie - Longcarcinoom [Internet]. 2019. Available from: [nvro.nl/images/documenten/rapporten/LIPP\\_longen\\_final\\_01122019.pdf](http://nvro.nl/images/documenten/rapporten/LIPP_longen_final_01122019.pdf).
- [3] Defraene G, Dankers FJWM, Price G, et al. Multifactorial risk factors for mortality after chemotherapy and radiotherapy for non-small cell lung cancer. *Radiotherapy and Oncology*. 2020;152:117–125.
- [4] Wijsman R, Dankers F, Troost EGC, et al. Multivariable normal-tissue complication modeling of acute esophageal toxicity in advanced stage non-small cell lung cancer patients treated with intensity-modulated (chemo-)radiotherapy. *Radiotherapy and Oncology*. 2015;117:49–54.











## OPEN ACCESS

EDITED BY  
Savino Cilla,  
Gemelli Molise Hospital, Italy

REVIEWED BY  
Nuradh Joseph,  
Government of Sri Lanka, Sri Lanka  
Hans Christiansen,  
Hannover Medical School, Germany

\*CORRESPONDENCE  
Liv Bolstad Hysing  
liv.bolstad.hysing@helse-bergen.no

SPECIALTY SECTION  
This article was submitted to  
Radiation Oncology,  
a section of the journal  
Frontiers in Oncology

RECEIVED 10 June 2022  
ACCEPTED 02 August 2022  
PUBLISHED 30 August 2022

CITATION  
Fjellanger K, Rossi L, Heijmen BJM,  
Pettersen HES, Sandvik IM,  
Breedveld S, Sulen TH and Hysing LB  
(2022) Patient selection, inter-fraction  
plan robustness and reduction of  
toxicity risk with deep inspiration  
breath hold in intensity-modulated  
radiotherapy of locally advanced non-  
small cell lung cancer.  
*Front. Oncol.* 12:966134.  
doi: 10.3389/fonc.2022.966134

COPYRIGHT  
© 2022 Fjellanger, Rossi, Heijmen,  
Pettersen, Sandvik, Breedveld, Sulen and  
Hysing. This is an open-access article  
distributed under the terms of the  
[Creative Commons Attribution License  
\(CC BY\)](https://creativecommons.org/licenses/by/4.0/). The use, distribution or  
reproduction in other forums is  
permitted, provided the original  
author(s) and the copyright owner(s)  
are credited and that the original  
publication in this journal is cited, in  
accordance with accepted academic  
practice. No use, distribution or  
reproduction is permitted which does  
not comply with these terms.

# Patient selection, inter-fraction plan robustness and reduction of toxicity risk with deep inspiration breath hold in intensity-modulated radiotherapy of locally advanced non-small cell lung cancer

Kristine Fjellanger<sup>1,2</sup>, Linda Rossi<sup>3</sup>, Ben J. M. Heijmen<sup>3</sup>,  
Helge Egil Seime Pettersen<sup>1</sup>, Inger Marie Sandvik<sup>1</sup>,  
Sebastian Breedveld<sup>3</sup>, Turid Husevåg Sulen<sup>1</sup>  
and Liv Bolstad Hysing<sup>1,2\*</sup>

<sup>1</sup>Department of Oncology and Medical Physics, Haukeland University Hospital, Bergen, Norway,

<sup>2</sup>Institute of Physics and Technology, University of Bergen, Bergen, Norway, <sup>3</sup>Department of Radiotherapy, Erasmus MC Cancer Institute, Erasmus University Medical Center, Rotterdam, Netherlands

**Background:** State-of-the-art radiotherapy of locally advanced non-small cell lung cancer (LA-NSCLC) is performed with intensity-modulation during free breathing (FB). Previous studies have found encouraging geometric reproducibility and patient compliance of deep inspiration breath hold (DIBH) radiotherapy for LA-NSCLC patients. However, dosimetric comparisons of DIBH with FB are sparse, and DIBH is not routinely used for this patient group. The objective of this simulation study was therefore to compare DIBH and FB in a prospective cohort of LA-NSCLC patients treated with intensity-modulated radiotherapy (IMRT).

**Methods:** For 38 LA-NSCLC patients, 4DCTs and DIBH CTs were acquired for treatment planning and during the first and third week of radiotherapy treatment. Using automated planning, one FB and one DIBH IMRT plan were generated for each patient. FB and DIBH was compared in terms of dosimetric parameters and NTCP. The treatment plans were recalculated on the repeat CTs to evaluate robustness. Correlations between  $\Delta$ NTCPs and patient characteristics that could potentially predict the benefit of DIBH were explored.

**Results:** DIBH reduced the median  $D_{\text{mean}}$  to the lungs and heart by 1.4 Gy and 1.1 Gy, respectively. This translated into reductions in NTCP for radiation pneumonitis grade  $\geq 2$  from 20.3% to 18.3%, and for 2-year mortality from 51.4% to 50.3%. The organ at risk sparing with DIBH remained significant in week 1 and week 3 of treatment, and the robustness of the target coverage was similar for FB and DIBH. While the risk of radiation pneumonitis was consistently

reduced with DIBH regardless of patient characteristics, the ability to reduce the risk of 2-year mortality was evident among patients with upper and left lower lobe tumors but not right lower lobe tumors.

**Conclusion:** Compared to FB, DIBH allowed for smaller target volumes and similar target coverage. DIBH reduced the lung and heart dose, as well as the risk of radiation pneumonitis and 2-year mortality, for 92% and 74% of LA-NSCLC patients, respectively. However, the advantages varied considerably between patients, and the ability to reduce the risk of 2-year mortality was dependent on tumor location. Evaluation of repeat CTs showed similar robustness of the dose distributions with each technique.

#### KEYWORDS

Deep inspiration breath hold (DIBH), gating, lung cancer radiotherapy, radiotherapy robustness, normal tissue complication probability (NTCP), autoplanning, iCE, radiation toxicity

## 1 Introduction

For patients with locally advanced non-small cell lung cancer (LA-NSCLC), only two thirds are expected to be alive after two years when immunotherapy is added to concurrent chemoradiotherapy (1). Reducing severe side effects caused by irradiation of the heart, immune cells, lungs, and esophagus could directly or indirectly improve survival (2–8).

Radiotherapy of LA-NSCLC is usually performed during free breathing (FB), with a planning margin around the tumor to ensure dose coverage in all breathing phases. As an alternative to FB, deep inspiration breath hold (DIBH) has been investigated for several tumor sites in the thorax and abdomen (9–11). DIBH is a respiratory gating technique where patients hold their breath at a specific level of inspiration during radiotherapy delivery, potentially increasing the separation between the target volume and organs at risk (OARs), and allowing smaller margins due to the elimination of breathing motion (9).

For LA-NSCLC, two planning studies have shown potential of a dosimetric benefit of treatment delivery in DIBH compared to FB for in total 42 patients, where the majority had tumors in the upper lobes (12, 13). In a VMAT planning study, significant dose reductions were found for the lungs, heart, esophagus, trachea and bronchi with DIBH compared to FB (12). Due to large variation between patients, this study recommended comparative planning, which may be challenging in clinical routine because of limitations in staff, equipment and machine capacity (11). A treatment planning study for 3D-CRT found reductions in all investigated lung dose parameters and some heart and esophagus parameters with DIBH (13). In the published planning studies comparing DIBH and FB for LA-NSCLC, manual planning was used for plan generation, which

introduces a risk of inconsistent plan quality. Many studies for various tumor sites, including LA-NSCLC, have shown significant improvements in plan quality with autoplanning compared to manual planning (14–16).

Previous studies have reported encouraging patient compliance of DIBH in radiotherapy for LA-NSCLC, with small intra- and inter-breath-hold uncertainties in tumor position registered in fluoroscopic movies of liquid markers during the treatment course (17) and evaluations of consecutive CT scans at treatment planning (18). However, DIBH and FB treatments have not yet been compared regarding robustness of the dose distributions against inter-fraction anatomical variations or slow inter-fraction time trends, e.g. caused by radiation-induced anatomical changes. It is not clear whether inter-fraction variations in DIBH inspiration level and FB breathing pattern affect the dose distributions differently, and how margin reduction with DIBH affects the target dose robustness.

The aims of the current study were to dosimetrically compare FB with DIBH for LA-NSCLC patients, including inter-fraction robustness, and to investigate which patients are more likely to benefit from DIBH. For this purpose, we initiated a prospective image collection study for LA-NSCLC patients treated with intensity-modulated radiotherapy (IMRT). To avoid bias, all treatment plans were generated with automated multi-criterial treatment planning with integrated beam-angle optimization (BAO) (14), and the same autoplanning configuration was used for both FB and DIBH (19). Comparisons were made in terms of dose-volume parameters and normal tissue complication probabilities (NTCPs), both on a population basis and with focus on the effect for individual patients. For these analyses, CT scans acquired in the treatment-

preparation phase were used. For assessment of dosimetric robustness against inter-fraction anatomical variations, repeat DIBH and FB CT scans (rCTs) were acquired during the fractionated treatment and used to recalculate dose. Finally, we investigated to what extent specific patient or tumor characteristics could be used to predict the best choice between treatment with DIBH or with FB for new patients, thereby avoiding unnecessary patient-specific comparative planning.

## 2 Materials and methods

### 2.1 Patients and clinical treatment

Between October 2019 and May 2022, 38 consecutive patients receiving radiotherapy with curative intent according to the protocol for LA-NSCLC at Haukeland University Hospital participated in prospective image collection for this simulation study. The study was approved by the regional committee for medical and health research ethics in Western Norway (protocol code 2019/749) and all participants gave informed consent. Clinical parameters describing the disease and condition of the patients as well as the prescribed treatments were collected.

Clinical treatments were delivered with IMRT in FB as a standard. For nine patients the oncologist chose treatment in DIBH instead, mainly due to high lung doses with FB. Thirty-three patients were treated with 6 IMRT beams. Based on patient-specific assessments, three patients had one field removed to reduce lung dose and were thus treated with 5 IMRT beams and two patients with large fields were treated with VMAT. The planning strategy and objectives are described in section S1. In accordance with national guidelines, the prescribed dose was 60 or 66 Gy for concomitant treatment and 66 or 70 Gy for sequential treatment (depending on lung function, lung dose and proximity of the brachial plexus to the PTV), all in 2 Gy fractions. The plans were normalized to the median PTV dose (PTV  $D_{\text{median}} = 100\%$ ). Daily CBCTs followed by table corrections with six degrees of freedom were used for on-line positioning.

To ensure high quality and consistency and avoid planner bias, the manually created clinical treatment plans were not used in this study. Instead, automated plans were generated as described in section 2.3.

### 2.2 Acquired CT scans and delineation

For each patient, a 10-phase 4DCT and three DIBH CTs were acquired for planning, and a repeated 4DCT and DIBH CT were acquired during the first week (W1) and third week (W3) of treatment. Imaging was performed on a Big Bore CT scanner

(Philips Healthcare, Best, The Netherlands), using a Posirest-2 support device (Civco Radiotherapy, Coralville, USA) for fixation in the supine position with arms resting above the head. The breathing curve for the 4DCT was acquired using the Philips Bellows device. DIBH was performed with the Respiratory Gating for Scanners (RGSC) system (Varian Medical Systems, Palo Alto, USA), using a marker box placed on the sternum, 2-3 mm gating window and visual feedback. The patients practiced breath holds before image acquisition at the planning CT session.

Gross tumor volumes (GTVs) for the primary tumor and lymph nodes were delineated according to ESTRO guidelines (20). For FB planning CTs and rCTs, the OARs and GTVs were delineated on the average intensity projection (AIP) of the 4DCT, and the internal GTV (IGTV) incorporated the GTV positions in all 4DCT phases. For DIBH planning, the OARs and GTVs were delineated on one of the DIBH CTs, and the IGTV incorporated the GTV positions in the two other DIBH CTs. In W1 and W3 only one DIBH rCT was acquired, hence no IGTV was delineated. For both FB and DIBH, the clinical target volume (CTV) was defined by expanding the IGTV (or GTV) by 5 mm without extending into uninvolved organs such as bone, heart, esophagus and major vessels. A 5 mm isotropic margin from the CTV was used to define the planning target volume (PTV). As OARs, the lungs, heart, esophagus, spinal canal and brachial plexus (if relevant) were delineated according to RTOG guidelines (21).

### 2.3 Automated treatment planning

The novel in-house “iCE” system for automated multi-criterial planning with integrated BAO was used to generate all the treatment plans in this study (14). In iCE, an initial Pareto-optimal, fluence-map-optimized treatment plan is automatically created in Erasmus-iCycle, based on a wish-list tuned to reflect the clinical priorities for this patient group (22). The dose distribution is then automatically reconstructed in Eclipse (Varian Medical Systems), resulting in a deliverable plan created without manual intervention. A detailed description of iCE and the applied wish-list can be found elsewhere (14).

In this study, iCE was used to automatically generate two deliverable 6-beam IMRT plans for each patient, one on the FB and one on the DIBH planning CT, each with optimized beam angles. The applied wish-list was the same for FB and DIBH planning, reflecting the common clinical protocols. The same prescription dose as in the clinical plan was used and the plans were normalized to the median dose in the PTV, as in clinical practice. The applied Eclipse version was 16.1, the Photon Optimizer algorithm was used for optimization and the Acuros External Beam algorithm was used for dose calculation.

## 2.4 Comparison of FB and DIBH

### 2.4.1 Dosimetric comparison based on planning CT scans

The FB and DIBH plans were compared using relevant dose-volume parameters for the PTV and OARs, the effective dose to immune cells (EDIC) given as equivalent uniform dose (see section S2.4. for details) and NTCPs (NB reference to subsection (needs numbering)). For lungs and heart, where the volume is expected to be different in FB and DIBH, we further estimated the integral dose (ID [Gy·L] =  $D_{\text{mean}}$  [Gy] · volume [L]). The mean dose to the lungs, heart and esophagus are clinically important and commonly reported parameters related to toxicity, and were therefore used for evaluation of per-patient differences.

### 2.4.2 Robustness of the dose distribution assessed with repeat CT scans

The W1 and W3 rCTs were rigidly matched to the corresponding planning CTs, using six degrees of freedom and a volume of interest covering the PTV and surrounding skeletal structures. The FB and DIBH plans were then recalculated on the respective rCTs. For the target volume, the robustness was considered sufficient if the CTV  $V_{95\%}$  was > 99%. For the OARs, the changes in dose-volume parameters from planning to each rCT were evaluated.

### 2.4.3 NTCPs

To evaluate the clinical impact of dosimetric differences between FB and DIBH, NTCPs for RP grade  $\geq 2$ , acute esophageal toxicity (AET) grade  $\geq 2$  and 2-year mortality based on heart dose (heart model) were calculated according to validated models used in the proton therapy selection framework in the Netherlands (23–26). An alternative model for 2-year mortality based on the EDIC was also applied (EDIC model) (6). A detailed description of the models is given in section S2.

## 2.5 Patient characteristics and benefit of DIBH

Correlations between the  $\Delta$ NTCPs [NTCP (DIBH) – NTCP (FB)] and patient characteristics that could potentially predict the benefit of DIBH were explored, with focus on characteristics that are known before or during the planning CT session:

- Primary tumor in the upper or lower lobes
- Primary tumor in the left or right lung
- Expansion of the lungs with DIBH (relative increase in lung volume compared to FB)
- Cranio-caudal motion extension of the primary tumor in FB (breathing motion)

The tumor breathing motion was determined by deformable mapping of the primary tumor GTV from the AIP to each phase of the 4DCT, followed by visual inspection of the structures to ensure accuracy, and measuring the motion extension of the GTV center of mass.

One patient had a primary tumor extending into both the right upper and middle lobes, and was grouped with the upper lobes for this analysis.

## 2.6 Statistical analysis

Statistical analyses were performed using SPSS Statistics v. 26 (IBM Corp., Armonk, USA). The two-tailed Wilcoxon signed-rank test was used for related samples. Linear regression was used to test correlations between two continuous variables.  $p$ -values  $\leq 0.05$  were considered statistically significant. Percentiles were established using a weighted average method.

## 3 Results

### 3.1 Patients and anatomy

Among the 38 included patients, most had stage IIIA-IIIIB disease. 29 had both a primary tumor and lymph nodes in the target volume, 1 had only lymph nodes and 8 had only a primary tumor. The primary tumor was located in the upper lobes for 20 patients and the lower lobes for 17. A summary of patient and treatment characteristics is given in Table 1.

At planning, the DIBH PTVs were on average 6% smaller than the FB PTVs (386 cm<sup>3</sup> vs. 409 cm<sup>3</sup>,  $p < 0.001$ ), the lung volumes increased by 50% (5656 cm<sup>3</sup> vs. 3776 cm<sup>3</sup>,  $p < 0.001$ ), and the heart volumes decreased by 7% (659 cm<sup>3</sup> vs. 709 cm<sup>3</sup>,  $p < 0.001$ ) with DIBH compared to FB (Figure 1).

### 3.2 Dosimetric comparison of FB and DIBH at planning

At planning, DIBH had a slightly lower median PTV  $V_{95\%}$  than FB (Table 2). The objective of  $V_{95\%} > 98\%$  was achieved in all plans except the DIBH plans for two patients, which had  $V_{95\%} > 95\%$ . All dosimetric parameters for the lungs, heart and spinal canal were significantly reduced with DIBH compared to FB, except for ID to the lungs (Table 2 and Figure 2). For the esophagus, no significant differences were found. There were large inter-patient variations in dosimetric differences between FB and DIBH (Figure 2). DIBH resulted in a lower lung  $D_{\text{mean}}$  than FB for 35/38 patients (range -4.5 to 0.6 Gy) and a lower heart  $D_{\text{mean}}$  for 28/38 patients (range -7.6 to 3.6 Gy), while for the esophagus around half the patients were better off with either technique and the difference in  $D_{\text{mean}}$  ranged from -7.5 Gy to 7.1

TABLE 1 Patient and treatment characteristics.

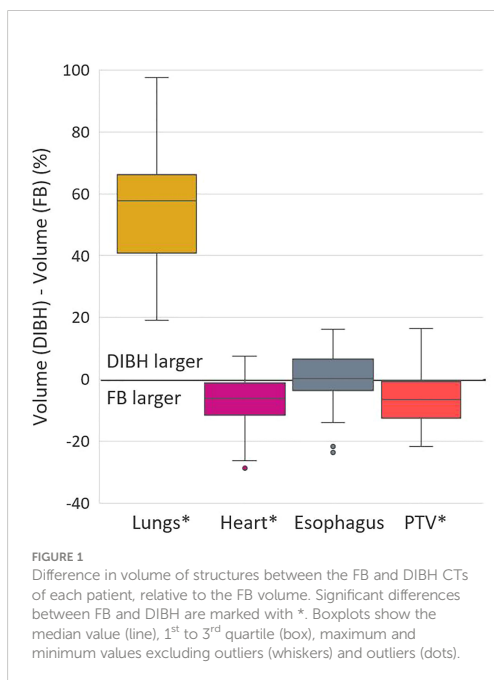
Characteristic		Number of Patients
Stage	IB <sup>1</sup>	1
	IIB	2
	IIIA	15
	IIIB	15
	IIIC	3
	IVA <sup>2</sup>	2
Target volume	Primary tumor and lymph nodes	29
	Primary tumor only	8
	Lymph nodes only	1
Primary tumor location (lobe)	Right upper	13
	Right upper + middle	1
	Right lower	7
	Left upper	6
	Left lower	10
Smoking habits	Active smoker	15
	Previous smoker	22
	Non-smoker	1
Pulmonary comorbidity	COPD	21
	Other	1
	None	16
Prescribed dose	60 Gy	14
	66 Gy	23
	70 Gy	1
Chemotherapy	Concurrent	36
	Sequential	2
Characteristic	Average	Range
Age (years)	66	53-82
GTV volume (cm <sup>3</sup> )	115	13-1021
Overall treatment time (days)	44	39-49
Tumor motion (mm) <sup>3</sup>	4	0-21

<sup>1</sup>This patient had an inoperable tumor due to the position in the main bronchus, and received radiotherapy according to the protocol for LA-NSCLC. <sup>2</sup>These patients had a solitary brain metastasis that was treated separately, and received radiotherapy with curative intent according to the protocol for LA-NSCLC. <sup>3</sup>Cranio-caudal motion of the primary tumor GTV in FB. The number of patients in each category is given for categorical variables. The average value and range is given for continuous variables.

Gy. Figure 3 illustrates how parts of the lungs and heart could be moved out of the treatment field with DIBH, resulting in substantial dose sparing.

### 3.3 Robustness of dose distributions assessed with rCTs

Repeat CTs in W1 were available for all 38 patients, while three patients did not complete the W3 scans due to poor



condition or covid-19. The 35 patients who completed all CT sessions were included in the statistical analyses of robustness.

The target coverage in W1 and W3 was satisfactory for most patients, the median CTV V<sub>95%</sub> was 100% for both FB and DIBH at all time points (Tables S3-S4), and there were no significant differences in CTV V<sub>95%</sub> between FB and DIBH in neither W1 ( $p = 0.2$ ) or W3 ( $p = 1.0$ ). However, the CTV V<sub>95%</sub> was <99% in FB for seven patients in W1 and five patients in W3, and in DIBH for five patients in W1 and three patients in W3 (Figure 2D).

Both for FB and DIBH, most OAR parameters were similar in the planning CT and rCTs, except for the esophagus which received a higher dose in W3 than at planning (Tables S3, S4, Figure 2). The lungs D<sub>mean</sub> was also slightly increased in W3 with both techniques. The dose to the lungs and heart remained significantly lower with DIBH than FB at all time points. Per-patient analysis showed that for the lungs and heart, the D<sub>mean</sub> and difference in D<sub>mean</sub> between FB and DIBH were quite stable for the different time points for most patients, while for the esophagus they varied more between planning and rCTs with changes in D<sub>mean</sub> of up to 8-10 Gy seen in some of the FB plans (Figures S2 and 2).

### 3.4 NTCPs

In addition to dose-volume parameters, a number of clinical parameters were collected and used in the NTCP calculations (Table 1).

TABLE 2 Dose-volume metrics and NTCPs for FB and DIBH plans at planning.

Metric	FB		DIBH		p-value	Patients with benefit of DIBH
	Median	10 <sup>th</sup> -90 <sup>th</sup> pctl	Median	10 <sup>th</sup> -90 <sup>th</sup> pctl		
PTV V <sub>95%</sub> (%)	99.4	98.7-99.7	99.1	98.0-99.5	<0.001*	24%
Patient D <sub>max</sub> (%)	104.9	103.9-105.9	104.7	104.0-106.1	0.8	50%
Lungs D <sub>mean</sub> (Gy)	15.2	9.3-18.9	13.8	7.7-17.2	<0.001*	92%
Lungs V <sub>5Gy</sub> (%)	58.7	41.4-78.7	54.3	38.0-73.5	0.007*	68%
Lungs V <sub>20Gy</sub> (%)	24.9	15.5-34.1	23.7	12.8-30.9	<0.001*	89%
Lungs ID (Gy*L)	51.9	32.1-84.7	70.8	47.5-100.8	<0.001*	0%
Heart D <sub>mean</sub> (Gy)	9.3	2.7-19.9	8.2	1.6-18.9	0.002 *	74%
Heart V <sub>5Gy</sub> (%)	42.6	9.9-84.6	35.5	5.3-93.6	0.05 *	66%
Heart V <sub>30Gy</sub> (%)	8.4	1.6-22.7	7.8	0.0-16.6	0.005*	68%
Heart ID (Gy*L)	5.6	0.4-12.7	5.2	0.3-11.5	<0.001*	71%
Esophagus D <sub>mean</sub> (Gy)	19.5	10.8-30.8	19.2	13.4-30.5	0.7	55%
Esophagus V <sub>20Gy</sub> (%)	36.7	23.6-55.2	36.3	26.1-56.4	0.1	39%
Esophagus V <sub>60 Gy</sub> (%)	4.9	0.0-27.9	5.8	0.0-24.3	0.8	50%
Spinal canal D <sub>max</sub> (Gy)	46.1	34.7-50.7	42.7	28.5-50.0	0.007 *	71%
EDIC (Gy)	4.6	2.9-6.8	4.2	2.7-6.1	<0.001*	89%
NTCP RP (%) <sup>1</sup>	20.3	9.1-39.7	18.3	7.1-35.5	<0.001*	92%
NTCP AET (%) <sup>2</sup>	38.9	21.9-55.4	38.8	25.3-55.9	0.8	55%
NTCP Mortality (heart) (%) <sup>3</sup>	51.4	37.1-65.2	50.3	36.5-64.4	0.002*	74%
NTCP Mortality (EDIC) (%) <sup>4</sup>	41.0	28.0-53.1	37.4	27.3-51.0	<0.001*	89%

<sup>1</sup> Radiation pneumonitis grade  $\geq 2$ , <sup>2</sup> acute esophageal toxicity grade  $\geq 2$ , <sup>3</sup> 2-year mortality (heart model), <sup>4</sup> 2-year mortality (EDIC model).

Median value and 10<sup>th</sup>-90<sup>th</sup> percentile (pctl) is given, along with p-values for comparison between the techniques. Significant differences are marked with \*. The percentage of patients with benefit of DIBH is also given for each parameter.

The NTCPs for RP, 2-year mortality (heart model) and 2-year mortality (EDIC model) were significantly lower with DIBH compared to FB, with average  $\Delta$ NTCPs of -3.8 percentage points (pp), -0.9 pp and -2.3 pp, respectively. There was no significant difference for AET (Table 2). The advantage of DIBH was generally larger for patients with higher risk of radiation-induced complication for RP ( $p = 0.002$ ), AET ( $p = 0.01$ ) and 2-year mortality (heart model) ( $p = 0.07$ ) but not for 2-year mortality (EDIC model) ( $p = 0.463$ ) (Figure 4).

While the 2-year mortality was lower with DIBH than FB according to both the applied models, the median NTCPs were 10-13 pp lower with the EDIC model than the heart dose model.

### 3.5 Patient characteristics and benefit of DIBH

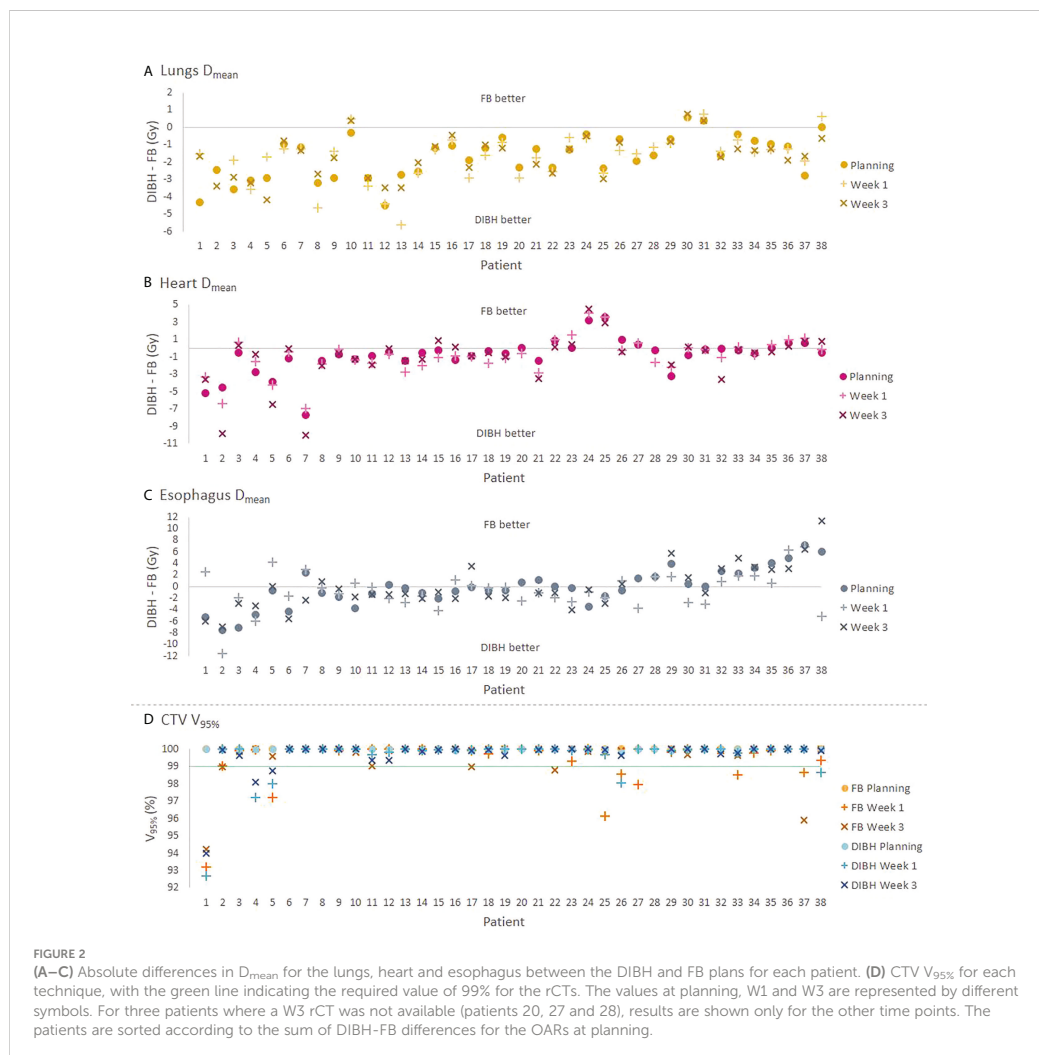
The NTCPs for RP and 2-year mortality (EDIC model) were significantly lower with DIBH than FB regardless of tumor position, and there was no correlation between  $\Delta$ NTCP and tumor motion in FB or lung expansion with DIBH (Tables S5-S6).

For 2-year mortality (heart model), the NTCP was significantly lower with DIBH than FB for the patients with

tumors in the upper lobe and left lung, but similar for patients with tumors in the lower lobe or right lung (Table S5). Separating the patients according to lobe, 83%, 79% and 80% of the patients with tumors in the left upper lobe, right upper lobe and left lower lobe had a lower NTCP for 2-year mortality (heart model) with DIBH than FB ( $\Delta$ NTCP range -4.6 to 0.6 pp), while this benefit was seen for only 43% of the patients with tumors in the right lower lobe ( $\Delta$ NTCP range -1.2 to 3.7 pp) (Figure 5).

## 4 Discussion

For LA-NSCLC patients treated with static beam IMRT, this study found significantly enhanced dosimetric sparing of the lungs and heart by using DIBH instead of FB. The dosimetric findings translated into reduced risks of RP and 2-year mortality. Patients with the highest complication risks benefited most from DIBH. The OAR sparing with DIBH remained similar in W1 and W3 of treatment. The robustness of the target coverage was similar for FB and DIBH, despite smaller margins in the DIBH plans. However, in 9%-14% of the DIBH plans and 14%-20% of the FB plans (depending on time point), there was not sufficient coverage of the CTV in the rCTs, suggesting a potential added value of adaptive protocols for this patient group (27).



Looking at individual patients, the sparing of the lungs with DIBH was consistent; more than 90% of the patients had a lower lung  $D_{mean}$  with DIBH than with FB. For the heart, DIBH was favorable around 70% of the patients: for these patients the deep inspiration could likely increase the separation of the heart from the PTV and enable a dose reduction. However, for two patients, the heart  $D_{mean}$  increased by more than 3 Gy and the NTCP for 2-year mortality (heart model) by 2–4 pp with DIBH. The median values for esophagus dose were similar between FB and DIBH, but there were large inter-patient differences both between the techniques and the different time points. Changes of

up to 10 Gy in the esophagus  $D_{mean}$  occurred between planning and rCTs, and the largest changes were seen in FB.

A clinical study of various respiratory gating techniques in 3D-CRT for lung cancer patients with different stages and prescriptions found less pulmonary and esophageal toxicity with respiratory gating compared to FB (28). Two previous planning studies with 3D-CRT and VMAT, although limited in the number of patients and performed with manual planning, have found an overall benefit of DIBH for LA-NSCLC patients in terms of reduced OAR doses compared to FB (12, 13). The current study showed the potential of DIBH also in static beam



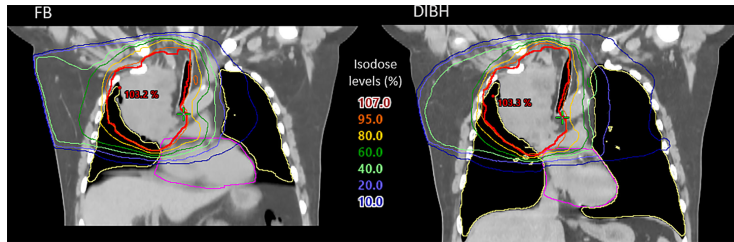


**FIGURE 3**  
Dose distributions superimposed on planning CT scans of patient 1, showing enhanced sparing of OARs in DIBH (right) compared to FB (left). Contours are shown for the PTV (red), lungs (yellow) and heart (magenta). Isodoses are shown in percentage of the prescribed dose (60 Gy).

IMRT, in a larger and more heterogeneous cohort of LA-NSCLC patients, and also reported on inter-patient differences and robustness in terms of inter-fractional changes in delivered dose. Although both VMAT and IMRT with a few static beams are used for treating LA-NSCLC patients with intensity modulation, the latter is particularly suited for avoiding large volumes of healthy lung tissue receiving low dose (15, 29). We have also experienced such an advantage with IMRT compared to VMAT in our clinic and have therefore concluded that in our

situation treatment with static beam IMRT is preferred for these patients.

Despite the promising results for OAR sparing and patient compliance, the use of DIBH for LA-NSCLC patients is still limited. In the POP-ART RT survey, the most important barriers stated for implementation or expanded use of respiratory motion management were resources in terms of equipment, staff and machine capacity (11). Identifying and prioritizing the patients with most benefit of DIBH could therefore be valuable.

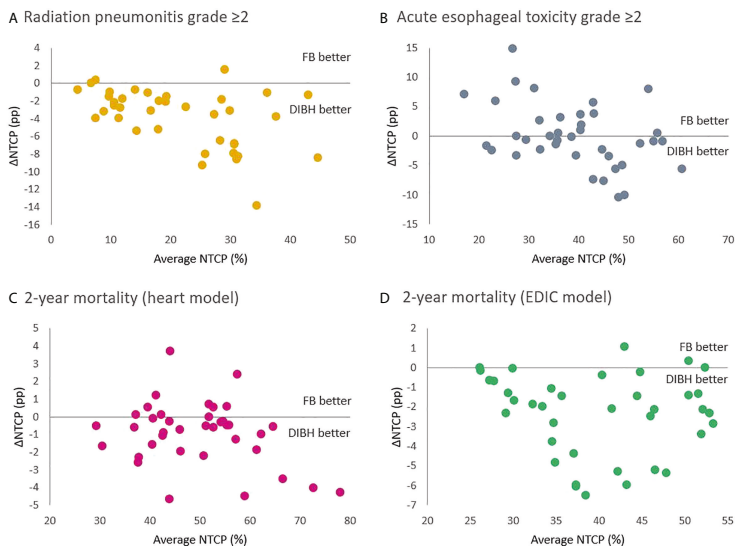
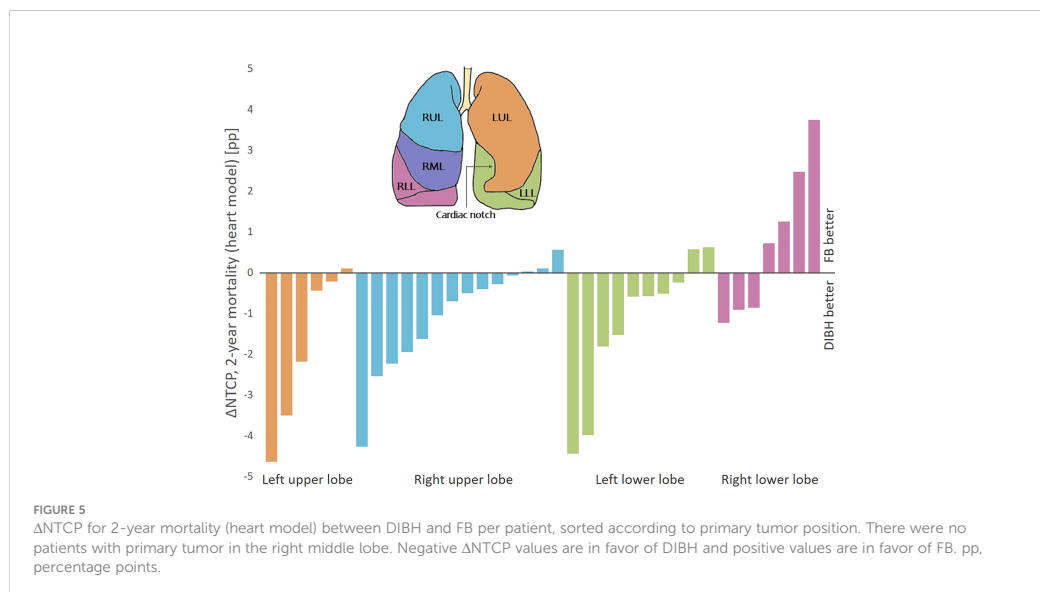


**FIGURE 4**  
 $\Delta$ NTCP between DIBH and FB as a function of the average NTCP value in the FB and DIBH plans for each patient, for (A) RP, (B) AET, (C) 2-year mortality (heart model) and (D) 2-year mortality (EDIC model). pp, percentage points.



This study showed a consistent reduction in the NTCP for RP with DIBH compared to FB, regardless of patient characteristics. Interestingly, despite lower-lobe tumors being more mobile and therefore having more potential for margin reduction with DIBH, increased  $\Delta$ NTCP for RP was not seen for neither lower-lobe compared to upper-lobe tumors, or with increased breathing motion. However, the NTCP for 2-year mortality (heart model) was reduced with DIBH for almost all patients with tumors in the upper lobes or left lower lobe, while it varied which technique was best for patients with tumors in the right lower lobe. As the mediastinum narrows during DIBH, the heart is compressed and caudal parts are moved from the left side towards the center of the body. This can increase the separation between tumors in the left lower lobe and the heart, while for tumors in the right lower lobe, decreased separation and compression of the heart could instead increase the heart dose with DIBH compared to FB. This analysis should, however, be seen as a preliminary investigation, as the number of patients in each group was small, and the interconnection between the parameters was, for this reason, not investigated. Persson et al. did not find a pattern in benefit regarding OAR doses between FB and DIBH depending on tumor position; however, their study included only three patients with lower lobe tumors, all in the left lung (12).

The NTCP models for RP, AET and 2-year mortality based on heart dose used in this study have been externally validated and carefully selected in the Dutch proton therapy selection framework (23). Recently, the radiation of immune cells and its impact on survival has received increased attention, and Jin et al.

published a method for approximating the EDIC, as well as a corresponding model for 2-year overall survival based on data from the RTOG0617 study (6). When applying their model for the patients in this study, the benefit of DIBH was retained, but the estimates for median 2-year mortality were 10–13 pp lower than with the heart dose model. The EDIC model is based on one patient cohort where the dose characteristics were quite different from the ones in this study; especially the heart dose was clearly higher. In a study by Thor et al. where IMRT was applied with similar heart doses to our cohort, the estimated dose of radiation to immune cells was not found to correlate with progression-free survival (30). In our cohort, the NTCP for 2-year mortality based on EDIC seems to be driven mainly by the mean lung dose. Because this parameter was lower with DIBH as a consequence of an increase in lung volume, we cannot know the clinical relevance of a lower EDIC with DIBH and this needs further investigation.

In this study, automated treatment planning with integrated BAO was applied to achieve several benefits. Plan comparison can be performed without planner bias, and due to short planning times and very limited planner interaction, a large number of patients can be included, increasing the quality and reliability of the study. In clinical routine, autoplanning could facilitate individualized selection between FB and DIBH with virtually zero workload.

The conclusions made in this study with regard to lung sparing depend on the assumption that the same mean dose will give the same side effects for FB and DIBH, or that the expansion of the lungs distributes the functional tissue evenly. Additionally, the applied NTCP models are developed using data from FB

treatment. More studies are therefore needed to determine the actual clinical benefit of DIBH in radiotherapy of LA-NSCLC.

This study has been evaluated using the RATING criteria for treatment planning studies and a score of 95% was achieved (31).

## 5 Conclusion

Compared to FB, DIBH allowed for smaller target volumes and similar target coverage. Furthermore, DIBH reduced the lung and heart dose, as well as the risks of radiation pneumonitis and 2-year mortality, for 92% and 74% of LA-NSCLC patients, respectively. The advantages of DIBH varied considerably between patients. Evaluation of rCTs showed similar robustness of the dose distributions with each technique. While DIBH reduced the risk of RP consistently regardless of patient characteristics, the ability to reduce the risk of 2-year mortality was evident among patients with upper and left lower lobe tumors but not right lower lobe tumors. Automated planning could facilitate individualized selection between FB and DIBH with no planner bias and virtually zero workload.

## Data availability statement

The data presented in this study are available on request from the corresponding author. The data are not publicly available due to privacy reasons as they are part of an ongoing study.

## Ethics statement

The study involved human participants and were reviewed and approved by the regional committee for medical and health research ethics in Western Norway (protocol code 2019/749). The patients provided their written informed consent to participate in this study.

## Author contributions

Conceptualization, KF, LR, BH, HP, SB and LH. methodology, KF, LR, BH, HP and LH. software, KF, LR, HP and SB. validation, KF. formal analysis, KF and LH. investigation, KF, IS and LH. resources, LH, BH, IS and TS. data curation, KF. writing—original draft preparation, KF. writing—review and editing, KF, LR, BH, HP, IS, TS, SB and LH. visualization, KF. supervision, LR, BH, HP and LH. project administration, LH. funding acquisition, KF and LH.

All authors contributed to the article and approved the submitted version.

## Funding

This research received funding from Helse Vest RHF (grant number F-12505) and the Trond Mohn Foundation (grant number BFS2017TMT07).

## Acknowledgments

The authors thank John-Vidar Hjørnevik, Ove Dalseid and other clinical personnel at Haukeland University Hospital for their contribution to data collection.

## Conflict of interest

LR, BH and SB: Erasmus MC Cancer Institute has research collaborations with Elekta AB (Stockholm, Sweden), Accuray, Inc. (Sunnyvale, USA) and Varian Medical Systems, Inc. (Palo Alto, USA). The funders had no role in the design of the study; in the collection, analyses, or interpretation of data; in the writing of the manuscript, or in the decision to publish the results.

The remaining authors declare that the research was conducted in the absence of any commercial or financial relationships that could be construed as a potential conflict of interest.

## Publisher's note

All claims expressed in this article are solely those of the authors and do not necessarily represent those of their affiliated organizations, or those of the publisher, the editors and the reviewers. Any product that may be evaluated in this article, or claim that may be made by its manufacturer, is not guaranteed or endorsed by the publisher.

## Supplementary material

The Supplementary Material for this article can be found online at: <https://www.frontiersin.org/articles/10.3389/fonc.2022.966134/full#supplementary-material>

## References

- Favre-Finn C, Vicente D, Kurata T, Planchard D, Paz-Ares L, Vansteenkiste JF, et al. Four-year survival with durvalumab after chemoradiotherapy in stage III NSCLC—an update from the PACIFIC trial. *J Thorac Oncol* (2021) 16(5):860–7. doi: 10.1016/j.jtho.2020.12.015
- Chun SG, Hu C, Choy H, Komaki RU, Timmerman RD, Schild SE, et al. Impact of intensity-modulated radiation therapy technique for locally advanced non–Small-Cell lung cancer: A secondary analysis of the NRG oncology RTOG 0617 randomized clinical trial. *JCO* (2017) 35(1):56–62. doi: 10.1200/JCO.2016.69.1378
- Dess RT, Sun Y, Matuszak MM, Sun G, Soni PD, Bazzi L, et al. Cardiac events after radiation therapy: Combined analysis of prospective multicenter trials for locally advanced non–Small-Cell lung cancer. *JCO* (2017) 35(13):1395–402. doi: 10.1200/JCO.2016.71.6142
- Marks LB, Bentzen SM, Deasy JO, Kong FM, Bradley JD, Vogelius IS, et al. Radiation dose–volume effects in the lung. *Int J Radiat Oncol Biol Phys* (2010) 76(3):570–6. doi: 10.1016/j.ijrobp.2009.06.091
- Monti S, Xu T, Mohan R, Liao Z, Palma G, Cella L. Radiation-induced esophagitis in non–Small-Cell lung cancer patients: Voxel-based analysis and NTCP modeling. *Cancers* (2022) 14(7):1833. doi: 10.3390/cancers14071833
- Jin JY, Hu C, Xiao Y, Zhang H, Paulus R, Ellsworth SG, et al. Higher radiation dose to the immune cells correlates with worse tumor control and overall survival in patients with stage III NSCLC: A secondary analysis of RTOG0617. *Cancers* (2021) 13(24):6193. doi: 10.3390/cancers13246193
- Antonia SJ, Villegas A, Daniel D, Vicente D, Murakami S, Hui R, et al. Overall survival with durvalumab after chemoradiotherapy in stage III NSCLC. *N Engl J Med* (2018) 379(24):2342–50. doi: 10.1056/NEJMoa1809697
- Bradley JD, Hu C, Komaki RR, Masters GA, Blumenschein GR, Schild SE, et al. Long-term results of NRG oncology RTOG 0617: Standard- versus high-dose chemoradiotherapy with or without cetuximab for unresectable stage III non–Small-Cell lung cancer. *JCO* (2020) 38(7):706–14. doi: 10.1200/JCO.19.01162
- Boda-Heggemann J, Knopf AC, Simeonova-Chergou A, Wertz H, Stieler F, Jahnke A, et al. Deep inspiration breath hold–based radiation therapy: A clinical review. *Int J Radiat Oncol Biol Phys* (2016) 94(3):478–92. doi: 10.1016/j.ijrobp.2015.11.049
- Latty D, Stuart KE, Wang W, Ahern V. Review of deep inspiration breath-hold techniques for the treatment of breast cancer. *J Med Radiat Sci* (2015) 62(1):74–81. doi: 10.1002/jmrs.96
- Anastasi G, Bertholet J, Poulsen P, Roggen T, Garibaldi C, Tilly N, et al. Patterns of practice for adaptive and real-time radiation therapy (POP-ART RT) part I: Intra-fraction breathing motion management. *Radiother Oncol* (2020) 153:79–87. doi: 10.1016/j.radonc.2020.06.018
- Persson GF, Scherman Rydhög J, Josipovic M, Maraldo MV, Nygård L, Costa J, et al. Deep inspiration breath-hold volumetric modulated arc radiotherapy decreases dose to mediastinal structures in locally advanced lung cancer. *Acta Oncologica* (2016) 55(8):1053–6. doi: 10.3109/0284186X.2016.1142115
- Marchand V, Zefkili S, Desrousseaux J, Simon L, Dauphinot C, Giraud P. Dosimetric comparison of free-breathing and deep inspiration breath-hold radiotherapy for lung cancer. *Strahlenther Onkol* (2012) 188(7):582–91. doi: 10.1007/s00066-012-0129-9
- Fjellanger K, Hysing LB, Heijmen BJM, Pettersen HES, Sandvik IM, Sulen TH, et al. Enhancing radiotherapy for locally advanced non-small cell lung cancer patients with iCE, a novel system for automated multi-criterial treatment planning including beam angle optimization. *Cancers* (2021) 13(22):5683. doi: 10.3390/cancers13225683
- Hoffmann L, Knap MM, Alber M, Møller DS. Optimal beam angle selection and knowledge-based planning significantly reduces radiotherapy dose to organs at risk for lung cancer patients. *Acta Oncologica* (2021) 60(3):293–9. doi: 10.1080/0284186X.2020.1856409
- Della Gala G, Dirx MLP, Hoekstra N, Franssen D, Lanconelli N, van de Pol M, et al. Fully automated VMAT treatment planning for advanced-stage NSCLC patients. *Strahlenther Onkol* (2017) 193(5):402–9. doi: 10.1007/s00066-017-1121-1
- Scherman Rydhög J, Riisgaard de Blanck S, Josipovic M, Irming Jølc R, Larsen KR, Clemetsen P, et al. Target position uncertainty during visually guided deep-inspiration breath-hold radiotherapy in locally advanced lung cancer. *Radiother Oncol* (2017) 123(1):78–84. doi: 10.1016/j.radonc.2017.02.003
- Josipovic M, Aznar MC, Thomsen JB, Scherman J, Damkjaer SM, Nygård L, et al. Deep inspiration breath hold in locally advanced lung cancer radiotherapy: validation of intrafractional geometric uncertainties in the INHALE trial. *BJR* (2019) 92(1104):20190569. doi: 10.1259/bjr.20190569
- Rossi L, Cambraia Lopes P, Marques Leitão J, Janus C, van de Pol M, Breedveld S, et al. On the importance of individualized, non-coplanar beam configurations in mediastinal lymphoma radiotherapy, optimized with automated planning. *Front Oncol* (2021) 11:619929. doi: 10.3389/fonc.2021.619929
- Nestle U, De Ruysscher D, Ricardi U, Geets X, Belderbos J, Pöttgen C, et al. ESTRO ACROP guidelines for target volume definition in the treatment of locally advanced non-small cell lung cancer. *Radiother Oncol* (2018) 127(1):1–5. doi: 10.1016/j.radonc.2018.02.023
- Kong FM, Ritter T, Quint DJ, Senan S, Gaspar LE, Komaki RU, et al. Consideration of dose limits for organs at risk of thoracic radiotherapy: Atlas for lung, proximal bronchial tree, esophagus, spinal cord, ribs, and brachial plexus. *Int J Radiat Oncol Biol Phys* (2011) 81(5):1442–57. doi: 10.1016/j.ijrobp.2010.07.1977
- Breedveld S, Storchi PRM, Voet PWJ, Heijmen BJM. iCycle: Integrated, multicriterial beam angle, and profile optimization for generation of coplanar and noncoplanar IMRT plans. *Med Phys* (2012) 39(2):951–63. doi: 10.1118/1.3676689
- Nederlandse vereniging voor radiotherapie en oncologie. *landelijk indicatie protocol protonen therapie - longcarcinoom* (Netherlands: National health care institute) (2019). Available at: [https://nvro.nl/images/documenten/rapporten/LIPP\\_longen\\_final\\_01122019.pdf](https://nvro.nl/images/documenten/rapporten/LIPP_longen_final_01122019.pdf)
- Appelt AL, Vogelius IR, Farr KP, Khalil AA, Bentzen SM. Towards individualized dose constraints: Adjusting the QUANTEC radiation pneumonitis model for clinical risk factors. *Acta Oncologica* (2014) 53(5):605–12. doi: 10.3109/0284186X.2013.820341
- Defraene G, Dankers FJWM, Price G, Schuit E, van Elmt W, Arredouani S, et al. Multifactorial risk factors for mortality after chemotherapy and radiotherapy for non-small cell lung cancer. *Radiother Oncol* (2020) 152:117–25. doi: 10.1016/j.radonc.2019.09.005
- Wijsman R, Dankers F, Troost EGC, Hoffmann AL, van der Heijden EHF, de Geus-Oei LF, et al. Multivariable normal-tissue complication modeling of acute esophageal toxicity in advanced stage non-small cell lung cancer patients treated with intensity-modulated (chemo-)radiotherapy. *Radiother Oncol* (2015) 117(1):49–54. doi: 10.1016/j.radonc.2015.08.010
- Møller DS, Lutz CM, Khalil AA, Alber M, Holt MI, Kandi M, et al. Survival benefits for non-small cell lung cancer patients treated with adaptive radiotherapy. *Radiother Oncol* (2022) 168:234–40. doi: 10.1016/j.radonc.2022.01.039
- Giraud P, Morvan E, Claude L, Mornex F, Le Pechoux C, Bachaud JM, et al. Respiratory gating techniques for optimization of lung cancer radiotherapy. *J Thorac Oncol* (2011) 6(12):2058–68. doi: 10.1097/JTO.0b013e3182307ec2
- Rosas S, Barbosa B, Couto JG. Intensity-modulated radiation therapy versus volumetric-modulated arc therapy in non-small cell lung cancer: Assessing the risk of radiation pneumonitis. *J Radiother Pract* (2018) 17(1):6–11. doi: 10.1017/S1460396917000358
- Thor M, Shepherd AF, Preeshagul I, Offin M, Gelblum DY, Wu AJ, et al. Pre-treatment immune status predicts disease control in NSCLCs treated with chemoradiation and durvalumab. *Radiother Oncol* (2022) 167:158–64. doi: 10.1016/j.radonc.2021.12.016
- Hansen CR, Crijs W, Hussein M, Rossi L, Gallego P, Verbakel W, et al. Radiotherapy treatment planning study guidelines (RATING): A framework for setting up and reporting on scientific treatment planning studies. *Radiother Oncol* (2020) 153:67–78. doi: 10.1016/j.radonc.2020.09.033

## *Supplementary Material*

### S1 Planning objectives

In the clinical treatment planning, there were maximum dose objectives for the spinal canal, brachial plexus and patient body. Additionally, the goal was to achieve sufficient target coverage and as low dose as possible to normal tissue, with the following order of priority: (1) PTV, (2) lungs, (3) heart, (4) esophagus, and (5) undefined normal tissue. These priorities are reflected in the wish-list applied for automated planning (1). A list of planning objectives is given in Table S1.

**Table S1.** Planning objectives for the PTV, OARs and normal tissue.  $D_p$  = prescribed dose.

<b>Volume</b>	<b>Dose objective</b>
PTV	$V_{95\%} > 98\%$
Lungs	$V_{5Gy} < 65\%$ $V_{20Gy} < 35\%$ $D_{mean} < 20$ Gy
Heart	$V_{30Gy} < 40\%$
Esophagus	$D_{mean} < 34$ Gy
Spinal canal	$D_{max} < 50$ Gy
Brachial plexus	$D_{max} < 66$ Gy
Patient body	$D_{max} < D_p \cdot 1.07$

### S2 NTCP calculations

#### S2.1 Radiation pneumonitis (RP)

The NTCP for RP grade  $\geq 2$  was calculated using a QUANTEC model refined by Appelt et al. (2,3):

$$NTCP = \frac{1}{1+e^{-S}} \text{ with } S = -4.12 + 0.138 \cdot MLD - 0.3711 \cdot (\text{Former smoker}) - 0.478 \cdot (\text{Current smoker}) + 0.8198 \cdot (\text{Co - morbidity}) + 0.6259 \cdot (\text{Tumor location}) + 0.5068 \cdot (\text{Old age}) + 0.47 \cdot (\text{Sequential chemo}),$$

where MLD is the mean lung dose in Gy and the other parameters are assigned value 1 or 0 according to Table S2.

**Table S2.** Variables in the NTCP model for radiation pneumonitis.

<b>Variable</b>	<b>Value = 1</b>	<b>Value = 0</b>
Former smoker	Yes	Never smoked/active smoker
Current smoker	Yes	Never smoked/stopped smoking
Co-morbidity <sup>1</sup>	Yes	No
Tumor location	Middle/lower lobe	Upper lobe
Old age	$\geq 63$ years	$< 63$ years
Sequential chemo	Yes	No

<sup>1</sup> Chronic obstructive pulmonary disease or other pre-existing lung disease.

### S2.2 2-year mortality (heart model)

The NTCP for 2-year mortality based on heart dose was calculated using a model developed by Defraene et al. and revised after external validation in several patient cohorts (3,4):

$$NTCP = \frac{1}{1+e^{-S}} \text{ with } S = -1.3409 + 0.0590 \cdot \sqrt{GTV} + 0.2635 \cdot \sqrt{MHD},$$

where GTV is the combined GTV volume of the primary tumor and nodes in  $\text{cm}^3$  and MHD is the mean heart dose in Gy. The GTV volume from the DIBH CT was used in the calculations for both FB and DIBH, as delineation on the DIBH CT was regarded more accurate than on the AIP (the average difference in GTV volume between DIBH and FB was 2.7%, with DIBH volumes being slightly larger).

### S2.3 Acute esophageal toxicity (AET)

The NTCP for AET grade  $\geq 2$  was calculated using a model developed by Wijnsman et al. and revised after external validation in several patient cohorts (3,5):

$$NTCP = \frac{1}{1+e^{-S}} \text{ with } S = -3.634 + 1.496 \cdot \ln(MED) - 0.0297 \cdot OTT,$$

where MED is the mean esophagus dose in Gy and OTT is the overall radiotherapy treatment time in days.

### S2.4 2-year mortality (EDIC model)

The effective radiation dose to immune cells (EDIC) in circulating blood, estimated as the equivalent uniform dose to the entire blood during the radiotherapy course, and the corresponding 2-year overall survival (OS) were calculated based on the models of Jin et al. (6), with some adjustments to accommodate the DIBH scenario:

$$EDIC = B_1\% \cdot MLD + B_2\% \cdot MHD + \left[ B_3\% + B_4\% \cdot k_1 \cdot \left( \frac{n}{45} \right)^{\frac{1}{2}} \right] \cdot MBD$$

where  $B_1\% = 0.12$ ,  $B_2\% = 0.08$ ,  $B_3\% = 0.45$  and  $B_4\% = 0.35$  represent the percentages of the total blood volume contained in the lungs, heart, great vessels, and small vessels in other organs, respectively, MLD, MHD and MBD are the mean doses to the lungs, heart and body, respectively,  $k_1 = 0.85$  is a dose effectiveness factor due to the small percentage of cardiac output for the small vessels, and  $n$  is the number of fractions.

The mean body dose was calculated as  $MBD = ID / (61.8 \cdot 10^3)$ , where  $61.8 \cdot 10^3 \text{ cm}^3$  is the estimated average body volume and ID is the integral dose to the body. The ID was not straightforwardly calculated in the DIBH vs. FB scenario. The increased lung volume leads to more air and more body volume around the treatment area and therefore more low dose in the patient body (Figure S1). This dose is, however, given to air; there is not more tissue or blood in the lungs. To correct for this, based on the fact that the amount of functional lung tissue is the same in FB and DIBH, a constant value approximating the lung volume was used for both techniques. To this purpose, the ID was split in two parts: the integral dose in the body volume included in the CT scan

minus the lungs,  $M(B - L)D \cdot V(B - L)$ , plus the integral dose in the lungs,  $MLD \cdot V(L)$ , where the average FB value of 3800 cm<sup>3</sup> was used as the lung volume in both FB and DIBH for all patients.

The integral dose in the whole patient was approximated as the integral dose in the body included in the CT scan. Because the CT scans always included the whole lungs and due to limitations in the 4DCT scan length depending on the patient's breathing frequency, the DIBH scan was usually longer than the FB scan for each patient. Therefore, more of the very low doses to the patient body were included in the dose statistics with DIBH. This difference was mainly seen for doses <0.5 Gy. Doses below this were therefore not included when calculating the ID. This had only a small impact on the calculated EDIC (-0.4% for FB and -0.6% for DIBH).

The 2-year OS based on the EDIC was calculated as

$$OS = 0.74 \cdot \left[ 1 - \frac{0.39}{1 + \left( \frac{4.5}{EDIC} \right)^6} \right] \cdot \left[ 1 - \frac{1}{1 + \left( \frac{9.9}{EDIC} \right)^{12}} \right]$$

with the resulting NTCP for 2-year mortality:  $NTCP = 1 - OS$ .

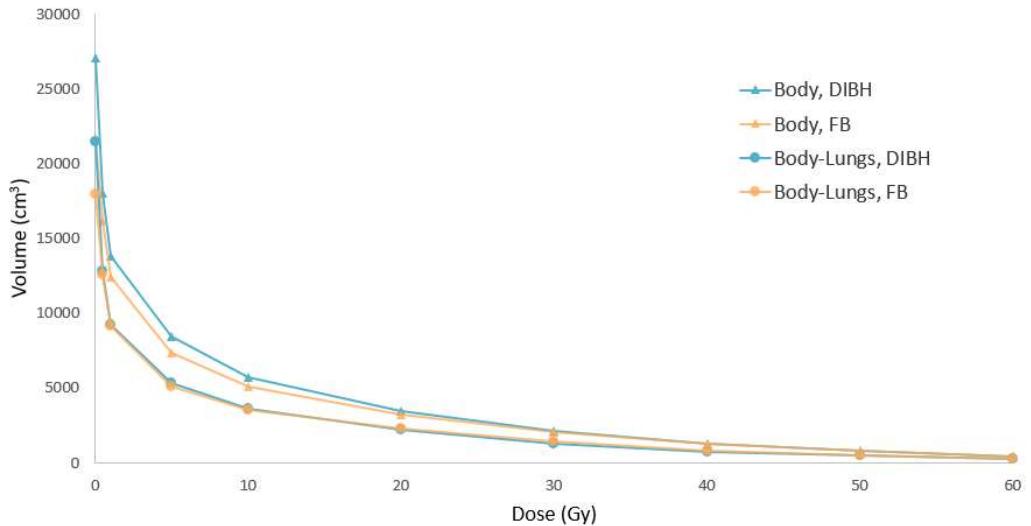


**Figure S1.** Average DVHs for the patient body and body without lungs in FB and DIBH plans. The figure illustrates that there is an increase in the absolute body volume receiving low doses with DIBH, but that this is solely due to the increased lung volume (more air in the lungs). The volume receiving very low doses (<0.5 Gy) is larger with DIBH due to increased scan length.

**S3 Robustness of the dose distribution****Table S3.** Dose-volume metrics for the planning FB plans, and the recalculated plans on the FB CTs in W1 and W3. Median value and 10<sup>th</sup>-90<sup>th</sup> percentile (pctl) is given for each time point, along with *p*-values for comparison with planning. Significant differences are marked with \*. The 35 patients who completed all three CT scans are included.

	FB planning		FB W1		<i>p</i> -value, planning vs. W1	FB W3		<i>p</i> -value, planning vs. W3
	Median	10 <sup>th</sup> -90 <sup>th</sup> pctl	Median	10 <sup>th</sup> -90 <sup>th</sup> pctl		Median	10 <sup>th</sup> -90 <sup>th</sup> pctl	
CTV $V_{95\%}$ (%)	100	–	100	98.0–100	<0.001 *	100	98.9–100	<0.001 *
Patient $D_{\max}$ (%)	104.9	103.9–106.0	105.6	103.8–109.1	<0.001 *	106.8	104.3–109.7	<0.001 *
Lungs $D_{\text{mean}}$ (Gy)	15.0	9.2–19.2	15.5	10.0–19.6	0.4	15.1	9.8–19.6	0.03 *
Lungs $V_{5\text{Gy}}$ (%)	58.7	41.0–79.8	59.8	41.6–78.6	0.7	59.6	41.6–79.2	0.09
Lungs $V_{20\text{Gy}}$ (%)	24.7	15.0–34.8	24.4	16.1–34.8	0.5	25.0	15.7–35.7	0.09
Heart $D_{\text{mean}}$ (Gy)	8.5	2.6–21.2	8.9	2.3–21.9	0.9	10.0	2.0–20.5	1.0
Heart $V_{5\text{Gy}}$ (%)	42.8	9.5–88.0	39.0	8.8–91.4	0.9	42.7	7.7–87.7	1.0
Heart $V_{30\text{Gy}}$ (%)	8.6	1.3–23.5	8.3	1.0–25.0	0.9	8.0	0.7–22.1	1.0
Esophagus $D_{\text{mean}}$ (Gy)	19.8	10.7–31.0	20.3	10.6–30.3	0.5	21.2	11.7–33.0	0.005 *
Esophagus $V_{20\text{Gy}}$ (%)	37.6	22.9–55.9	38.9	17.2–55.3	0.6	41.7	24.9–58.6	0.002 *
Esophagus $V_{60\text{Gy}}$ (%)	5.2	0.0–29.1	4.7	0.1–29.6	0.03 *	7.2	0.0–34.6	0.01 *
Spinal canal $D_{\max}$ (Gy)	46.5	33.8–51.1	46.2	34.4–51.8	0.9	46.8	34.3–52.6	0.07
EDIC (Gy)	4.6	2.9–6.8	4.7	2.8–6.7	0.6	4.7	3.0–7.0	0.1
NTCP RP (%) <sup>1</sup>	20.3	8.2–38.1	21.9	6.8–39.4	0.4	21.2	7.3–37.5	0.03 *
NTCP AET (%) <sup>2</sup>	39.3	21.3–55.4	39.3	20.4–54.6	0.5	43.3	21.1–57.1	0.01 *
NTCP Mortality_Heart (%) <sup>3</sup>	51.4	37.1–66.2	50.1	37.0–66.0	0.9	50.8	37.0–68.0	0.8
NTCP Mortality_EDIC (%) <sup>4</sup>	41.7	27.8–53.3	42.0	27.6–52.9	0.8	42.1	28.1–53.7	0.1

<sup>1</sup> Radiation pneumonitis grade  $\geq 2$ , <sup>2</sup> acute esophageal toxicity grade  $\geq 2$ , <sup>3</sup> 2-year mortality (heart model), <sup>4</sup> 2-year mortality (EDIC model).



**Table S4.** Dose-volume metrics for the planning DIBH plans, and the recalculated plans on the DIBH CTs in W1 and W3. Median value and 10<sup>th</sup>-90<sup>th</sup> percentile (pctl) is given for each time point, along with *p*-values for comparison with planning. Significant differences are marked with \*. The 35 patients who completed all three CT scans are included.

	DIBH planning		DIBH W1		<i>p</i> -value, planning vs. W1	DIBH W3		<i>p</i> -value, planning vs. W3
	Median	10 <sup>th</sup> -90 <sup>th</sup> pctl	Median	10 <sup>th</sup> -90 <sup>th</sup> pctl		Median	10 <sup>th</sup> -90 <sup>th</sup> pctl	
CTV V <sub>95%</sub> (%)	100	99.9–100	100	98.0–100	0.007 *	100	99.1–100	0.002 *
Patient D <sub>max</sub> (%)	104.7	104.0–106.0	106.6	103.8–109.2	<0.001 *	107.0	105.5–109.9	<0.001 *
Lungs D <sub>mean</sub> (Gy)	13.5	7.5–17.2	13.7	7.8–17.2	0.5	13.5	7.8–17.3	0.02 *
Lungs V <sub>5Gy</sub> (%)	55.5	36.0–74.2	55.1	36.0–74.1	1.0	55.6	35.9–74.4	0.07
Lungs V <sub>20Gy</sub> (%)	22.5	12.2–31.4	22.6	12.5–31.1	0.8	22.9	12.4–31.8	0.07
Heart D <sub>mean</sub> (Gy)	7.9	1.5–19.6	8.2	1.6–20.3	0.6	9.2	1.6–19.7	0.6
Heart V <sub>5Gy</sub> (%)	31.3	4.9–94.8	32.4	5.0–96.7	0.2	34.9	5.3–94.6	0.3
Heart V <sub>30Gy</sub> (%)	7.6	0.0–16.7	6.9	0.2–17.6	0.7	7.0	0.2–17.4	0.9
Esophagus D <sub>mean</sub> (Gy)	19.4	13.0–30.6	19.7	12.3–28.0	0.06	21.9	13.0–32.5	0.003 *
Esophagus V <sub>20Gy</sub> (%)	37.5	25.9–56.4	37.0	24.2–62.7	0.1	40.3	27.2–61.2	0.01 *
Esophagus V <sub>60 Gy</sub> (%)	5.7	0.0–24.4	6.4	0.0–22.1	0.8	9.2	0.0–27.3	0.001 *
Spinal canal D <sub>max</sub> (Gy)	42.9	29.1–50.9	43.3	29.9–52.7	0.4	44.4	30.6–53.0	0.02 *
EDIC (Gy)	4.4	2.7–6.2	4.1	2.7–6.4	0.4	4.4	2.6–6.3	0.1
NTCP RP (%) <sup>1</sup>	18.3	6.9–32.7	18.2	6.8–34.1	0.4	18.5	6.8–34.4	0.009 *
NTCP AET (%) <sup>2</sup>	39.2	23.9–56.1	38.6	22.1–53.9	0.04 *	42.0	26.5–58.4	0.005 *
NTCP Mortality Heart (%) <sup>3</sup>	50.9	36.5–64.5	49.1	37.2–64.4	0.7	50.7	37.2–65.1	0.6
NTCP Mortality EDIC (%) <sup>4</sup>	39.5	27.2–51.2	36.9	27.2–51.9	0.7	39.6	27.1–51.8	0.2

<sup>1</sup> Radiation pneumonitis grade  $\geq 2$ , <sup>2</sup> acute esophageal toxicity grade  $\geq 2$ , <sup>3</sup> 2-year mortality (heart model), <sup>4</sup> 2-year mortality (EDIC model).

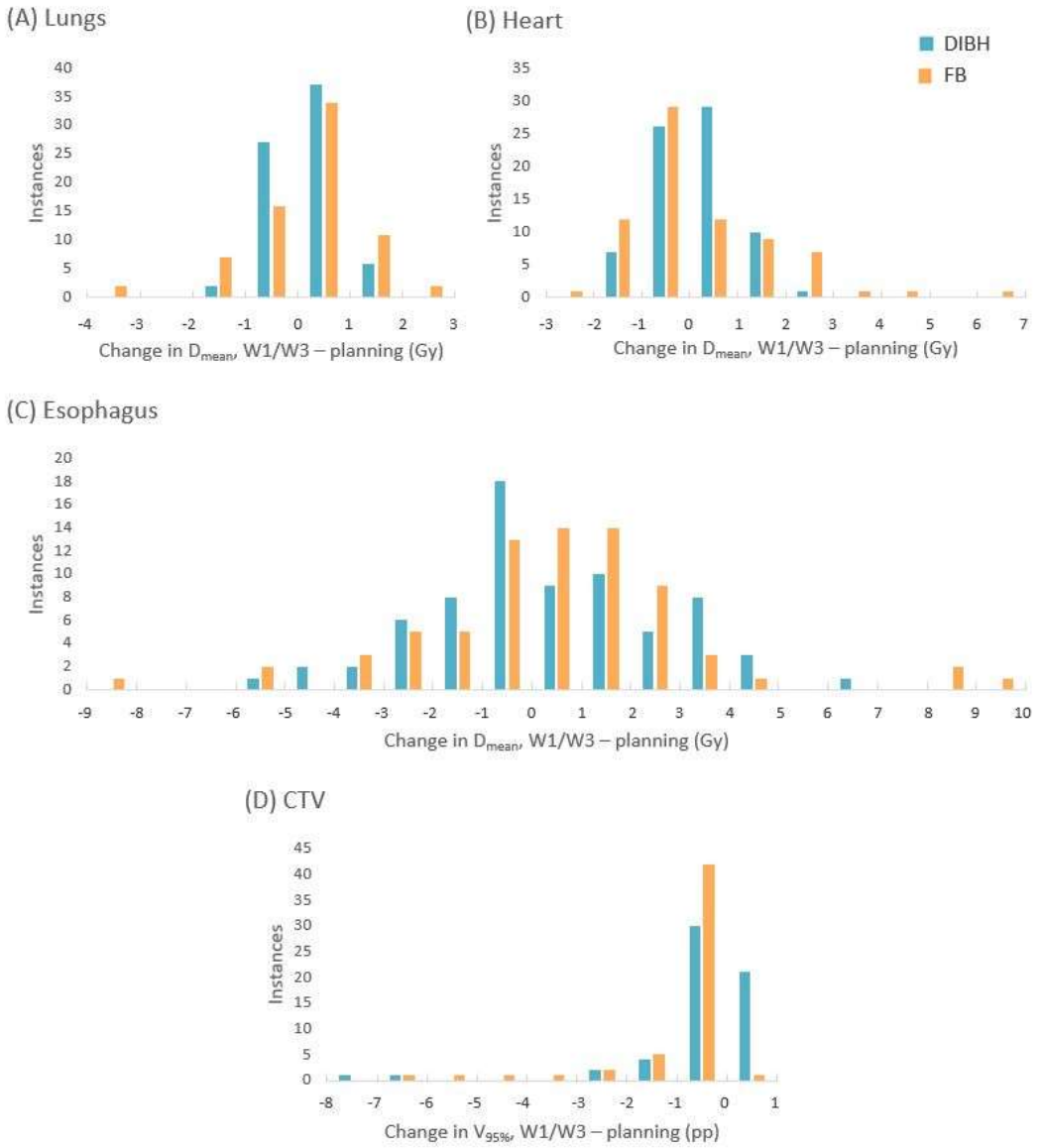


**Figure S2.** Intra-patient changes in the mean doses to (A) lungs, (B) heart and (C) esophagus, and (D) CTV  $V_{95\%}$ , from planning to week 1 and planning to week 3 evaluated together. pp = percentage points.

## S4 Patient characteristics and benefit of DIBH

**Table S5.** Average  $\Delta$ NTCP between DIBH and FB for radiation pneumonitis grade  $\geq 2$  (RP), acute esophageal toxicity grade  $\geq 2$  (AET) and 2-year mortality with the heart dose and EDIC models for patients with primary tumor in the upper or lower lobe and left or right lung. Negative  $\Delta$ NTCP values are in favor of DIBH and positive values are in favor of FB.  $p$ -values are given for comparison between FB and DIBH within each group, and significant differences are marked with \*.

	Upper lobe (n=20)			Lower lobe (n=17)			Left lung (n=16)			Right lung (n=21)		
	Avg	STD	$p$	Avg	STD	$p$	Avg	STD	$p$	Avg	STD	$p$
$\Delta$ NTCP, RP (pp)	-3.7	3.4	<0.001 *	-4.1	3.2	0.001 *	-3.2	2.9	0.001 *	-4.4	3.5	<0.001 *
$\Delta$ NTCP, AET (pp)	0.5	5.0	0.7	-0.3	6.0	0.5	2.2	6.4	0.2	-1.5	4.1	0.09
$\Delta$ NTCP, Mortality_Heart (pp)	-1.3	1.5	0.001 *	-0.4	2.0	0.3	-1.5	1.8	0.007 *	-0.5	1.7	0.1
$\Delta$ NTCP, Mortality_EDIC (pp)	-2.6	2.2	<0.001 *	-2.2	1.9	0.001 *	-2.1	1.9	0.001 *	-2.6	2.2	<0.001 *

**Table S6.** Results from the linear regressions between the  $\Delta$ NTCPs for radiation pneumonitis grade  $\geq 2$  (RP), acute esophageal toxicity grade  $\geq 2$  (AET) and 2-year mortality with the heart dose and EDIC models vs. the cranio-caudal motion of the primary tumor GTV in FB, and vs. the expansion of the lungs with DIBH. The reported parameters are the intercept (a), slope (b), coefficient of determination ( $r^2$ ) and  $p$ -value of the linear regression. There were no statistically significant correlations.

	Tumor motion				Lung expansion			
	a	b	$r^2$	$p$	a	b	$r^2$	$p$
$\Delta$ NTCP, RP (pp)	-3.0	-0.2	0.07	0.1	-1.5	-0.04	0.06	0.2
$\Delta$ NTCP, AET (pp)	0.9	-0.2	0.02	0.4	-1.9	0.04	0.02	0.5
$\Delta$ NTCP, Mortality_Heart (pp)	-1.2	0.06	0.03	0.3	-1.0	0.003	0.001	0.9
$\Delta$ NTCP, Mortality_EDIC (pp)	-2.1	-0.1	0.02	0.4	-1.2	-0.02	0.04	0.3

## References

1. Fjellanger K, Hysing LB, Heijmen BJM, Pettersen HES, Sandvik IM, Sulen TH, et al. Enhancing Radiotherapy for Locally Advanced Non-Small Cell Lung Cancer Patients with iCE, a Novel System for Automated Multi-Criterial Treatment Planning Including Beam Angle Optimization. *Cancers*. 2021 Nov 13;13(22):5683.
2. Appelt AL, Vogelius IR, Farr KP, Khalil AA, Bentzen SM. Towards individualized dose constraints: Adjusting the QUANTEC radiation pneumonitis model for clinical risk factors. *Acta Oncologica*. 2014 May;53(5):605–12.
3. Nederlandse Vereniging voor Radiotherapie en Oncologie. Landelijk Indicatie Protocol Protonen Therapie - Longcarcinoom [Internet]. 2019 Jun. Available from: [nvro.nl/images/documenten/rapporten/LIPP\\_longen\\_final\\_01122019.pdf](http://nvro.nl/images/documenten/rapporten/LIPP_longen_final_01122019.pdf)
4. Defraene G, Dankers FJWM, Price G, Schuit E, van Elmpt W, Arredouani S, et al. Multifactorial risk factors for mortality after chemotherapy and radiotherapy for non-small cell lung cancer. *Radiotherapy and Oncology*. 2020 Nov;152:117–25.

5. Wijsman R, Dankers F, Troost EGC, Hoffmann AL, van der Heijden EHF, de Geus-Oei LF, et al. Multivariable normal-tissue complication modeling of acute esophageal toxicity in advanced stage non-small cell lung cancer patients treated with intensity-modulated (chemo-)radiotherapy. *Radiotherapy and Oncology*. 2015 Oct;117(1):49–54.
6. Jin JY, Hu C, Xiao Y, Zhang H, Paulus R, Ellsworth SG, et al. Higher Radiation Dose to the Immune Cells Correlates with Worse Tumor Control and Overall Survival in Patients with Stage III NSCLC: A Secondary Analysis of RTOG0617. *Cancers*. 2021 Dec 8;13(24):6193.




IV



## Article

# Substantial Sparing of Organs at Risk with Modern Proton Therapy in Lung Cancer, but Altered Breathing Patterns Can Jeopardize Target Coverage

Camilla Grindeland Boer<sup>1</sup>, Kristine Fjellanger<sup>1,2,\*</sup>, Inger Marie Sandvik<sup>1</sup>, Maren Ugland<sup>1</sup>, Grete May Engeseth<sup>1,3</sup> and Liv Bolstad Hysing<sup>1,2</sup>

- <sup>1</sup> Department of Oncology and Medical Physics, Haukeland University Hospital, 5021 Bergen, Norway; camilla.grindeland.boer@helse-bergen.no (C.G.B.); inger.marie.sandvik@helse-bergen.no (I.M.S.); maren.ugland@helse-bergen.no (M.U.); grete.may.engeseth@helse-bergen.no (G.M.E.); liv.bolstad.hysing@helse-bergen.no (L.B.H.)
- <sup>2</sup> Institute of Physics and Technology, University of Bergen, 5007 Bergen, Norway
- <sup>3</sup> Department of Clinical Science, University of Bergen, 5021 Bergen, Norway
- \* Correspondence: kristine.fjellanger@helse-bergen.no

**Simple Summary:** Treatment of locally advanced non-small cell lung cancer (LA-NSCLC) is a fine balance between toxicity and cure. Modern proton therapy might offer a more gentle radiation treatment compared to state-of-the-art photon radiotherapy, but is also more susceptible to the influence of breathing motion and anatomical changes. In this study, the influence of such uncertainties on treatment delivery was thoroughly investigated. Modern proton therapy did indeed show potential to reduce the risk of toxicity for the heart and lungs. This potential was maintained under the influence of anatomical and delivery uncertainties. However, changes in breathing motion jeopardized the target dose distribution in a subset of patients. We therefore recommend imaging at onset or early in treatment to recognize these patients and adapt the treatment.

**Abstract:** Enhancing treatment of locally advanced non-small cell lung cancer (LA-NSCLC) by using pencil beam scanning proton therapy (PBS-PT) is attractive, but little knowledge exists on the effects of uncertainties occurring between the planning (Plan) and the start of treatment (Start). In this prospective simulation study, we investigated the clinical potential for PBS-PT under the influence of such uncertainties. Imaging with 4DCT at Plan and Start was carried out for 15 patients that received state-of-the-art intensity-modulated radiotherapy (IMRT). Three PBS-PT plans were created per patient: 3D robust single-field uniform dose (SFUD), 3D robust intensity-modulated proton therapy (IMPT), and 4D robust IMPT (4DIMPT). These were exposed to setup and range uncertainties and breathing motion at Plan, and changes in breathing motion and anatomy at Start. Target coverage and dose-volume parameters relevant for toxicity were compared. The organ at risk sparing at Plan was greatest with IMPT, followed by 4DIMPT, SFUD and IMRT, and persisted at Start. All plans met the preset criteria for target robustness at Plan. At Start, three patients had a lack of CTV coverage with PBS-PT. In conclusion, the clinical potential for heart and lung toxicity reduction with PBS-PT was substantial and persistent. Altered breathing patterns between Plan and Start jeopardized target coverage for all PBS-PT techniques.

**Keywords:** locally advanced non-small cell lung cancer; NSCLC; pencil beam scanning proton therapy; robustness; toxicity; breathing motion



**Citation:** Boer, C.G.; Fjellanger, K.; Sandvik, I.M.; Ugland, M.; Engeseth, G.M.; Hysing, L.B. Substantial Sparing of Organs at Risk with Modern Proton Therapy in Lung Cancer, but Altered Breathing Patterns Can Jeopardize Target Coverage. *Cancers* **2022**, *14*, 1365. <https://doi.org/10.3390/cancers14061365>

Academic Editors: Laura Cella, Giuseppe Palma and Andrew Hope

Received: 31 January 2022

Accepted: 4 March 2022

Published: 8 March 2022

**Publisher's Note:** MDPI stays neutral with regard to jurisdictional claims in published maps and institutional affiliations.



**Copyright:** © 2022 by the authors. Licensee MDPI, Basel, Switzerland. This article is an open access article distributed under the terms and conditions of the Creative Commons Attribution (CC BY) license (<https://creativecommons.org/licenses/by/4.0/>).

## 1. Introduction

State-of-the-art treatment for inoperable locally advanced non-small cell lung cancer (LA-NSCLC) is concurrent chemotherapy and intensity-modulated photon radiotherapy (IMRT) to a dose of 60 Gy. Still, 5-year survival rates for stage III disease are only around



30%, and side effects from treatment are common and potentially fatal, limiting the possibility for dose escalation with IMRT [1,2].

Proton therapy (PT) has advantageous depth dose characteristics with the potential to reduce side effects and facilitate dose escalation in LA-NSCLC patients [3–7]. Although phase II clinical trials have been promising [8–10], PT showed no advantage over IMRT in a randomized trial by Liao and colleagues [11,12]. These early clinical trials have mainly applied passive scattering PT, but state-of-the-art PT uses pencil beam scanning (PBS), allowing more conformal dose distributions with lower doses to critical organs [3,13].

PBS-PT is, however, not straightforwardly delivered in the thoracic region due to the inherent sensitivity to uncertainties [14,15]. Much concern has been dedicated to how the breathing motion of the primary tumor can interplay with PBS-PT spot delivery [16,17]. PBS-PT has therefore mainly been offered to patients with limited breathing motion [14]. However, recent studies with PBS-PT confirm that interplay uncertainties are canceled out by fractionation—as for IMRT—and more attention should be focused on changes in breathing patterns and anatomy [15,18–21].

Various optimization techniques for PBS-PT exist, and it is believed that these are differently influenced by uncertainties [14,16]. With single-field uniform dose (SFUD), each field delivers a uniform dose to the entire target volume, while intensity-modulated proton therapy (IMPT) contains non-uniform dose distributions for the individual fields. 3D and 4D robust optimization can be applied to account for uncertainties due to patient setup and proton range as well as breathing motion, respectively [22–24].

In theory, IMPT has the potential to produce the most conformal treatment plans, while SFUD and 4D robust optimization are strategies to increase robustness [17]. There is, however, limited knowledge on how different robustly optimized PBS-PT techniques perform in practice for LA-NSCLC patients, as the planning CT is commonly used for both optimization and evaluation [16]. We see a need to investigate this in order to guide the use of PBS-PT, balancing organ at risk (OAR) sparing and robustness for both targets and OARs. Furthermore, little knowledge exists on the dosimetric advantages of PBS-PT compared to state-of-the-art IMRT at the start of treatment. Comparisons for, e.g., patient selection between protons and photons are also usually carried out on the planning scan, even though it is known that robustness towards changes matters [25]. A few studies have focused on the impact of anatomical changes occurring during the six weeks of treatment that should be handled by means of adaptive radiotherapy (ART) [26–28].

The purpose of this prospective simulation study was to compare 3D robust SFUD, 3D robust IMPT and 4D robust IMPT in terms of target coverage and OAR sparing under the influence of setup and range uncertainties, breathing motion and interplay at planning, as well as changes in the breathing motion pattern and anatomy from the planning to the start of treatment. Further, using the clinical IMRT plan as a reference, our objective was to evaluate if the potential for OAR sparing expected at planning was persistent at the start of treatment.

## 2. Materials and Methods

### 2.1. Patient Material and Clinical IMRT Planning

Fifteen consecutive patients with stage III NSCLC receiving radiochemotherapy with curative intent at Haukeland University Hospital in Bergen, Norway, in 2019–2020 were prospectively included in an *in silico* simulation study. All patients gave informed consent, and the study was approved by the regional committee for medical and health research ethics (protocol code 2019/749).

Imaging was performed on a Big Bore CT scanner (Philips Healthcare, Best, The Netherlands), using a Posirest-2 support device (Civco Radiotherapy, Coralville, IA, USA) for fixation in the supine position with arms resting above the head, and the Philips bellows device for registration of the breathing curve.

4DCTs with 10 respiratory phases and deep inspiration breath hold (DIBH) CTs were acquired at planning (Plan) and at the start of treatment (fraction 2 or 3; Start). The average

intensity projection (AIP) of the 4DCT was used for delineation and treatment planning. Gross tumor volumes (GTVs) for the primary tumor and lymph nodes were defined on the AIP, based on a diagnostic CT with intravenous contrast, an FDG-PET-CT, and biopsy of mediastinal lymph nodes. To define the internal GTVs (IGTVs), each 4DCT phase was blended with the AIP, and the structure was expanded to include the GTV positions on all phases. Exceptions from this were three patients treated in DIBH due to lung dose exceeding the constraints or large tumor motion blurring the 4DCT. In these cases, IGTV delineation included the GTV on three consecutive planning DIBH scans. A clinical target volume (CTV) was created using a 5 mm margin from the IGTV, without extending into uninvolved organs such as bone, heart, esophagus and major vessels. The GTVs and CTV were deformably mapped to all phases of the 4DCT and later used in 4DIMPT optimization. For clinical IMRT planning, a planning target volume (PTV) with 5 mm margin from the CTV was used. Target delineation was performed by the same oncologist (I.M.S.) on all Plan and Start scans. The lungs, heart, esophagus, spinal canal and, if relevant, the brachial plexus were delineated according to RTOG guidelines [29].

Clinical treatment planning was performed in Eclipse v. 15.6 (Varian Medical Systems, Palo Alto, CA, USA). All patients received IMRT with a prescribed dose of 60 or 66 Gy in 2 Gy fractions, depending on lung function, lung dose and proximity of the brachial plexus to the PTV. The beam configuration was adjusted to fit the anatomy of each patient, mainly using six beams and avoiding entry through the contralateral lung. For the PTV,  $D_{98\%} > 95\%$  of prescribed dose was required, and the maximum dose in the plan should be  $< 107\%$ . Dose constraints for OARs are listed in Table A1. The Acuros External Beam algorithm was used for dose calculation, and the plans were normalized to the median dose in the PTV.

The motion amplitude of the primary tumor at Plan and Start was evaluated in Eclipse, using deformable mapping of the primary tumor GTV from the AIP to each breathing phase of the 4DCT and measuring the motion of the GTV center of mass in all directions.

The AIP of the 4DCT acquired at Start was rigidly matched to the AIP at Plan using six degrees of freedom and a volume of interest covering the PTV, as well as skeletal structures and the body contour in proximity to the PTV.

## 2.2. Proton Therapy Planning

Proton planning was performed in RayStation v. 8B (RaySearch Laboratories, Stockholm, Sweden). To ensure high plan quality, all plans were made by an experienced planning expert within photon therapy and comparative proton planning (C.G.B.) and reviewed by an experienced medical physicist (M.U.). The 4DCT phases were deformably registered to their respective AIP, and the deformed target volumes (GTVs and CTVs) and OARs were mapped onto each phase. For the AIP scan, a density override representative for tumor tissue ( $1.06 \text{ g/cm}^3$ ,  $\sim 40 \text{ HU}$ ) was used for all plans for the IGTV. For the 4DCT phases, the original density values were applied (i.e., no density override).

For each patient, three PBS-PT treatment plans were created on the Plan AIP using different optimization techniques: SFUD, 4DIMPT and IMPT. 3D robust optimization according to the minimax approach with setup uncertainty of 5 mm in each direction and 3.5% range uncertainty (21 scenarios) was used for SFUD and IMPT [22]. 4D robust optimization, applying the same settings for setup and range uncertainty on all 4DCT breathing phases (231 scenarios), was used for 4DIMPT [23]. In 3D and 4D robust optimization, the reference plan is evaluated in each uncertainty scenario, and in each iteration, the scenario with the currently worst objective value is improved. 3D and 4D robust optimization were applied for the CTV, and for the spinal canal if close to the CTV. Rescanning methods were not used.

Each plan had two (10 patients) or three (5 patients) coplanar fields with gantry angles carefully selected with regard to the patient anatomy and the distance between the beam entry and the CTV (Figure A1). For each patient, beam angles were individually selected, and the same field setup was used in the three PT plans. Range shifters of 4 cm or 7.5 cm were used for all fields, and the air gaps were 5–12 cm from the body contour depending

on beam angles and risk of collision. Sigma of spot sizes in air at isocenter (without range shifter) were 3.7 to 7.2 mm depending on energy.

The same prescription as in the clinical plan was used, applying a relative biological effectiveness of 1.1 for protons. A generic IBA beam model was used for planning, and a Monte Carlo algorithm was used for dose calculation (using 0.5% statistical uncertainty).

### 2.3. Robustness Evaluation

An overview of the acquired image data and the robustness evaluation is shown in Figure 1. Robustness towards *setup and range* variations (Plan S/R) was evaluated on the Plan AIP using combined isocenter shifts of 2.9 mm in 3 directions simultaneously (corresponding to 5 mm isotropic shifts) and 3.5% range uncertainty (16 scenarios).

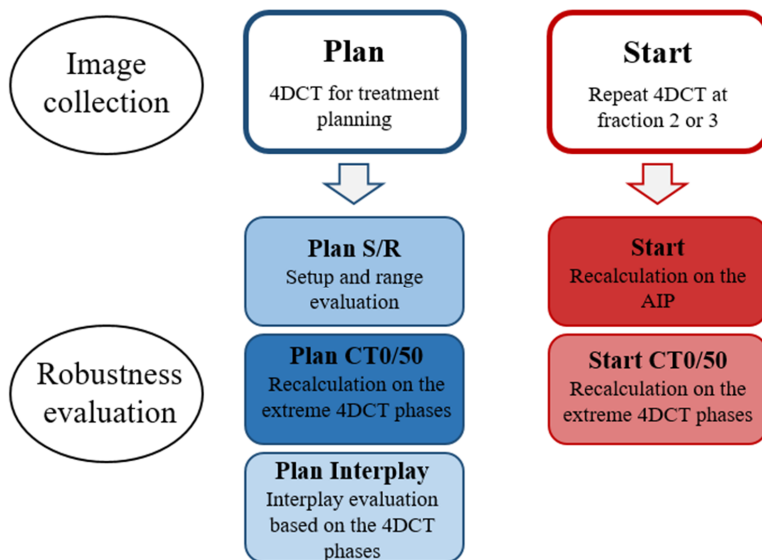


Figure 1. Overview of the acquired image data and the robustness evaluation.

Robustness towards *breathing motion* at Plan (Plan CT0/50) was evaluated by recalculating all PT plans on the extreme breathing phases of the 4DCT: CT0 (maximum inspiration) and CT50 (maximum expiration). In addition, *interplay* evaluation was performed at Plan (Plan Interplay) using a script provided by RaySearch. The 10 breathing phases of the 4DCT were in turn used as the starting phase for treatment delivery, and the spots were distributed on the CTs of the different phases based on delivery time and breathing cycle length. Constant breathing periods of five seconds were used for all patients. The dose on each phase was calculated and mapped to the reference image (AIP), where the total dose was calculated. This resulted in 10 different interplay dose distributions depending on which phase delivery started in. For all robustness simulations, reported values represent the worst-case scenario for each parameter.

All PT plans were also recalculated on the AIP (Start), CT0 and CT50 (Start CT0/50) of the Start 4DCT to evaluate robustness towards *changes in breathing motion and anatomy* that can occur between planning and onset of treatment.

### 2.4. Dosimetric Evaluation

Dose distributions at Plan were compared using  $D_{98\%}$  and  $D_{2\%}$  for the CTV, as well as the homogeneity index  $HI = (D_{2\%} - D_{98\%})/D_{50\%}$ , and the conformity index  $CI = (TV_{RI}/TV) \times (TV_{RI}/V_{RI})$ , where TV is the target volume,  $TV_{RI}$  is the target volume

covered by the reference (95%) isodose and  $V_{RI}$  is the volume of the reference isodose [30]. For healthy tissue and OARs, the following parameters relevant for toxicity were evaluated:  $D_{2cc}$  for the patient body,  $D_{mean}$ ,  $V_{5Gy}$  and  $V_{20Gy}$  for the lungs,  $D_{mean}$  and  $V_{30Gy}$  for the heart,  $D_{mean}$  for the esophagus and  $D_{max}$  for the spinal canal.

For OARs, the planning criteria (Table A1) were also required in robustness evaluation. In addition, the  $D_{2cc}$  to the patient body should be <107% of the prescribed dose. CTV  $D_{98} > 95\%$  and CTV  $D_{2\%} < 107\%$  were required in setup and range and extreme phase evaluation as well as in the Start recalculations. The interplay effect is expected to cause under- and overdosage in the tumor and OARs that average out during fractionated treatment. Ensuring at least 1.8 Gy per fraction, i.e., CTV  $D_{98} > 90\%$ , and CTV  $D_{2\%}$  and body  $D_{2cc} < 110\%$  were considered acceptable in interplay evaluation.

A structured overview of the various evaluations and criteria is shown in Table A2. Initially, we present the target coverage and OAR sparing for the various techniques at Plan. Thereafter, we investigate the robustness of the target dose and OAR doses, respectively. For evaluation of the actual clinical potential of proton therapy compared to photon therapy, we lastly compare target coverage and OAR sparing at Start.

### 2.5. Statistical Analysis

Statistical analyses were performed in IBM SPSS Statistics (IBM Corp., Armonk, NY, USA). Friedman's test (non-parametric two-way analysis of variance by ranks) was used for comparison of the different techniques. Bonferroni correction was applied to adjust the  $p$ -value for multiple testing in post hoc analysis. A significance level of 0.05 was used.

## 3. Results

### 3.1. Patient Characteristics and Breathing Motion

The median CTV volume was 137 cc (range 66–435 cc). Nine patients had disease stage IIIA, five IIIB and one IIIC. Primary tumor positions were left upper (3), left lower (4), right upper (4) and right lower (3) lobe. One patient only had mediastinal lymph nodes and one only had a primary tumor; the rest had both primary tumor and lymph nodes included in the target volume. The prescribed dose was 60 Gy for 6 patients and 66 Gy for 9 patients.

The breathing motion of the primary tumor was largest in the cranio–caudal direction, with a median amplitude of 4 mm and a maximum of 15 mm in the planning 4DCTs. Large variability in breathing motion was observed between patients. Six patients had a motion amplitude >5 mm, all in the cranio–caudal direction. Median breathing motion amplitudes were similar at Plan and Start (Table A3), and for most patients, the change in amplitude from Plan to Start was  $\leq 2$  mm in all directions. Three patients had a larger change in amplitude in the cranio–caudal direction (−6 mm, +4 mm and −3 mm), and these were also the three patients with the largest breathing motion amplitudes at Plan.

### 3.2. Target Coverage and OAR Sparing at Plan

All treatment plans achieved the required CTV  $D_{98\%} > 95\%$  and  $D_{2\%} < 107\%$  of the prescribed dose at Plan (Table 1). The median CTV  $D_{98\%}$  was, however, significantly higher for IMRT than for all PT techniques. The median PTV  $D_{98\%}$  in the IMRT plans was 95.7% (range 94.6–97.0%). Healthy tissue and OAR doses were lower for all proton techniques than for IMRT (Table 1, Figure 2). The only exception was the  $D_{2cc}$  of the body, where IMRT gave the lowest dose. Among the PT techniques, significant differences were found between SFUD and IMPT in  $D_{mean}$  for the lungs and esophagus and  $V_{20Gy}$  for the lungs, all in favor of IMPT. The mean rank was the worst with IMRT and the best with IMPT for all of the evaluated OAR parameters.

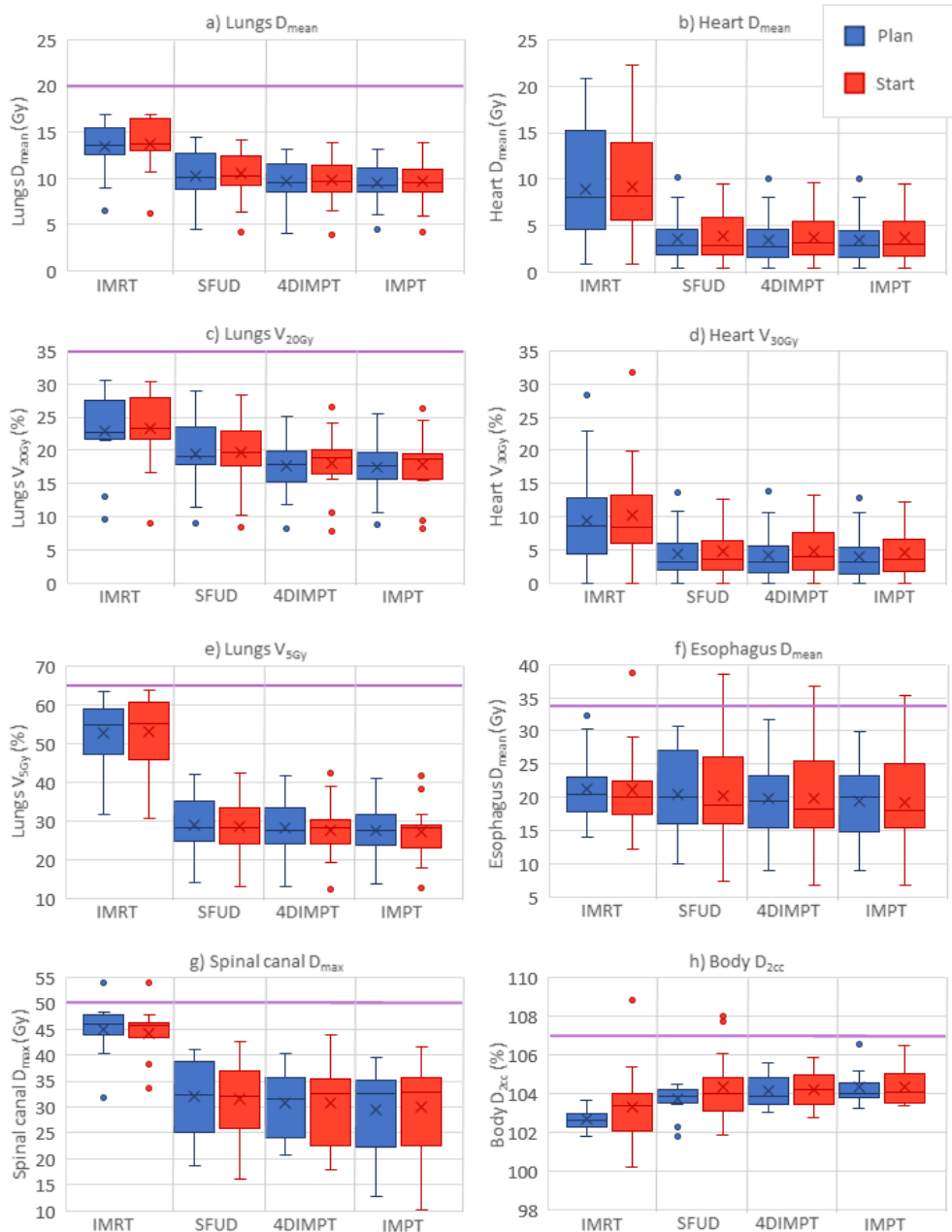


**Figure 2.** OAR and normal tissue doses at Plan (blue) and Start (red) for the different optimization techniques; panel (a–h) shows each of the evaluated parameters. Purple horizontal lines indicate planning constraints in cases where the value is included in the plot. Boxplots show the median (line), mean (cross) and spread, with outliers as dots outside the box. IMRT = intensity-modulated radiotherapy, SFUD = single-field uniform dose, 4DIMPT = 4D robustly optimized intensity-modulated proton therapy, IMPT = 3D robustly optimized intensity-modulated proton therapy.

**Table 1.** Dose-volume parameters for the target, patient body, and OARs for the different optimization techniques, evaluated on the planning scan. The mean rank (obtained by Friedman’s test) for each technique regarding each evaluated parameter is also shown. A mean rank of 1 would mean that this was the best plan for all patients, while a mean rank of 4 means that this was the worst plan for all patients. Statistically significant differences ( $p < 0.05$ ) compared to the IMRT plan are shown in bold.

	IMRT		SFUD		4DIMPT		IMPT	
	Median (Range)	Mean Rank	Median (Range)	Mean Rank	Median (Range)	Mean Rank	Median (Range)	Mean Rank
CTV D <sub>98%</sub> (%)	98.6 (98.2–98.8)	1.20	<b>98 (97.4–98.8)</b>	2.93	<b>98 (97.1–98.9)</b>	2.93	<b>98 (97.1–98.7)</b>	2.93
CTV D <sub>2%</sub> (%)	102.2 (101.7–102.7)	1.93	102.5 (101.5–103.0)	2.13	102.6 (102–103.4)	2.93	102.4 (102.2–103.9)	3.00
CTV CI	0.41 (0.33–0.62)	1.70	<b>0.34 (0.26–0.53)</b>	3.33	0.34 (0.25–0.64)	2.50	0.34 (0.26–0.61)	2.47
CTV HI	0.036 (0.030–0.044)	1.27	<b>0.046 (0.027–0.051)</b>	2.53	<b>0.047 (0.038–0.059)</b>	3.13	<b>0.044 (0.036–0.068)</b>	3.07
Body D <sub>2cc</sub> (Gy)	67.5 (61.3–68.4)	1.20	<b>68.3 (61.1–69.0)</b>	2.47	<b>68.1 (62.1–69.7)</b>	3.07	<b>68.5 (61.9–69.4)</b>	3.27
Lungs D <sub>mean</sub> (Gy)	13.6 (6.6–16.8)	3.93	10.2 (4.5–14.5) *	2.87	<b>9.6 (4.1–13.2)</b>	1.87	<b>9.2 (4.5–13.1)</b>	1.33
Lungs V <sub>5Gy</sub> (%)	54.9 (31.8–63.2)	4.00	<b>28.3 (14.0–41.9)</b>	2.47	<b>27.5 (13.1–41.6)</b>	2.00	<b>27.6 (13.7–40.9)</b>	1.53
Lungs V <sub>20Gy</sub> (%)	22.6 (9.6–30.6)	3.80	19.0 (9.0–29.0) *	2.93	<b>18.0 (8.2–25.1)</b>	1.93	<b>17.6 (8.8–25.5)</b>	1.33
Heart D <sub>mean</sub> (Gy)	8.1 (0.9–20.7)	4.00	<b>2.8 (0.5–10.1)</b>	2.53	<b>2.8 (0.5–10.0)</b>	1.93	<b>2.8 (0.5–10.0)</b>	1.53
Heart V <sub>30Gy</sub> (%)	8.6 (0.0–28.2)	3.90	<b>3.2 (0.0–13.7)</b>	2.30	<b>3.3 (0.9–13.9)</b>	2.37	<b>3.3 (0.0–13.7)</b>	1.43
Esophagus D <sub>mean</sub> (Gy)	20.4 (14.1–32.2)	3.33	20.0 (10.0–30.8) *	3.00	19.5 (8.9–31.8)	2.27	<b>20.0 (9.0–29.9)</b>	1.40
Spinal Canal D <sub>max</sub> (Gy)	46.0 (31.8–53.9)	4.00	<b>32.3 (18.8–41.1)</b>	2.40	<b>31.4 (20.6–40.3)</b>	2.00	<b>32.5 (12.8–39.6)</b>	1.60

\* Statistically significant difference between SFUD and IMPT.

### 3.3. Target Dose Robustness at Plan and Start

All IMPT and 4DIMPT plans achieved the criteria for D<sub>98%</sub> and D<sub>2%</sub> for the CTV on setup and range evaluation and extreme phase evaluation at Plan (Figure 3). One SFUD plan narrowly failed with a D<sub>98%</sub> of 94.8% on CT0. In interplay evaluations, all plans fulfilled the goal of D<sub>98%</sub> > 90%. CTV D<sub>2%</sub> slightly exceeded 107% in interplay evaluations of three plans, two of which were SFUD and one was 4DIMPT. Thus, all PBS-PT techniques had satisfying target robustness at Plan. The results from the extensive robustness evaluation at Plan and Start for CTV D<sub>98%</sub> are shown in Figure 3, and a summary of D<sub>98%</sub> and D<sub>2%</sub> values for all evaluations of all proton techniques are listed in the Appendix A (Table A4).

For the Start AIP recalculation, the CTV D<sub>98%</sub> was above 95% of the prescribed dose for 13/15 patients with SFUD and 4DIMPT and 12/15 with IMPT (Figure 3). In general, the CTV D<sub>98%</sub> decreased in extreme-phase evaluations, but for 11/15 patients, it was still above 95%, independent of the optimization technique. The differences in the median CTV D<sub>98%</sub> between the PT techniques were small for both AIP and CT0/50 recalculations at Start (Figure 3, Table A4). It was, however, statistically significant between 4DIMPT and IMPT on CT0/50, in disfavor of IMPT. D<sub>2%</sub> was similar and <107% for all plans on all scans.

One of the patients that stood out with insufficient CTV coverage at Start (AIP) was patient 3, with D<sub>98%</sub> of 87.2%, 91.7% and 82.7% for SFUD, 4DIMPT and IMPT, respectively. This patient had a change in breathing pattern between Plan and Start, causing the CTV in the mediastinum to expand 15 mm caudally and 3 mm cranially (Figure A2). Similar changes were seen for patients 11 and 15. The CTV coverage at Start for these patients was not sufficient with any PT optimization technique (Figure 3). For one of the patients with insufficient and one of the patients with sufficient CTV coverage at Start, dose distributions for all PT techniques are shown in Figure A3. For patient 8, the low CTV D<sub>98%</sub> at the Start CT0/50 was likely caused by delineation uncertainty. The IMRT plans for patients 3 and 11 were planned and recalculated on DIBH CTs. The values for IMRT and PT techniques can therefore not be directly compared.

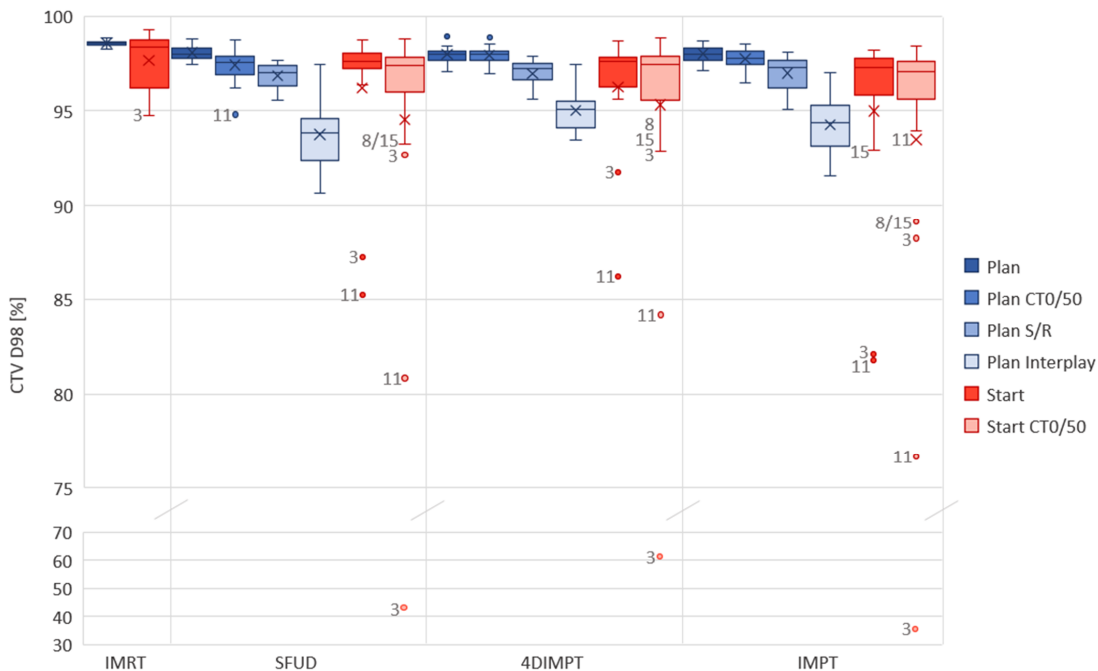


**Figure 3.** Robust evaluation on the Plan (blue) and Start (red) CTs for each optimization technique. The acceptance criteria were  $D_{98\%} > 90\%$  for interplay evaluation and  $>95\%$  for other robust evaluations. In cases where the criteria were not met, the patient number is given next to the observation in the figure. DIBH CT was used in IMRT for patients 3 and 11, hence planning and recalculation were not performed on the same scans as for the PT plans. CT0/50 includes two observations (both extreme phases) per patient. Boxplots show the median (line), mean (cross) and spread, with outliers as dots outside the box. Plan = planning CT, Start = start of treatment CT, CT0/50 = extreme phase evaluation, S/R = setup and range evaluation.

### 3.4. OAR Dose Robustness at Plan and Start

In setup and range and extreme-phase evaluations at Plan, both IMPT and 4DIMPT achieved the constraints for OARs (Table A1) in all plans. One of the SFUD plans failed in the setup and range evaluation, exceeding the  $D_{max}$  criterion for the spinal canal with 52.0 Gy in the worst-case scenario. In interplay evaluation, 26 out of 45 plans had a  $D_{2cc}$  to the body  $>107\%$ ; however, only three plans exceeded 110% of the prescribed dose. Two of these were IMPT plans, and one was 4DIMPT. The OAR constraints were met for all patients and all techniques in interplay evaluation.

Relevant dose-volume parameters for OARs at Plan and Start for IMRT and all PT techniques are shown in Figure 2. The pattern of OAR sparing with PT compared to IMRT persisted at Start. Median changes in dose-volume parameters from Plan to Start were 6% or lower for all parameters and all techniques (Table A5). Nevertheless, large variations between patients in the relative change of dose-volume parameters (ranging from  $-58\%$  to  $103\%$ ) from Plan to Start were seen for individual patients with all techniques. For most of the patients, constraints were still achieved for all OARs. For one patient, the esophagus shifted towards the CTV, causing a  $\sim 30\%$  increase in mean dose to above 35 Gy for all techniques. Hotspots ( $D_{2cc} > 107\%$ ) to the healthy tissue occurred at Start with one IMRT plan and two SFUD plans.

### 3.5. Target Coverage and OAR Sparing at Start

Out of the PBS-PT techniques, IMPT showed the greatest potential for toxicity reduction. A comparison of all 105 OAR dose-volume parameters calculated at Start resulted in the best mean rank for IMPT (1.51), followed by 4DIMPT (2.06), SFUD (2.56) and IMRT (3.87), with all pairwise comparisons being significant. Figure 4 shows the per-patient advantage of IMPT in the sparing of OAR mean doses, as well as the price to pay in target coverage. The latter was, however, only significantly different between IMPT and IMRT, probably influenced by the use of DIBH for IMRT.

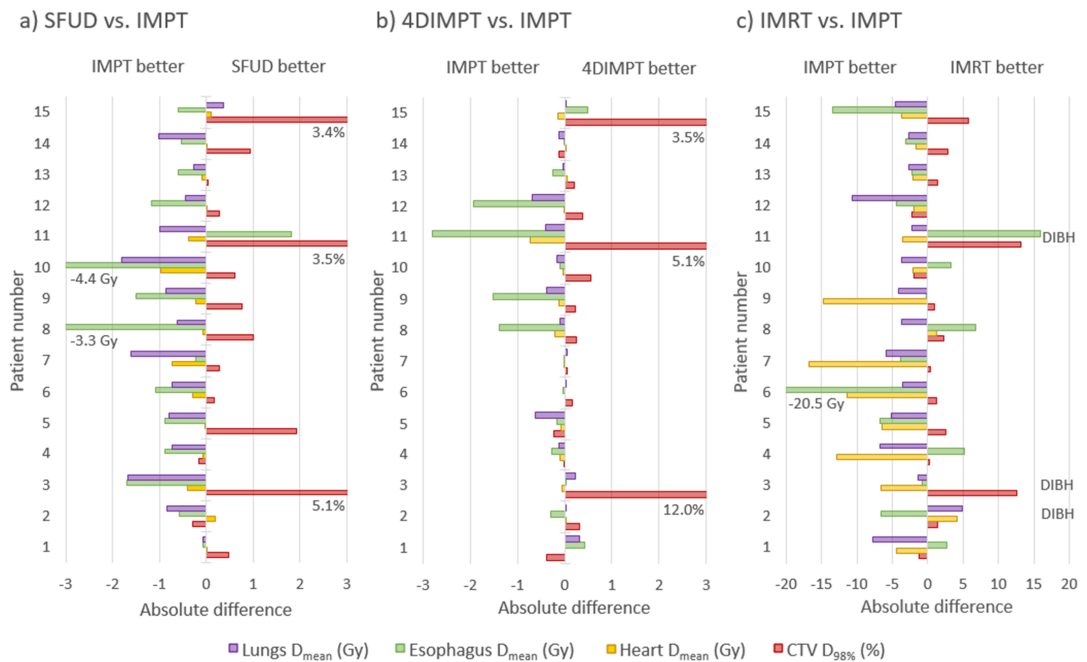


**Figure 4.** Absolute difference in mean OAR dose and CTV  $D_{98\%}$  per patient between IMPT and SFUD (a), IMPT and 4DIMPT (b) and IMPT and IMRT (c) as calculated on the AIP at Start. Negative values are always in favor of IMPT (for the OARs, the other technique is subtracted from IMPT, while for the CTV, IMPT is subtracted from the other technique). The patients are sorted according to increasing breathing motion. Patient 1 had no primary tumor, patients 2–7 had tumor motion amplitude  $>0.5$  cm and patients 8–15 had tumor motion amplitude  $<0.5$  cm. Notably, the patients with a large advantage in CTV  $D_{98\%}$  for SFUD and 4DIMPT (patients 3, 11 and 15) are the same patients where changes in breathing pattern and anatomy deteriorated CTV coverage for all proton techniques. Note also that three of the patients (2, 3 and 11) received IMRT in DIBH and cannot be directly compared in (c).

Substantial dose reductions were achieved with IMPT compared to state-of-the-art IMRT for the lungs, heart and spinal canal (Figures 4 and 5). For the lungs, the median  $D_{mean}$  was reduced from 13.7 to 9.6 Gy,  $V_{5Gy}$  from 55.1 to 28.4% and  $V_{20Gy}$  from 23.4 to 18.6% with IMPT compared to IMRT. The median heart  $D_{mean}$  was reduced from 8.2 to 3.0 Gy, with  $D_{mean} < 10$  Gy for all patients with IMPT and 10/15 with IMRT. The median heart  $V_{30Gy}$  was reduced from 8.3 to 3.6%, the median esophagus  $D_{mean}$  was reduced from 20.1 to 18.1 Gy and the median spinal canal  $D_{max}$  was reduced from 45.5 to 32.7 Gy. All differences were statistically significant, and among the 105 individual parameters compared, 102 were in favor of IMPT, 2 were in favor of IMRT, and 1 was tied.



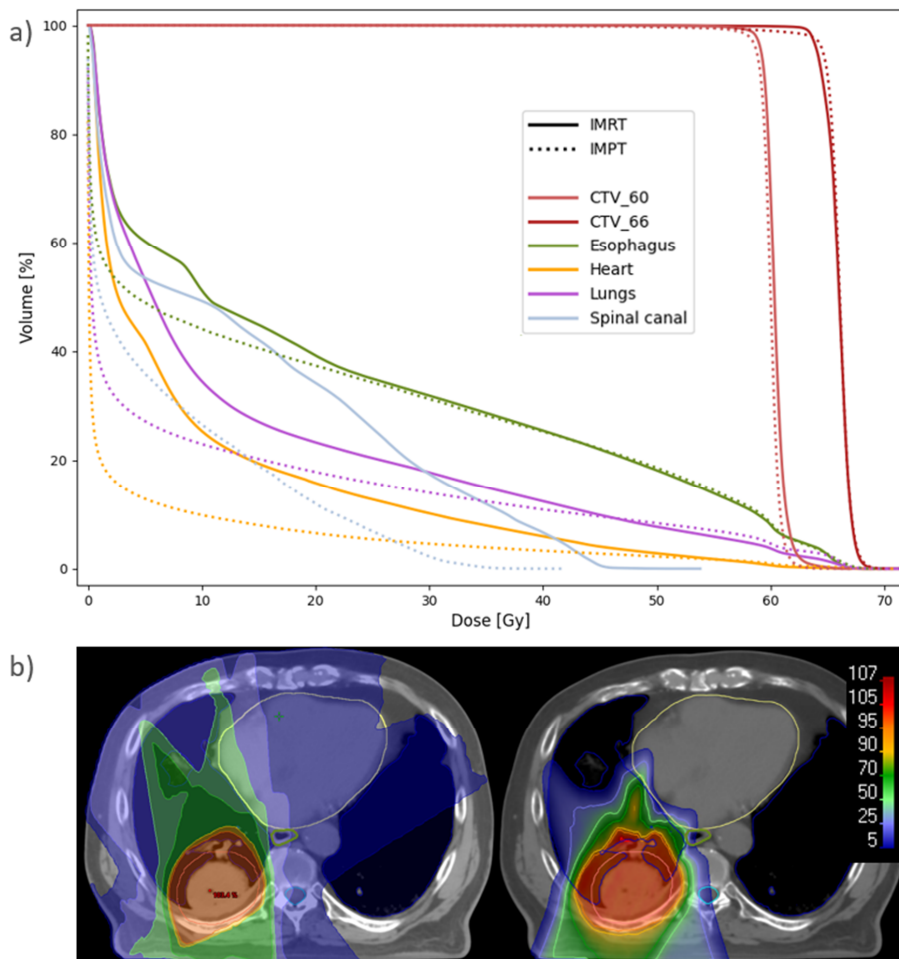


**Figure 5.** (a) Population average DVH for IMRT and IMPT plans recalculated at Start. Six patients had CTV\_60 and nine had CTV\_66. (b) Dose distribution for patient 7 with IMRT (left) and IMPT (right), recalculated at Start. The spread of the low and medium doses results in higher mean doses to the lungs (blue), esophagus (green) and heart (yellow) with IMRT. The CTV is delineated in pink, and the spinal canal in cyan.

#### 4. Discussion

This study shows that the potential for OAR sparing with PBS-PT compared to state-of-the-art IMRT was substantial and persistent from the planning to the start of treatment. Among the various optimization techniques, IMPT spared OARs the most. There were surprisingly small differences between the PBS-PT techniques in the response to various uncertainties, but IMPT was slightly less robust towards breathing motion than 4DIMPT. All techniques were acceptable with respect to robustness evaluations at Plan, including interplay, and also at Start for the majority of patients. However, all robust optimization techniques failed to account for changes in breathing motion patterns occurring in three patients, causing unacceptable coverage of the mediastinal lymph nodes.

Given strategies to recognize patients with altered breathing motion and account for the lack of target robustness in these patients, we believe robustly optimized IMPT and

4DIMPT can reduce the risk of both radiation pneumonitis and heart toxicity compared to IMRT. Lung  $D_{\text{mean}}$ ,  $V_{5\text{Gy}}$  and  $V_{20\text{Gy}}$  were all significantly reduced with IMPT and 4DIMPT, and these parameters have previously been correlated to the probability of radiation pneumonitis [31]. Interestingly, this could potentially be a key to better outcome as well, since patients with radiation pneumonitis have been excluded from adjuvant treatment with immune checkpoint inhibitors [32]. Note that SFUD did not reduce lung doses compared to IMRT in our study, and therefore we would not expect any reduced risk of pneumonitis with SFUD. The reductions in heart dose seen with all PBS-PT techniques are also likely clinically relevant. Atkins et al. showed that a heart  $D_{\text{mean}} > 10$  Gy significantly increased the risk of mortality in LA-NSCLC [33]. In our study, a mean dose to the heart below 10 Gy was achieved for 10/15 patients with IMRT and for all patients across all PBS-PT techniques.

Sparing of the spinal canal beyond the max dose constraint is not expected to give a clinical benefit in itself. However, with the large reduction seen with all PBS-PT techniques compared to IMRT, less effort must be spent on this highly prioritized constraint in the optimization, possibly giving room for the considerable dose reduction seen for other OARs.

Mean doses to the esophagus were slightly reduced with IMPT compared to IMRT in our study. It is unknown whether this would lead to a reduction in esophagitis [34], especially since there are additional uncertainties in elevated LET that were not considered in the current study. The esophagus is highly mobile and often located in close proximity to the target volume, and can move into the high-dose region. This was the case for one of the patients in our study. In a recent clinical dose-escalation study (including 47 patients with stage III NSCLC) by Iwata et al., ART was used to monitor the position of the esophagus and adjust treatment accordingly if needed [8]. Dose-escalated PT was well tolerated in this phase II study, with no grade  $\geq 3$  radiation pneumonitis and one case of acute grade 3 esophagitis. Additionally, the 5-year overall survival of 59% (probably influenced by combination with immunotherapy) shows promise. This study mainly used passive scattering PT, although some patients with small tumor motion had single-field optimized spot-scanning plans.

Recently, Ribeiro et al. published a comprehensive robustness analysis, including weekly imaging during treatment, for 10 stage III NSCLC patients with small to moderate tumor motion, showing the feasibility of PBS-PT in the majority of patients [27]. Our study strengthens these findings by confirming the results in an independent patient group with larger motion variability. Inoue et al. also investigated the robustness of 3D robustly optimized IMPT in stage III NSCLC [35]. They reported a limited impact of setup and range uncertainties, breathing motion and interplay effects on the dose distribution when using properly selected robust optimization parameters. This is in line with our analysis for the planning scan.

A strength of our study was the prospective study design with repeated imaging at the start of treatment. At this time point, we expected a small probability of anatomical changes in need of ART, based on experience from photon therapy [36]. A CT at fraction 2 or 3 was therefore chosen for robustness evaluation, as it would reveal if any of the optimization techniques were particularly sensitive towards interfractional variations such as changes in breathing pattern or positioning of the patient.

Indeed our results show that none of the optimization techniques for PBS-PT were able to handle substantial changes in the breathing pattern. With current robust optimization methods, it is therefore important to verify dose delivery at the onset of treatment. Adaptive protocols in PT are commonly based on weekly 4DCTs, starting at the end of the first treatment week, but imaging at the onset of treatment could recognize these patients earlier. Importantly, the observed target under-dosage was mainly located in the mediastinal lymph nodes (and not the primary tumor), which are hard to locate on, e.g., CBCT. A possibility is to use the carina as a surrogate structure in addition to the diaphragm, as done by Møller et al. in their ART protocol [36]. The carina position has been shown to correlate better with lung volume than, e.g., diaphragm position [37]. Alternative strategies

to avoid dose degradation due to breathing motion changes could be respiratory gating or breath-hold strategies. Although images in DIBH were acquired in the current study and used clinically in IMRT for three patients, analysis of PBS-PT in DIBH was beyond the scope of the current study.

Both Ribeiro et al. and Hoffmann et al. reported that altered shoulder position caused a loss in robustness when evaluating dose during treatment [27,28]. This was not observed in our study, but in principle, this could also occur from the planning to the start of treatment and should be kept in mind when evaluating robustness at the onset of treatment. Our study design was limited to observing changes between the planning and start of treatment, and hence anatomical changes such as atelectasis or pleural effusion were not observed. Such changes can occur during treatment and largely impact the delivered dose, but they are well known and can be corrected for by existing adaptive protocols [28]. The novelty of our study lies in focusing on uncertainties that so far have received less attention. We have shown that these are neither handled by current robust optimization techniques nor adaptive protocols.

Regarding the comparison of different PBS-PT optimization techniques, Ribeiro et al. compared 3D and 4D robustly optimized IMPT plans with layered rescanning in their study [27]. Similar to us, they found only small differences in robustness between the techniques. However, IMPT was (somewhat surprisingly) slightly more robust than 4DIMPT in their study, while we found the opposite. This might be explained by the difference in the use of density override for the target. In the study by Ribeiro et al., density override was only used for the IMPT plans, while we used it on the AIP for both techniques. This is an example of one out of several technical details that might influence robustness; rescanning is another [14]. Indeed, with the use of rescanning, the uncertainties due to the interplay effect could be limited even further than reported here. Liao and colleagues have pointed out the importance of treatment planning experience in PT for NSCLC [11]. In addition to comprehensive treatment planning guidelines, solutions for automated treatment planning could be useful to ensure the high plan quality needed in PBS-PT for LA-NSCLC [38].

The number of treatment fields could also influence the robustness of the PT plans. In this study, two fields were used for ten patients and three fields for five patients. On the one hand, adding a third field could increase the robustness, as the dose contribution is divided between more treatment angles, and changes in anatomy affecting one of the fields have a lesser impact on the dose distribution. However, some issues came with increasing the number of fields. For some patients, finding a third, robust angle could be difficult due to, e.g., arm position or large breasts or fat folds, where it was preferred to avoid beam entry due to positioning uncertainty. In the 4D optimization, splitting the fields with field-specific targets was not possible, so the fields had to be able to contribute to both the primary tumor and the lymph node volumes, giving some limitations for robust angles because of the surrounding anatomy. Hence, the requirement for the field setup to work for all optimization techniques was a limitation in this study.

Another limitation of the current study is the low number of included patients. Despite this, there was a large variation in tumor size and position, and breathing motion ranged from negligible to substantial. These parameters also varied among the patients that failed the robustness criteria at Start. Finally, the 4D optimization and extreme phase and interplay evaluations performed in this study required deformable image registration and mapping of contours to each phase of the 4DCT. As delineation was performed on the AIP as a part of the clinical routine, the contours were mapped from the AIP to each phase. Due to blurring of the edges, the GTV on the AIP may be slightly larger than in reality, and the plans may therefore be slightly more robust than if delineation had been performed on one of the phase images.

## 5. Conclusions

The potential of IMPT and 4DIMPT for reducing heart and lung toxicity in the treatment of LA-NSCLC was substantial and persistent at Start. SFUD only showed potential

for reduced heart toxicity. All proton optimization techniques responded similarly to uncertainties and were sufficiently robust towards setup and range uncertainties as well as interplay at Plan, and for the majority of patients in recalculations at Start. Altered breathing patterns between Plan and Start jeopardized target coverage for all PBS-PT techniques. Adaptive protocols for free-breathing PBS-PT should include imaging at onset of or early in treatment, and possibly a surrogate for visualization of the mediastinal target. Given such strategies to recognize patients with altered breathing patterns, we believe there is great potential for PBS-PT to improve the treatment of LA-NSCLC.

**Author Contributions:** Conceptualization, C.G.B., I.M.S., M.U. and L.B.H.; methodology, C.G.B., M.U., G.M.E. and L.B.H.; software, C.G.B. and M.U.; validation, K.F., I.M.S. and M.U.; formal analysis, C.G.B., K.F. and L.B.H.; investigation, C.G.B., K.F., I.M.S., M.U., G.M.E. and L.B.H.; resources, L.B.H.; data curation, K.F., I.M.S. and L.B.H.; writing—original draft preparation, C.G.B., K.F. and L.B.H.; writing—review and editing, C.G.B., K.F., I.M.S., M.U., G.M.E. and L.B.H.; visualization, C.G.B., K.F. and L.B.H.; supervision, G.M.E. and L.B.H.; project administration, L.B.H.; funding acquisition, C.G.B., K.F. and L.B.H. All authors have read and agreed to the published version of the manuscript.

**Funding:** This research received funding from the Trond Mohn Foundation (grant number BFS2017TMT07) and Helse Vest RHF (grant number F-12505).

**Institutional Review Board Statement:** This study was conducted in accordance with the Declaration of Helsinki and approved by the regional committee for medical and health research ethics in Western Norway (protocol code 2019/749, 21 June 2019).

**Informed Consent Statement:** Informed consent was obtained from all subjects involved in the study. Written informed consent has been obtained from the patients to publish this paper.

**Data Availability Statement:** The data presented in this study are available on request from the corresponding author. The data are not publicly available due to privacy reasons as they are part of an ongoing study.

**Acknowledgments:** The authors are thankful to Sara Pilskog for scientific discussions and clinical personnel at Haukeland University Hospital for data collection.

**Conflicts of Interest:** The authors declare no conflict of interest. The funders had no role in the design of the study; in the collection, analyses, or interpretation of data; in the writing of the manuscript, or in the decision to publish the results.

## Appendix A

**Table A1.** Planning dose constraints for organs at risk.

Organ	Dose Constraint
Lungs	$V_{5Gy} < 65\%$
	$V_{20Gy} < 35\%$
	$D_{mean} < 20 \text{ Gy}$
Esophagus	$D_{mean} < 34 \text{ Gy}$
	$V_{30Gy} < 40\%$
Heart	$D_{max} < 50 \text{ Gy}$
Spinal canal	$D_{max} < 66 \text{ Gy}$
Brachial plexus	$D_{max} < 66 \text{ Gy}$

**Table A2.** Overview of the performed robustness evaluations, and the criteria used in each evaluation. The criteria in parentheses were used for interplay evaluation. \* OAR constraints are shown in Table A1.

Evaluations of	Evaluations at Plan	Evaluations at Start	Evaluation Criteria
Target coverage and OAR sparing at Plan	Plan AIP		CTV D <sub>98%</sub> > 95% CTV D <sub>2%</sub> < 107% Body D <sub>2cc</sub> < 107% OARs within constraints *
Target dose robustness	Plan S/R Plan CT0/50 Plan Interplay	Start AIP Start CT0/50	CTV D <sub>98%</sub> > 95% (90%) CTV D <sub>2%</sub> < 107% (110%)
OAR dose robustness	Plan S/R Plan CT0/50 Plan Interplay	Start AIP Start CT0/50	Body D <sub>2cc</sub> < 107% (110%) OARs within constraints *
Target coverage and OAR sparing at Start		Start AIP	CTV D <sub>98%</sub> > 95% CTV D <sub>2%</sub> < 107% Body D <sub>2cc</sub> < 107% OARs within constraints *

**Table A3.** Breathing motion amplitudes of the primary tumor in the Plan and Start 4DCTs. Median value and range are given for each direction.

Direction	Motion—Plan	Motion—Start
x (left–right)	1 mm (0–5)	1 mm (0–6)
y (anterior–posterior)	2 mm (1–4)	2 mm (1–4)
z (cranio–caudal)	4 mm (1–15)	4 mm (1–13)

**Table A4.** Robust evaluation of CTV dose, showing median values and range.

Parameter	Evaluation	SFUD	4DIMPT	IMPT
CTV D <sub>98%</sub> (%)	Plan CT0/50	97.5 (94.8–98.8)	98.0 (97.0–99.0)	97.8 (96.5–98.5)
	Plan setup/range	97.0 (95.6–97.7)	97.2 (95.6–97.7)	97.3 (95.1–98.1)
	Plan interplay	93.6 (90.7–97.5)	95.0 (93.5–97.0)	94.6 (91.8–97.0)
	Start	97.6 (85.3–98.8)	97.6 (86.2–98.7)	97.5 (81.8–98.2)
	Start CT0/50	97.4 (43.2–98.8)	97.4 (61.3–98.9)	97.1 (35.6–98.4)
CTV D <sub>2%</sub> (%)	Plan CT0/50	102.2 (101.2–103.2)	102.5 (102.0–103.5)	102.5 (102.0–103.9)
	Plan setup/range	103.3 (102.2–104.5)	103.2 (102.3–104.2)	103.3 (102.5–105.5)
	Plan interplay	104.9 (102.7–107.6)	105.3 (103.2–107.5)	105.5 (104.1–106.7)
	Start	102.6 (101.4–104.4)	102.8 (102.0–103.7)	102.6 (101.8–103.7)
	Start CT0/50	102.3 (101.1–104.9)	102.5 (102.0–104.0)	102.5 (101.8–103.8)

**Table A5.** Difference in OAR parameters from Plan to Start, relative to the Plan value. Median and range are shown for each technique. Positive values indicate a higher dose and negative values indicate a lower dose at Start.

Structure	Difference, Plan vs. Start			
	IMRT	SFUD	4DIMPT	IMPT
Lungs D <sub>mean</sub> (Gy)	1 (–6/20)	0 (–11/20)	0 (–11/33)	0 (–12/32)
Lungs V <sub>5Gy</sub> (%)	–1 (–5/7)	–1 (–11/26)	–2 (–11/26)	–1 (–12/28)
Lungs V <sub>20Gy</sub> (%)	1 (–7/29)	3 (–13/30)	2 (–10/30)	3 (–11/31)
Heart D <sub>mean</sub> (Gy)	–4 (–13/68)	–6 (–55/70)	–4 (–47/78)	–6 (–51/78)
Heart V <sub>30Gy</sub> (%)	0 (–29/162)	0 (–58/84)	0 (–42/97)	0 (–50/103)
Esophagus D <sub>mean</sub> (Gy)	–3 (–17/28)	–5 (–27/30)	–4 (–31/31)	–4 (–31/35)
Spinal canal D <sub>max</sub> (Gy)	–1 (–9/6)	1 (–14/6)	0 (–16/9)	1 (–21/8)
Body D <sub>2cc</sub> (Gy)	0 (–2/6)	0 (–1/4)	0 (0/1)	0 (–3/1)

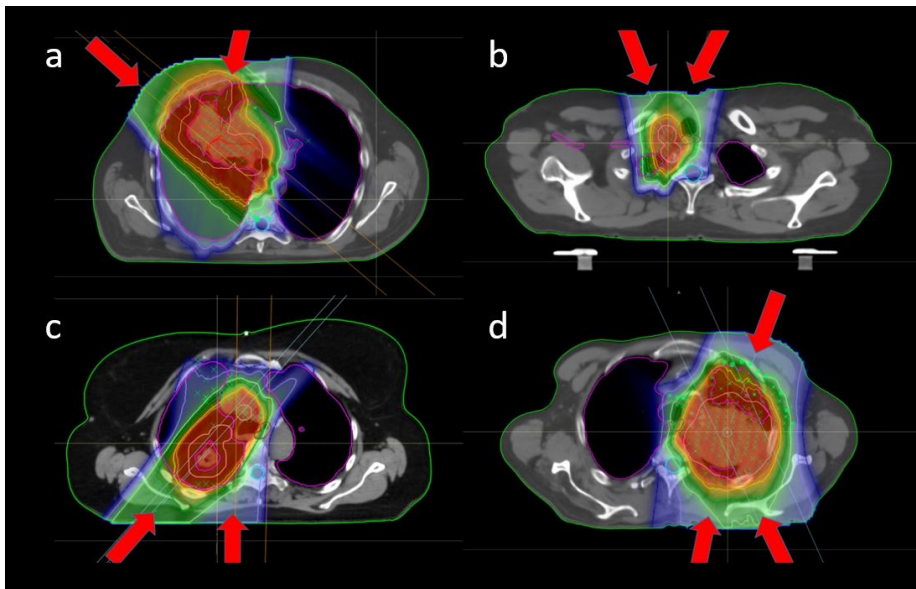


**Figure A1.** Common beam configurations for different tumor locations: (a) frontal oblique tumor with oblique and frontal fields, (b) nodes in the frontal part of the mediastinum with two slightly frontal oblique fields, (c) dorsal tumor with dorsal oblique and dorsal fields, and (d) large tumor near the brachial plexus, with slightly frontal oblique, dorsal and dorsal oblique fields.

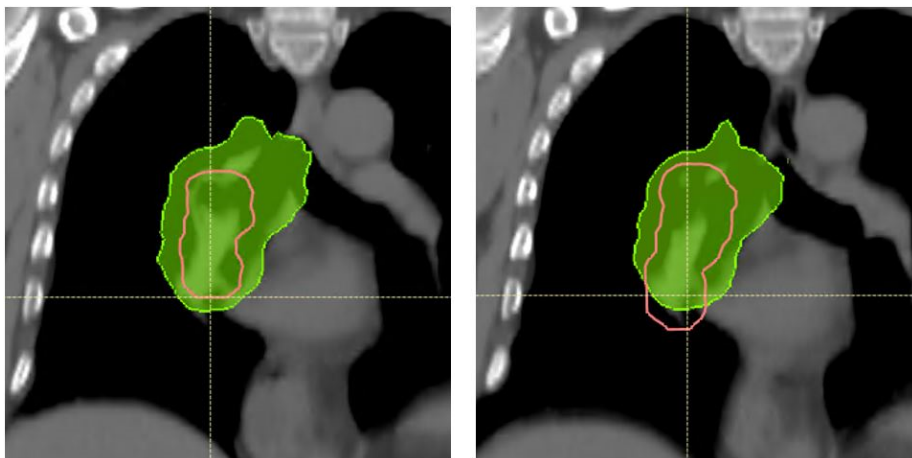


**Figure A2.** SFUD plan for patient 3. Deeper breathing and increased breathing motion causes the CTV (pink) in the mediastinum to extend 15 mm more caudally and 3 mm more cranially on the Start AIP (right) compared to the Plan AIP (left). The yellow cross shows a reference position in both images. The 95% isodose (green) does not cover the caudal area of the CTV at Start. Notably, the diaphragm position had also changed in this patient, and this change would be detectable on CBCT imaging.

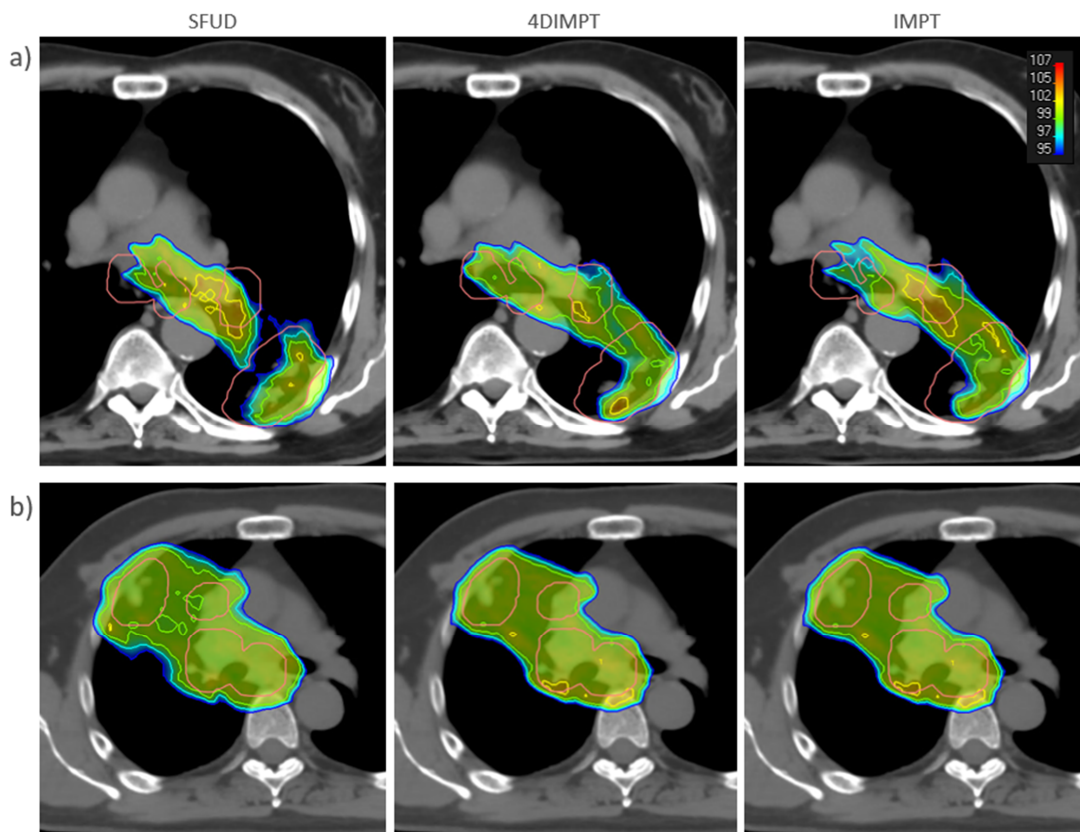


**Figure A3.** SFUD (left), 4DIMPT (middle), and IMPT (right) plans recalculated on the Start AIP for (a) one of the patients that failed the robustness criteria (patient 11) and (b) one of the patients with satisfactory target coverage (patient 10). The CTV is delineated in pink. Doses higher than 95% of the prescribed dose are shown, according to the color scale in the top right corner.

## References

- Bradley, J.D.; Hu, C.; Komaki, R.R.; Masters, G.A.; Blumenschein, G.R.; Schild, S.E.; Bogart, J.A.; Forster, K.M.; Magliocco, A.M.; Kavadi, V.S.; et al. Long-Term Results of NRG Oncology RTOG 0617: Standard-versus High-Dose Chemoradiotherapy with or without Cetuximab for Unresectable Stage III Non-Small-Cell Lung Cancer. *J. Clin. Oncol.* **2020**, *38*, 706–714. [[CrossRef](#)] [[PubMed](#)]
- Ma, L.; Men, Y.; Feng, L.; Kang, J.; Sun, X.; Yuan, M.; Jiang, W.; Hui, Z. A Current Review of Dose-Escalated Radiotherapy in Locally Advanced Non-Small Cell Lung Cancer. *Radiol. Oncol.* **2019**, *53*, 6–14. [[CrossRef](#)] [[PubMed](#)]
- Gjyshi, O.; Liao, Z. Proton Therapy for Locally Advanced Non-Small Cell Lung Cancer. *Br. J. Radiol.* **2020**, *93*, 20190378. [[CrossRef](#)] [[PubMed](#)]
- Ramella, S.; D'Angelillo, R.M. Proton Beam or Photon Beam Radiotherapy in the Treatment of Non-Small-Cell Lung Cancer. *Lancet Oncol.* **2020**, *21*, 873–875. [[CrossRef](#)]
- Chang, J.Y.; Zhang, X.; Wang, X.; Kang, Y.; Riley, B.; Bilton, S.; Mohan, R.; Komaki, R.; Cox, J.D. Significant Reduction of Normal Tissue Dose by Proton Radiotherapy Compared with Three-Dimensional Conformal or Intensity-Modulated Radiation Therapy in Stage I or Stage III Non-Small-Cell Lung Cancer. *Int. J. Radiat. Oncol. Biol. Phys.* **2006**, *65*, 1087–1096. [[CrossRef](#)]
- Zhang, X.; Li, Y.; Pan, X.; Xiaoqiang, L.; Mohan, R.; Komaki, R.; Cox, J.D.; Chang, J.Y. Intensity-Modulated Proton Therapy Reduces the Dose to Normal Tissue Compared with Intensity-Modulated Radiation Therapy or Passive Scattering Proton Therapy and Enables Individualized Radical Radiotherapy for Extensive Stage IIIB Non-Small-Cell Lung Cancer: A Virtual Clinical Study. *Int. J. Radiat. Oncol. Biol. Phys.* **2010**, *77*, 357–366. [[CrossRef](#)]

7. Kim, N.; Myoung Noh, J.; Lee, W.; Park, B.; Park, H.; Young Park, J.; Pyo, H. Proton Beam Therapy Reduces the Risk of Severe Radiation-Induced Lymphopenia during Chemoradiotherapy for Locally Advanced Non-Small Cell Lung Cancer: A Comparative Analysis of Proton versus Photon Therapy. *Radiother. Oncol.* **2021**, *156*, 166–173. [[CrossRef](#)] [[PubMed](#)]
8. Iwata, H.; Akita, K.; Yamaba, Y.; Kunii, E.; Takakuwa, O.; Yoshihara, M.; Hattori, Y.; Nakajima, K.; Hayashi, K.; Toshito, T.; et al. Concurrent Chemo-Proton Therapy Using Adaptive Planning for Unresectable Stage 3 Non-Small Cell Lung Cancer: A Phase 2 Study. *Int. J. Radiat. Oncol. Biol. Phys.* **2021**, *109*, 1359–1367. [[CrossRef](#)]
9. Chang, J.Y.; Verma, V.; Li, M.; Zhang, W.; Komaki, R.; Lu, C.; Allen, P.K.; Liao, Z.; Welsh, J.; Lin, S.H.; et al. Proton Beam Radiotherapy and Concurrent Chemotherapy for Unresectable Stage III Non-Small Cell Lung Cancer: Final Results of a Phase 2 Study. *JAMA Oncol.* **2017**, *3*, e172032. [[CrossRef](#)] [[PubMed](#)]
10. Nguyen, Q.-N.; Ly, N.B.; Komaki, R.; Levy, L.B.; Gomez, D.R.; Chang, J.Y.; Allen, P.K.; Mehran, R.J.; Lu, C.; Gillin, M.; et al. Long-Term Outcomes after Proton Therapy, with Concurrent Chemotherapy, for Stage II–III Inoperable Non-Small Cell Lung Cancer. *Radiother. Oncol.* **2015**, *115*, 367–372. [[CrossRef](#)]
11. Liao, Z.; Lee, J.J.; Komaki, R.; Gomez, D.R.; O'Reilly, M.S.; Fossella, F.V.; Blumenschein, G.R.; Heymach, J.V.; Vaporciyan, A.A.; Swisher, S.G.; et al. Bayesian Adaptive Randomization Trial of Passive Scattering Proton Therapy and Intensity-Modulated Photon Radiotherapy for Locally Advanced Non-Small-Cell Lung Cancer. *J. Clin. Oncol.* **2018**, *36*, 1813–1822. [[CrossRef](#)] [[PubMed](#)]
12. Yang, P.; Xu, T.; Gomez, D.R.; Deng, W.; Wei, X.; Elhalawani, H.; Jin, H.; Guan, F.; Mirkovic, D.; Xu, Y.; et al. Patterns of Local-Regional Failure after Intensity Modulated Radiation Therapy or Passive Scattering Proton Therapy with Concurrent Chemotherapy for Non-Small Cell Lung Cancer. *Int. J. Radiat. Oncol. Biol. Phys.* **2019**, *103*, 123–131. [[CrossRef](#)]
13. Gjyshi, O.; Xu, T.; Elhammali, A.; Boyce-Fappiano, D.; Chun, S.G.; Gandhi, S.; Lee, P.; Chen, A.B.; Lin, S.H.; Chang, J.Y.; et al. Toxicity and Survival after Intensity-Modulated Proton Therapy versus Passive Scattering Proton Therapy for NSCLC. *J. Thorac. Oncol.* **2021**, *16*, 269–277. [[CrossRef](#)] [[PubMed](#)]
14. Chang, J.Y.; Zhang, X.; Knopf, A.; Li, H.; Mori, S.; Dong, L.; Lu, H.-M.; Liu, W.; Badiyan, S.N.; Both, S.; et al. Consensus Guidelines for Implementing Pencil-Beam Scanning Proton Therapy for Thoracic Malignancies on Behalf of the PTCOG Thoracic and Lymphoma Subcommittee. *Int. J. Radiat. Oncol. Biol. Phys.* **2017**, *99*, 41–50. [[CrossRef](#)] [[PubMed](#)]
15. Meijers, A.; Knopf, A.-C.; Crijs, A.P.G.; Ubbels, J.F.; Niezink, A.G.H.; Langendijk, J.A.; Wijsman, R.; Both, S. Evaluation of Interplay and Organ Motion Effects by Means of 4D Dose Reconstruction and Accumulation. *Radiother. Oncol.* **2020**, *150*, 268–274. [[CrossRef](#)] [[PubMed](#)]
16. Jie, A.W.; Marignol, L. Pro-Con of Proton: Dosimetric Advantages of Intensity-Modulation over Passive Scatter for Thoracic Malignancies. *Tech. Innov. Patient Support Radiat. Oncol.* **2020**, *15*, 37–46. [[CrossRef](#)] [[PubMed](#)]
17. Paganetti, H.; Grassberger, C.; Sharp, G.C. Physics of Particle Beam and Hypofractionated Beam Delivery in NSCLC. *Semin. Radiat. Oncol.* **2021**, *31*, 162–169. [[CrossRef](#)]
18. Selvaraj, J.; Uzan, J.; Baker, C.; Nahum, A. 4D Radiobiological Modelling of the Interplay Effect in Conventionally and Hypofractionated Lung Tumour IMRT. *Br. J. Radiol.* **2015**, *88*, 20140372. [[CrossRef](#)]
19. Den Otter, L.A.; Anakotta, R.M.; Weessies, M.; Roos, C.T.G.; Sijtsema, N.M.; Muijs, C.T.; Dieters, M.; Wijsman, R.; Troost, E.G.C.; Richter, C.; et al. Investigation of Inter-fraction Target Motion Variations in the Context of Pencil Beam Scanned Proton Therapy in Non-small Cell Lung Cancer Patients. *Med. Phys.* **2020**, *47*, 3835–3844. [[CrossRef](#)] [[PubMed](#)]
20. Möller, D.S.; Khalil, A.A.; Knap, M.M.; Hoffmann, L. Adaptive Radiotherapy of Lung Cancer Patients with Pleural Effusion or Atelectasis. *Radiother. Oncol.* **2014**, *110*, 517–522. [[CrossRef](#)]
21. Kwint, M.; Conijn, S.; Schaake, E.; Knegejs, J.; Rossi, M.; Remeijer, P.; Sonke, J.-J.; Belderbos, J. Intra Thoracic Anatomical Changes in Lung Cancer Patients during the Course of Radiotherapy. *Radiother. Oncol.* **2014**, *113*, 392–397. [[CrossRef](#)] [[PubMed](#)]
22. Fredriksson, A.; Forsgren, A.; Hårdemark, B. Minimax Optimization for Handling Range and Setup Uncertainties in Proton Therapy: Minimax Optimization for Handling Uncertainties in Proton Therapy. *Med. Phys.* **2011**, *38*, 1672–1684. [[CrossRef](#)] [[PubMed](#)]
23. Engwall, E.; Fredriksson, A.; Glimelius, L. 4D Robust Optimization Including Uncertainties in Time Structures Can Reduce the Interplay Effect in Proton Pencil Beam Scanning Radiation Therapy. *Med. Phys.* **2018**, *45*, 4020–4029. [[CrossRef](#)]
24. Ge, S.; Wang, X.; Liao, Z.; Zhang, L.; Sahoo, N.; Yang, J.; Guan, F.; Mohan, R. Potential for Improvements in Robustness and Optimality of Intensity-Modulated Proton Therapy for Lung Cancer with 4-Dimensional Robust Optimization. *Cancers* **2019**, *11*, 35. [[CrossRef](#)] [[PubMed](#)]
25. Teoh, S.; Fiorini, F.; George, B.; Vallis, K.A.; Van den Heuvel, F. Proton vs Photon: A Model-Based Approach to Patient Selection for Reduction of Cardiac Toxicity in Locally Advanced Lung Cancer. *Radiother. Oncol.* **2020**, *152*, 151–162. [[CrossRef](#)]
26. Chen, M.; Yang, J.; Liao, Z.; Chen, J.; Xu, C.; He, X.; Zhang, X.; Zhu, R.X.; Li, H. Anatomic Change over the Course of Treatment for Non-Small Cell Lung Cancer Patients and Its Impact on Intensity-Modulated Radiation Therapy and Passive-Scattering Proton Therapy Deliveries. *Radiat. Oncol.* **2020**, *15*, 55. [[CrossRef](#)]
27. Ribeiro, C.O.; Visser, S.; Korevaar, E.W.; Sijtsema, N.M.; Anakotta, R.M.; Dieters, M.; Both, S.; Langendijk, J.A.; Wijsman, R.; Muijs, C.T.; et al. Towards the Clinical Implementation of Intensity-Modulated Proton Therapy for Thoracic Indications with Moderate Motion: Robust Optimised Plan Evaluation by Means of Patient and Machine Specific Information. *Radiother. Oncol.* **2021**, *157*, 210–218. [[CrossRef](#)] [[PubMed](#)]



28. Hoffmann, L.; Alber, M.; Jensen, M.F.; Holt, M.I.; Møller, D.S. Adaptation Is Mandatory for Intensity Modulated Proton Therapy of Advanced Lung Cancer to Ensure Target Coverage. *Radiother. Oncol.* **2017**, *122*, 400–405. [[CrossRef](#)]
29. Kong, F.-M.; Ritter, T.; Quint, D.J.; Senan, S.; Gaspar, L.E.; Komaki, R.U.; Hurkmans, C.W.; Timmerman, R.; Bezjak, A.; Bradley, J.D.; et al. Consideration of Dose Limits for Organs at Risk of Thoracic Radiotherapy: Atlas for Lung, Proximal Bronchial Tree, Esophagus, Spinal Cord, Ribs, and Brachial Plexus. *Int. J. Radiat. Oncol. Biol. Phys.* **2011**, *81*, 1442–1457. [[CrossRef](#)] [[PubMed](#)]
30. Feuvret, L.; Noël, G.; Mazeran, J.-J.; Bey, P. Conformity Index: A Review. *Int. J. Radiat. Oncol. Biol. Phys.* **2006**, *64*, 333–342. [[CrossRef](#)] [[PubMed](#)]
31. Marks, L.B.; Bentzen, S.M.; Deasy, J.O.; Kong, F.-M.; Bradley, J.D.; Vogelius, I.S.; El Naqa, I.; Hubbs, J.L.; Lebesque, J.V.; Timmerman, R.D.; et al. Radiation Dose–Volume Effects in the Lung. *Int. J. Radiat. Oncol. Biol. Phys.* **2010**, *76*, S70–S76. [[CrossRef](#)] [[PubMed](#)]
32. Antonia, S.J.; Villegas, A.; Daniel, D.; Vicente, D.; Murakami, S.; Hui, R.; Kurata, T.; Chiappori, A.; Lee, K.H.; de Wit, M.; et al. Overall Survival with Durvalumab after Chemoradiotherapy in Stage III NSCLC. *N. Engl. J. Med.* **2018**, *379*, 2342–2350. [[CrossRef](#)]
33. Atkins, K.M.; Rawal, B.; Chaunzwa, T.L.; Lamba, N.; Bitterman, D.S.; Williams, C.L.; Kozono, D.E.; Baldini, E.H.; Chen, A.B.; Nguyen, P.L.; et al. Cardiac Radiation Dose, Cardiac Disease, and Mortality in Patients with Lung Cancer. *J. Am. Coll. Cardiol.* **2019**, *73*, 2976–2987. [[CrossRef](#)] [[PubMed](#)]
34. Wang, Z.; Chen, M.; Sun, J.; Jiang, S.; Wang, L.; Wang, X.; Sahoo, N.; Gunn, G.B.; Frank, S.J.; Nguyen, Q.-N.; et al. Lyman–Kutcher–Burman Normal Tissue Complication Probability Modeling for Radiation-Induced Esophagitis in Non-Small Cell Lung Cancer Patients Receiving Proton Radiotherapy. *Radiother. Oncol.* **2020**, *146*, 200–204. [[CrossRef](#)] [[PubMed](#)]
35. Inoue, T.; Widder, J.; van Dijk, L.V.; Takegawa, H.; Koizumi, M.; Takashina, M.; Usui, K.; Kurokawa, C.; Sugimoto, S.; Saito, A.I.; et al. Limited Impact of Setup and Range Uncertainties, Breathing Motion, and Interplay Effects in Robustly Optimized Intensity Modulated Proton Therapy for Stage III Non-Small Cell Lung Cancer. *Int. J. Radiat. Oncol. Biol. Phys.* **2016**, *96*, 661–669. [[CrossRef](#)] [[PubMed](#)]
36. Møller, D.S.; Holt, M.I.; Alber, M.; Tvillum, M.; Khalil, A.A.; Knap, M.M.; Hoffmann, L. Adaptive Radiotherapy for Advanced Lung Cancer Ensures Target Coverage and Decreases Lung Dose. *Radiother. Oncol.* **2016**, *121*, 32–38. [[CrossRef](#)] [[PubMed](#)]
37. Van der Weide, L.; van Sörnsen de Koste, J.R.; Lagerwaard, F.J.; Vincent, A.; van Triest, B.; Slotman, B.J.; Senan, S. Analysis of Carina Position as Surrogate Marker for Delivering Phase-Gated Radiotherapy. *Int. J. Radiat. Oncol. Biol. Phys.* **2008**, *71*, 1111–1117. [[CrossRef](#)]
38. Kouwenberg, J.; Penninkhof, J.; Habraken, S.; Zindler, J.; Hoogeman, M.; Heijmen, B. Model Based Patient Pre-Selection for Intensity-Modulated Proton Therapy (IMPT) Using Automated Treatment Planning and Machine Learning. *Radiother. Oncol.* **2021**, *158*, 224–229. [[CrossRef](#)] [[PubMed](#)]



Graphic design: Communication Division, UIB / Print: Skjipes Kommunikasjon AS



[uib.no](http://uib.no)

ISBN: 9788230850664 (print)  
9788230869727 (PDF)